EVALUATION OF THE USGS NATIONAL ELEVATION DATASET AND THE KANSAS BIOLOGICAL SURVEY'S FLDPLN ("FLOODPLAIN") MODEL FOR INUNDATION EXTENT ESTIMATION

By

Kevin E. Dobbs

Submitted to the Department of Geography and the
Faculty of the Graduate School of the University of Kansas
in partial fulfillment of the requirements for the degree of
Master of Arts

Committee:

Dr. Stephen L. Egbert
(Chair)

Dr. Jerome E. Dobson
(Committee Member)

Dr. William C. Johnson
(Committee Member)

December 2nd, 2009
Date Submitted

The Thesis Committee for Kevin Dobbs certifies
that this is the approved version of the following thesis:

EVALUATION OF THE USGS NATIONAL ELEVATION DATASET AND THE KANSAS BIOLOGICAL SURVEY'S FLDPLN ("FLOODPLAIN") MODEL FOR INUNDATION EXTENT ESTIMATION

Committee:

_____
Dr. Stephen L. Egbert
(Chair)

_____
Dr. Jerome E. Dobson
(Committee Member)

_____
Dr. William C. Johnson
(Committee Member)

April 26th, 2010
Date Submitted

ABSTRACT
Kevin E. Dobbs, April 2010
The University of Kansas

While riverine flooding is a natural and ecologically beneficial phenomenon, severe flood events continue to result in loss of life and property. Recent major flood events in the Midwest, including record flooding in Kansas in 2007 and Iowa in 2008, have shown that currently available inundation extent information is insufficient from both a planning and a response perspective. Current initiatives at the Kansas Biological Survey are aiming to bridge the gap between limited information that is presently available and what is needed to adequately prepare for and respond to a range of inevitable, and in some cases unprecedented, flood events. The focus of this effort is the development of a library of modeled flood inundation extents, using the FLDPLN model, for major streams across the state that can be accessed in near real-time to provide valuable information to disaster responders. This research 1) examines the USGS National Elevation Dataset (NED) and evaluates the affects of errors in the elevation data on flood inundation extent estimation and 2) evaluates the capabilities and limitations of the FLDPLN model for inundation extent estimation. Results showed that, although the accuracy of pre-LiDAR NED for the Kansas study area is better than published figures, modeled flood extents vary significantly when using LiDAR-derived vs. pre-LiDAR NED elevation data inputs. Comparison of modeled flood extents for HEC-RAS, HAZUS, and FLDPLN models for both hypothetical and empirical floods events showed greater correspondence at high flood stages. Improved elevation data and empirical low flood data would offer improved flood extent estimates and more robust model evaluation.

ACKNOWLEDGMENTS

I would like to thank the members of my committee, Drs. Steve Egbert (my advisor), Bill Johnson, and Jerry Dobson, for their keen insight and suggestions in the writing of this thesis. I can always count on Steve to be the calm voice of reason and encouragement, provided sound advice, and make delicious freezer jam for the holidays.

I also want to express my deep appreciation to Dr. Ed Martinko, director of the Kansas Biological Survey, for his ongoing support toward my education, career, and personal development. His encouragement and understanding have been invaluable. Dr. Jude Kastens has been an integral part of this work. I wish to thank him for affording me the opportunity to test the FLDPLN model, which was the basis for part of his dissertation work, for his diligent review of this manuscript, and for being a valuable source of information, inspiration, and reason. I would like to extend a special thank you to Deb and Ron Teeter for all of their support and encouragement, and for providing a safe haven in which to find refuge when I've needed it.

Without the unwavering support of my wife Rachel, and amazing children Willow, Finn, Persephone, and Jet, I don't know what I would have done - you are my inspiration. Thank you so much for tolerating my absence for so many nights and weekends. I'll try to make it up to you …I can't wait for "family time."

To my parents, Kay and Luther Dobbs, whom, from day one, have sacrificed so much for me and provided invaluable support in every way - thank you for believing in me. To my sister Heather, thank for the encouragement, you are truly a special person. And to my brother Kelly……you're a lot nicer now than when we were kids.

TABLE OF CONTENTS

LIST OF TABLES

LIST OF FIGURES

CHAPTER 1

INTRODUCTION

With the increasing availability of GIS functionality and applications as decision support tools in desktop, web-based, and field environments, disaster preparedness and response personnel and emergency managers are fast becoming key consumers of geospatial information (Mansourian et al. 2006). This complex environment of disaster preparedness and response drives both application and data development. Recent major flood events in Kansas have shown the need for timely flood inundation extent estimate information that is currently not available, and heretofore would have been cost prohibitive to produce. Recent advances in both computational capacity and geospatial applications development have created new opportunities for research and applications development for flood preparedness and response (Sagun, Bouchlaghem and Anumba 2009, Joyce et al. 2009).

In June and July of 2007, severe flooding triggered federal disaster declarations for twenty counties in southeast Kansas. Inadequate tools for relating both the real-time and predicted river stages to actual spatial flood extents hampered response efforts and led to the unintentional release of 90,000 gallons of crude oil into the Verdigris River as flood waters inundated an oil refinery in Coffeyville, Kansas (Vardi 2007) (Figure 1). It was over seven days after flood crest that ASTER and Landsat satellite imagery was acquired and available to map the inundation extent over most of the flooded area. Inherent limitations of optical remotely sensed imagery (Voigt et al. 2007) and the lack of any additional timely information led the author and colleagues to investigate the

application of the FLDPLN model (Kastens 2008), which was developed at the Kansas Biological Survey, for production of flood inundation libraries that could be accessed during flood events to produce real-time flood maps with only actual or predicted flood stage as the input variable.

In researching the wide range of alternative modeling options it was determined that the FLDPLN model offers unique features, namely simplicity of implementation and ease of adaptability for inundation library development, that could made it an economical alternative, both in terms of time an cost, to other modeling options for library development. During subsequent efforts to secure funding to develop a library of inundation extents for major streams in eastern Kansas using the FLDPLN model, two primary questions emerged: 1) is the 1/3 arc second (10 m) National Elevation Dataset (NED) adequate for inundation library development, and 2) is the FLDPLN model an appropriate tool for developing the inundation library.

Elevation data

Elevation data are an important input to flood models, and their quality and resolution influence model inundation extent estimates. Choice of terrain data is guided by concerns for data quality, availability, and computational capacity. For many areas the 1/3 arc second NED (also referred to as the 10-meter NED) is the most accurate and current dataset used for flood mapping, and this is certainly true for the state of Kansas. The source data for the NED varies (Gesch 2007), but for Kansas the two primary sources are: 1) cartographic contours and mapped hydrography, source material for which dates from 1933 through 1996, and 2) LiDAR, which presently accounts for less that 10%

of the state, although there are efforts underway to update additional areas of the state with LiDAR-derived data (Figure 2). For the foreseeable future, it is likely that additional LiDAR coverage will be achieved in piecemeal fashion through a series of *ad hoc* initiatives supported by coalitions of local, state, and federal agencies as funding becomes available. The result of this approach will be an ever changing patchwork of moderate and high quality elevation data. As such, it important to assess and communicate the accuracy and applicability of the NED for flood model applications.

A majority of the NED evaluation done to date has been performed by Dean Gesch of the United States Geological Survey (USGS). Most notably, Gesch (2007) used National Geodetic Survey GPS-over-benchmark points to show that the overall absolute vertical accuracy of the 1/3 arc second NED is 2.44 meters (RMSE), with a relative vertical accuracy of 1.64 meters, both of which are significantly better than the generally accepted, and USGS stated, accuracy of ± 7 meters. Gesch has also done work in identifying topographic changes by comparing the NED to the Shuttle Radar Topography Mission (SRTM) data (Gesch 2006). This analysis showed that SRTM data were useful for detecting major topographic changes that have occurred since the original NED data were collected, such as highway construction and quarrying activates, and for mapping tall vegetation, like forests, since SRTM data maps the top of the vegetation canopy height.

Recent work has been done on two river reaches, one in North Carolina and one in Texas, to evaluate discrepancies between modeled results for multiple elevation data sets, which included 1 arc second NED, 1/3 arc second NED, LiDAR, and integration of surveyed cross-sections with all three aforementioned data sets (Cook and Merwade

2009). Two models, HEC-RAS 4.0 and FESWMS-2DH 3.1.5, were run using all six topographic data sets. Results were evaluated to determine the effect of horizontal resolution and vertical accuracy on flood extent mapping, as well as to highlight the discrepancies between these two models at varying resolutions and vertical accuracies. In general, the flood extents mapped using the FESWMS-2DH model were smaller compared to the HEC-RAS results, and flood area tended to be reduced with greater horizontal resolution and greater vertical accuracy. There were no empirical flood data available, therefore evaluation of modeled flood extent accuracy was not possible.

Modeling for flood preparedness and response

One of the most effective ways to enhance flood preparedness and response is to model flood events. This is one of the primary activities of the National Flood Insurance Program's (NFIP) Map Modernization Program (Map Mod) (National Research Council (U.S.). Committee on FEMA Flood Maps., United States. Federal Emergency Management Agency. and United States. National Oceanic and Atmospheric Administration. 2009). The most common map product of the NFIP is known as the 100-year floodplain, commonly referred to as "the" floodplain. More accurately, it is the 1-percent-annual-chance (100-year) floodplain. Although the arbitrary area comprised by the 100-year floodplain is useful for determining flood risk, particularly for insurance purposes, it has only a 1% chance of coinciding with an actual flood event within a given year. A more useful approach for disaster response is to develop a library of inundation extents for a range of river stages that cover an expected range of events from low flow to

above-record levels (Bales and Wagner 2009). During an actual flood event, appropriate extent maps can be created based on actual and predicted river levels.

Ad hoc flood mapping has been done in Kansas with FEMA HAZUS-MH software at a local level, particularly in response to isolated flood events. KBS evaluations have shown that HAZUS modeling has a number of limitations that make it cumbersome and potentially unsuitable for inundation extent library production. These limitations include program crashes, discontinuous flood depth values, insufficient stream buffer distances, difficulty handling backwater effects, and excessive required user interaction for library development. Use of HAZUS is certainly appropriate for many applications (Scawthorn et al. 2006a, Gall, Boruff and Cutter 2007), but for large area inundation extent library development it is not suitable.

In a limited number of areas the National Weather Service has partnered with state and local cooperators to develop inundation libraries for river segments directly surrounding NWS and USGS gage locations (Merwade et al. 2008b). The library extents are limited to approximately one mile upstream and downstream from the gage location. As per NWS specifications, the development of these libraries requires the use of elevation data that will support 2-foot contours, generally LiDAR or photogrammetrically derived elevation, and the use of approved hydrodynamic flow models, such as HEC-RAS.

Sources of Uncertainty

Uncertainties involved in flood mapping exist at virtually every step of the mapping process. While this is true of all modeling, it is important to be aware of these

uncertainties, have a sense of their magnitude, and be aware of how they might affect modeled results.

Hydrologic modeling concerns estimating the timing and magnitude of stream discharge (flow) based on watershed and rainfall parameters. This component of flood modeling is subject to a number of uncertainties, primarily; 1) watershed characteristics; 2) storm precipitation dynamics, 3) infiltration, and 4) antecedent conditions (Singh 1997). Each of these parameters has associated uncertainties also. Implementation of flood extent libraries using predicted stage does rely on hydrologic models, but stage forecasts are issued by the NWS and evaluation of them is beyond the scope of this study.

Streamflow is calculated by measuring flow velocity along a stream cross section, following standard protocols, for a range of river stages and combining them with surveyed cross section information to produce an estimated flow volume, usually reported in cubic feet per second (cfs). From these data a stage discharge relationship can calculated to produce a stage discharge table for any stage. For typical conditions, streamflow value errors can range from 3% to 19%, and as high as 42% in the least favorable cases (Harmel et al. 2009).

Flood frequency is commonly used to as a tool to guide design and development decisions by examining the recorded stream flows to determine areas that are likely to flood with a specified frequency, often the 100-year flood. The most commonly used specifications for determining flood frequency are outlined in Bulletin No.17B authored by the Interagency Advisory Committee on Water Data ((IACWD) 1982), which recommends using a Log-Person Type III probability distribution (Merwade et al. 2008b). This analysis relies on historical stream flow records, and often these records

have a baseline shorter than the design storm of interest. More recent work suggests that this method needs to be updated to a hybrid approach that includes paleoflood data, when available, and also uses an iterative least squares regression in a pooled regression technique (England, Jarrett and Salas 2003, Griffis and Stedinger 2007a, Griffis and Stedinger 2007b). In addition to the uncertainty of the techniques themselves, additional factors such as selection of data series, assumptions about probability distributions, climate trends, land use changes, years where no floods have occurred, and missing data (Merwade et al. 2008b). Regional flood frequency analysis where no flow data exist relies on hydrologic models that use watershed characteristics and rainfall records to develop estimated flood frequencies. There is significant error associated with these approaches, like those used in the National Streamflow Statistics, which range from 15% to more than 100% (Ries and Atkins 2007) .

Because terrain data represent the 3-dimensional surface over which flood water pass, its quality has a direct effect on flood extent estimates. It affects hydrologic model discharge values (Brasington and Richards 1998, Valeo and Moin 2000, Hancock 2005, Kenward et al. 2000), water surface elevations derived from flood models (Marks and Bates 2000, Casas et al. 2006), and the estimated horizontal extent of flood inundation (Tate et al. 2002, Wang and Zheng 2005, Merwade, Cook and Coonrod 2008a, Merwade et al. 2008b). There is a wide range of uncertainties associated with elevation datasets, which include source data, interpolation techniques, cell resolution, data fusion, hydrologic conditioning, and others (Merwade et al. 2008b). When combined, these uncertainties and the uncertainties associated with streamflow, flood frequency, hydrologic modeling, and hydraulic models themselves point to the need to develop an

approach that integrates an uncertainty analysis into mapped flood extent estimates (Smemoe, Nelson and Zundel 2004, Crosetto, Tarantola and Saltelli 2000, Merwade et al. 2008b, Weichel, Pappenberger and Schulz 2007). Although it is beyond the scope of this study to examine each of these in detail, the affect of elevation data quality on flood extent estimation is the focal point of this study.

Elevation data and modeling

Evaluation of model performance and uncertainties is an important part of understanding the model appropriateness for practical implementation (Harmel et al. 2009). There is a range of uncertainties with any modeling approach. Mason et al. (2009) used ERS-1 synthetic aperture radar (SAR) data, acquired during a 5-year flood event in Oxford, England, fused with LiDAR elevation data and modeled flood extent from LISFLOOD-FP to evaluate the use of the height-based probability statistic versus the F statistic (Bates and De Roo 2000), a performance based measure of areal extent mapped. The height-base statistic, using an active contour model for the fused SAR/LiDAR data as the reference value, which effectively extracts elevation values at the waterline as determined by the SAR imagery, was found to offer less uncertainty in the flood map than F statistic when evaluating the LISFLOOD-FP based model. It is worth noting that SAR imagery, as opposed to optically based sensors, has the advantages of acquisition by day or night, in all weather conditions, and is able to penetrate tree canopies. This makes it an ideal reference against which to evaluate modeled flood event, and a tool to calibrate models. Although this is and interesting and

valuable approach, it requires both high accuracy elevation data, like LiDAR, and SAR imagery of a flood event to be replicable.

While there are many other flood models that are in use that have been implemented and evaluated for a variety of applications, it is beyond the scope of this study to review them all. There are two widely used models, FEMA's HAZUS-MH and USACE's HEC-RAS, that are of particular importance because they are used in a similar capacity and scope, and are used as for evaluation and comparisons in this study. The HAZUS-MH software is specifically designed for risk assessment applications for earthquakes, hurricanes, and flooding. In recent years it has become more widely used for risk assessment, preparedness, and response for flooding applications (Ding et al. 2008, Scawthorn et al. 2006b), and promises to become more widely used as the software and applications community develops (Moffatt and Laefer). Although the software offers a complex range of features and capabilities, what is known as a "level 1" analysis, which requires very little user input to delineate flood boundaries, is a common use for flood extent estimation. The HAZUS software is free and is run in conjunction with ArcGIS software.

HEC-RAS (USACE 2010) has been an industry standard floodplain determination model for a number of years, and is a widely used for FEMA floodplain delineation. Most existing FEMA 100 yr floodplains in Kansas were generated using HEC-RAS. The specific models developed for each county, usually under contract with commercial engineering firms, are available for use so that the upfront work of determining cross sections and hydrology does not need to be repeated. After the 2007 floods, URS Corporation used the HEC-RAS model to construct "flood recovery maps" for

Montgomery County, Kansas, and other counties most heavily impacted by the flood of that year. The flood recovery maps, while not being official boundaries, delineated the 100 yr floodplain for the county for all streams with catchments greater than one square mile. The prepared model was one of the URS project deliverables, so it was also readily available to produce flood extent maps for discharges other than the 100 yr flood.

FLDPLN Model

The FLDPLN model (Kastens 2008), is a static model that relies entirely on topographic data. After standard fill, flow direction, and flow accumulation procedures are applied to a DEM, this model utilizes an iterative two-step, backfill and spillover procedure that is seeded with stream pixels derived from the flow accumulation layer. In essence, each stream pixel is flooded to a specified depth, so that all upstream, connected pixels, as specified by the corresponding flow direction layer, are assigned a depth-to-flood (DTF) reflecting elevation differences between the stream pixel in question and the indentified flooded pixels. This is followed by a spillover step that addresses discontinuities created by flow divides and allows for the creation of new floodwater flow paths. These steps are repeated in small vertical step size increments to create a DTF map from which a library of inundation extents can be derived. The advantages to the using the FLDPLN model are the minimal inputs required, and an architecture that makes it ideal for inundation extent library production.

After the 2007 flood, initial investigations at KBS were aimed at using the FLDPLN model to create a mask that could be used to eliminate upland areas from image based classification approaches. The results of these investigations indicated that the

model's performance might be good enough to be used independently as a way to map inundation extents for major floods. A pilot project was conducted for stretches of the Marais des Cygnes, Little Osage, and Osage Rivers in western Missouri (Figure 3). The results showed good correspondence between flood extent predicted by the FLDPLN model, which was calibrated to USGS gage data, and actual flooding that was mapped using Landsat imagery acquired at or near flood crest during the 2007 event, with an overall map accuracy of 81.7%. The only inputs to generate the FLDPLN-modeled flood extent were the 1 arc second NED DEM (30-meter) and USGS stage data from three gauging stations for peak discharges during the flood event. These results provided the impetus to develop the flood mapping application further.

Objectives

In order to assess the needs and capabilities of current flood preparedness initiatives at KBS, this research addresses two key questions: 1) what is the utility and what are the limitations of the currently available elevation data for Kansas with regard to flood modeling, 2) what are the capabilities and limitations of the FLDPLN model for inundation estimation.

Elevation data evaluations

Chapter 2 of this study focuses on the fist study objective through evaluation of currently available NED elevation data in Douglas County, Kansas, and is performed in three steps. The first step uses high accuracy, high precision National Geodetic Survey GPS-on-benchmark (GPSBM) point elevations as a reference to evaluate the accuracy of

2 m LiDAR (LIDAR2) elevation data, and to compare its accuracy to both LiDAR-derived and pre-LiDAR NED elevation datasets. This is important for establishing the accuracy of the LiDAR-derived NED data, which are used as reference elevations in the second step, and for examining the accuracies of all of these dataset against a common reference. GPSBM, LIDAR2, and NED data are also drawn from adjacent Jefferson and Shawnee Counties to increase the sample size.

The second step establishes the accuracy of the pre-LiDAR 10 m NED (NED10) by comparing corresponding elevation values to higher accuracy LiDAR-derived 10 m NED (NED10L) values for nearly 3000 randomly selected points across Douglas County. Error summary statistics are evaluated by cover type, based on the 2005 Kansas Land Cover Patterns dataset, for urban, woodland, cropland, grassland, and overall. Error vs. elevation, slope, aspect, and local relief are also evaluated for anomalies and systematic error. Determining the NED10 accuracy for data in Kansas establishes the context for uncertainty and expectations for flood modeling, and ultimately gives decision-makers a basis understanding model results.

The third step compares modeled flood extents for the same magnitude flood with the same model using the NED10 and the NED10L as elevation data sources in two separate model runs. This comparison is performed at two flood magnitudes, the 50-year and the 100-year flood, using two difference models, HEC-RAS and the FLDPLN model, on two separate rivers, the Kansas and Wakarusa. This combination of magnitudes, models, and rivers produces eight unique comparisons showing the impact of discrepancies between the NED10 and the NED10L on modeled flood extents, which are quantified by calculating the F-static (Bates and De Roo 2000) (a measure of

correspondence between the modeled flood extents) for each case. This side-by-side comparison of modeled results for two levels of elevation data quality gives direct evidence of the discrepancies between the two sources on modeled flood extent estimates.

Flood model evaluations

Chapter 3 focuses on evaluation of FLDPLN model performance in three steps. The study area is located in Montgomery County, Kansas, on a segment of the Verdigris River that was heavily impacted during the floods of 2007. The first step compares modeled flood extents for a range of hypothetical flood levels, ranging from the 10 to 45 ft stage, in five foot increments. Flood extents are modeled using HEC-RAS, HAZUS and the FLDPLN models, and correspondence of flood extent among all three models are quantified using the F-statistic, as in Chapter 2. Correspondence statistics and trends are evaluated. Comparison of modeled results over a large range of flood magnitudes for three separate models gives insight into model behavior and potential uncertainties.

The second step evaluates HEC-RAS, HAZUS, and FLDPLN model performance using 13 high-water-mark (HWM) elevations from a post-flood field survey that was conducted shortly after the 2007 floods (FEMA 2008). Modeled water surface elevations from all three models using the Verdigris River's 169,000 cfs peak discharge value from the 2007 event are differenced from the surveyed HWMs. Error statistics are used to evaluate the model's performance. Referencing empirical flood data allows for an objective evaluation of the FLDPLN model, and, by comparing the models performance

with two other models, shows where it falls relative to other commonly used flood extent estimators.

The third step uses manually digitized flood shoreline points derived from ASTER satellite imagery (n= 200) and 1-foot aerial imagery (n=260) captured over the study area within a week after the 2007 flood crest. Each set of imagery-derived points evaluated against modeled flood surface elevations for each model by differencing the NED10 elevation value corresponding to the point's location from the NED10 elevation value of the closest modeled flood boundary to which each point has been "snapped," or moved, using Hawth's Tools "snap to line" feature. Error statistics are used to evaluate each model's performance.

As whole, this study establishes a basis for future development of the FLPLN model by addressing questions that were posed during efforts to seek funding to support development of a segmented library of inundation extents (SLIE) for eastern Kansas. The SLIE has now been developed for 40 counties in eastern Kansas, with the intent to eventually have statewide coverage (http://www.kars.ku.edu/maps/depthtoflood/). These study results will be an important resource for communicating expectations and uncertainties to future users of the data. Beyond applications for emergency response, the model is also being adapted for several ecological applications and as a tool for reservoir site suitability determination. The results from this study will be an important reference for this research as well.

References Cited

(IACWD), I. A. C. o. W. D. 1982. Guidelines for determining flood flow frequency. In *Bulletin 17B of the Hydrology Subcommittee*.

Bales, J. D. & C. R. Wagner (2009) Sources of uncertainty in flood inundation maps. *Journal of Flood Risk Management,* 2**,** 139-147.

Bates, P. D. & A. P. J. De Roo (2000) A simple raster-based model for flood inundation simulation. *Journal of Hydrology,* 236**,** 54-77.

Brasington, J. & K. Richards (1998) Interactions between model predictions, parameters and DTM scales for TOPMODEL. *Computers & Geosciences,* 24**,** 299-314.

Casas, A., G. Benito, V. R. Thorndycraft & M. Rico (2006) The topographic data source of digital terrain models as a key element in the accuracy of hydraulic flood modelling. *Earth Surface Processes and Landforms,* 31**,** 444-456.

Cook, A. & V. Merwade (2009) Effect of topographic data, geometric configuration and modeling approach on flood inundation mapping. *Journal of Hydrology,* 377**,** 131-142.

Crosetto, M., S. Tarantola & A. Saltelli (2000) Sensitivity and uncertainty analysis in spatial modelling based on GIS. *Agriculture, Ecosystems & Environment,* 81**,** 71-79.

Ding, A., J. F. White, P. W. Ullman & A. O. Fashokun (2008) Evaluation of HAZUS-MH Flood Model with Local Data and Other Program. *Natural Hazards Review,* 9**,** 20-28.

England, J. F., R. D. Jarrett & J. D. Salas (2003) Data-based comparisons of moments estimators using historical and paleoflood data. *Journal of Hydrology,* 278**,** 172-196.

FEMA. 2008. Base Flood Elevation Determination, Mongomery County, Kansas. Wahshington, DC.

Gall, M., B. J. Boruff & S. L. Cutter (2007) Assessing Flood Hazard Zones in the Absence of Digital Floodplain Maps: Comparison of Alternative Approaches. *Natural Hazards Review,* 8**,** 1-12.

Gesch, D. B. 2006. An inventory and assessment of significant topographic changes in the United States. xvii, 217 leaves. Geography Dept., South Dakota State University, 2006.

---. 2007. Chapter 4 – The National Elevation Dataset. In *Digital Elevation Model Technologies and Applications: The DEM Users Manual,* ed. D. Maune, 99-118. Bethesda, Maryland: American Society for Photogrammetry and Remote Sensing.

Griffis, V. W. & J. R. Stedinger (2007a) The use of GLS regression in regional hydrologic analyses. *Journal of Hydrology,* 344**,** 82-95.

--- (2007b) Evolution of Flood Frequency Analysis with Bulletin 17. *Journal of Hydrologic Engineering,* 12**,** 283-297.

Hancock, G. R. (2005) The use of digital elevation models in the identification and characterization of catchments over different grid scales. *Hydrological Processes,* 19**,** 1727-1749.

Harmel, R. D., D. R. Smith, K. W. King & R. M. Slade (2009) Estimating storm discharge and water quality data uncertainty: A software tool for monitoring and modeling applications. *Environmental Modeling & Software,* 24**,** 832-842.

Joyce, K. E., S. E. Belliss, S. V. Samsonov, S. J. McNeill & P. J. Glassey (2009) A review of the status of satellite remote sensing and image processing techniques for mapping natural hazards and disasters. *Progress in Physical Geography,* 33**,** 183-207.

Kastens, J. H. 2008. Some New Devolopments On Two Separate Topoics: Statistical Cross Validation and Floodplain Mapping. In *Mathematics*, 191. Lawrence: The University of Kansas.

Kenward, T., D. P. Lettenmaier, E. F. Wood & E. Fielding (2000) Effects of Digital Elevation Model Accuracy on Hydrologic Predictions. *Remote Sensing of Environment,* 74**,** 432-444.

Mansourian, A., A. Rajabifard, M. J. Valadan Zoej & I. Williamson (2006) Using SDI and web-based system to facilitate disaster management. *Computers & Geosciences,* 32**,** 303-315.

Marks, K. & P. Bates (2000) Integration of high-resolution topographic data with floodplain flow models. *Hydrological Processes,* 14**,** 2109-2122.

Merwade, V., A. Cook & J. Coonrod (2008a) GIS techniques for creating river terrain models for hydrodynamic modeling and flood inundation mapping. *Environmental Modelling & Software,* 23**,** 1300-1311.

Merwade, V., F. Olivera, M. Arabi & S. Edleman (2008b) Uncertainty in Flood Inundation Mapping: Current Issues and Future Directions. *Journal of Hydrologic Engineering,* 13**,** 608-620.

Moffatt, S. & D. Laefer An Open-Source Vision for HAZUS. *Journal of Computing in Civil Engineering,* 24**,** 1-2.

National Research Council (U.S.). Committee on FEMA Flood Maps., United States. Federal Emergency Management Agency. & United States. National Oceanic and Atmospheric Administration. 2009. *Mapping the zone : improving flood map accuracy*. Washington, D.C.: National Academies Press.

Ries, K. G. & J. B. Atkins. 2007. *The National streamflow statistics program : a computer program for estimating streamflow statistics for ungaged sites*. Reston, Va.: U.S. Department of the Interior, U.S. Geological Survey.

Sagun, A., D. Bouchlaghem & C. J. Anumba (2009) A scenario-based study on information flow and collaboration patterns in disaster management. *Disasters,* 33**,** 214-238.

Scawthorn, C., N. Blais, H. Seligson, E. Tate, E. Mifflin, W. Thomas, J. Murphy & C. Jones (2006a) HAZUS-MH Flood Loss Estimation Methodology. I: Overview and Flood Hazard Characterization. *Natural Hazards Review,* 7**,** 60-71.

Scawthorn, C., P. Flores, N. Blais, H. Seligson, E. Tate, S. Chang, E. Mifflin, W. Thomas, J. Murphy, C. Jones & M. Lawrence (2006b) HAZUS-MH Flood Loss Estimation Methodology. II. Damage and Loss Assessment. *Natural Hazards Review,* 7**,** 72-81.

Singh, V. P. (1997) Effect of spatial and temporal variability in rainfall and watershed characteristics on stream flow hydrograph. *Hydrological Processes,* 11**,** 1649-1669.

Smemoe, C., J. Nelson & A. Zundel. 2004. Risk Analysis Using Spatial Data in Flood Damage Reduction Studies. 262-262. Salt Lake City, Utah, USA: ASCE.

Tate, E. C., D. R. Maidment, F. Olivera & D. J. Anderson (2002) Creating a Terrain Model for Floodplain Mapping. *Journal of Hydrologic Engineering,* 7**,** 100-108.
USACE. 2010. HEC-RAS.
Valeo, C. & S. M. A. Moin (2000) Variable source area modelling in urbanizing watersheds. *Journal of Hydrology,* 228**,** 68-81.
Vardi, N. (2007) Slick. *Forbes,* 180**,** 50-50.
Voigt, S., T. Kemper, T. Riedlinger, R. Kiefi, K. Scholte & H. Mehi (2007) Satellite Image Analysis for Disaster and Crisis-Management Support. *IEEE Transactions on Geoscience & Remote Sensing,* 45**,** 1520-1528.
Wang, Y. & T. Zheng (2005) Comparison of Light Detection and Ranging and National Elevation Dataset Digital Elevation Model on Floodplains of North Carolina. *Natural Hazards Review,* 6**,** 34-40.
Weichel, T., F. Pappenberger & K. Schulz (2007) Sensitivity and uncertainty in flood inundation modelling; concept of an analysis framework. *Advances in Geosciences,* 11**,** 31-36.

Figures

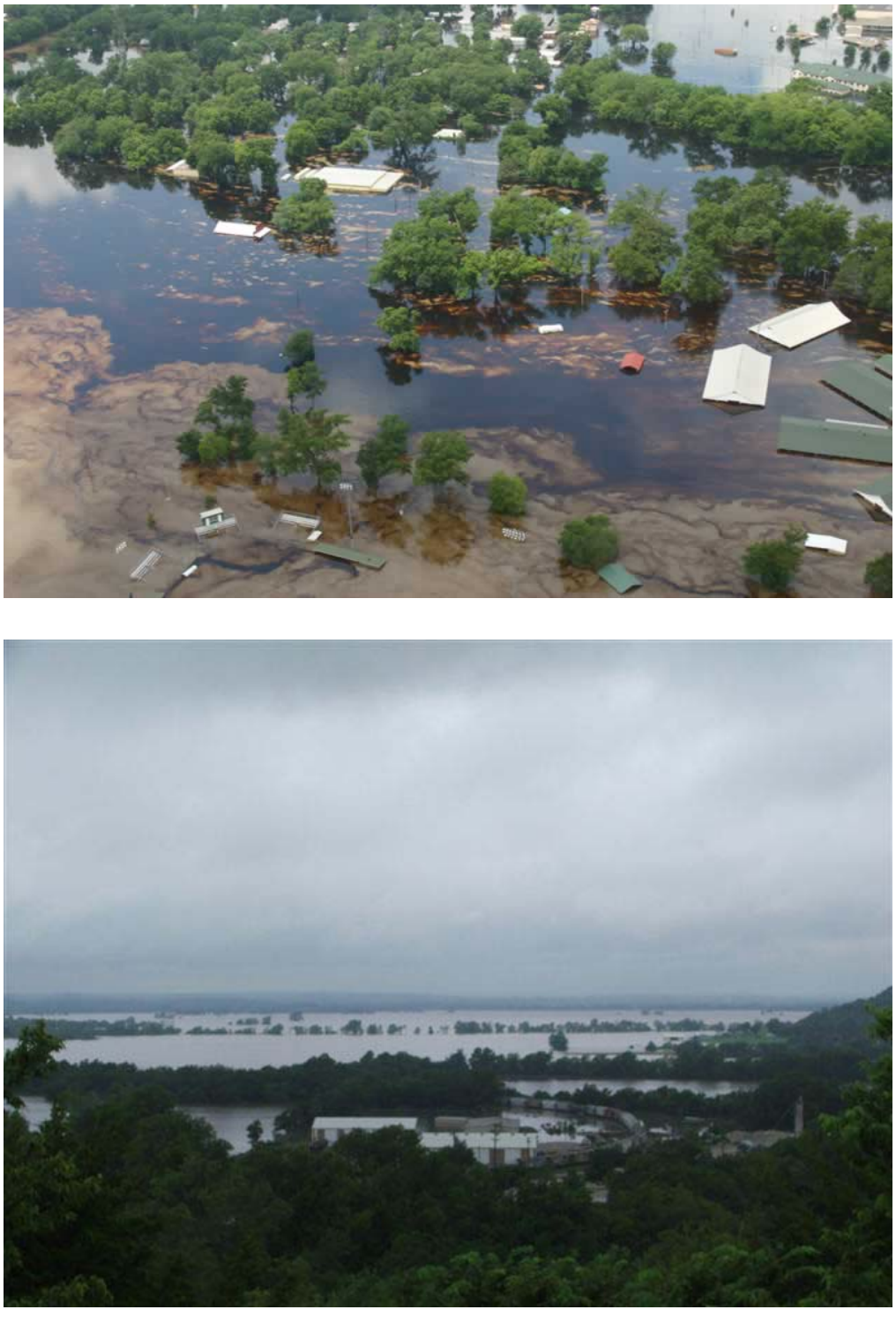

Figure 1-1. Aerial photographs taken during the peak flooding in Montgomery County in July of 2007. The top two photos show oil release from a refinery in Coffeyville, which flowed south in the Verdigris River into Oklahoma. (www.kansasgis.org)

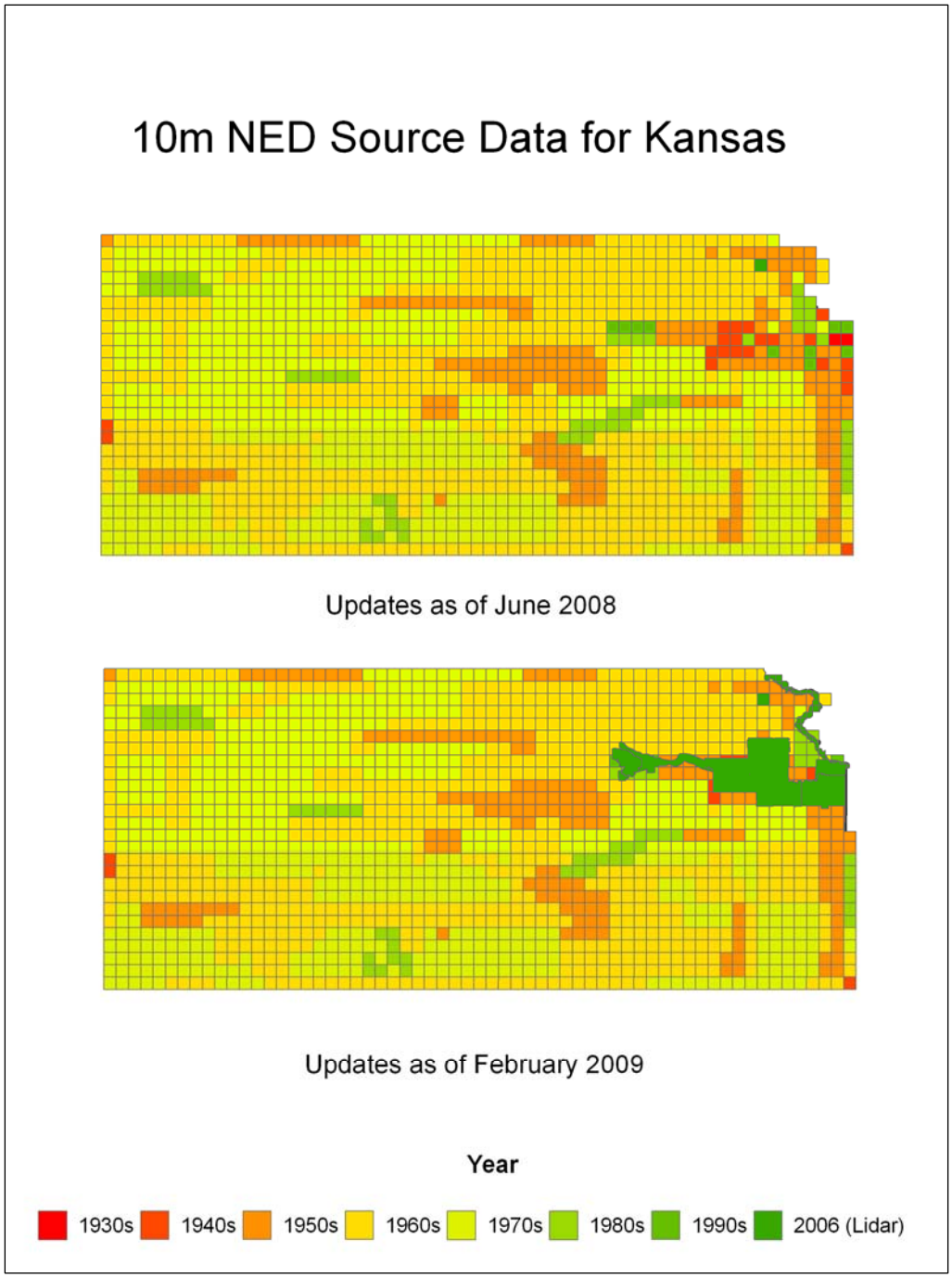

Figure 1-2. Kansas National Elevation Dataset (NED) source data dates, grouped by decade. In 2006 a consortium of stakeholders at the state and local level coordinated LiDAR data acquisition along the Kansas River corridor. These higher resolution and higher precision data were eventually incorporated into the NED.

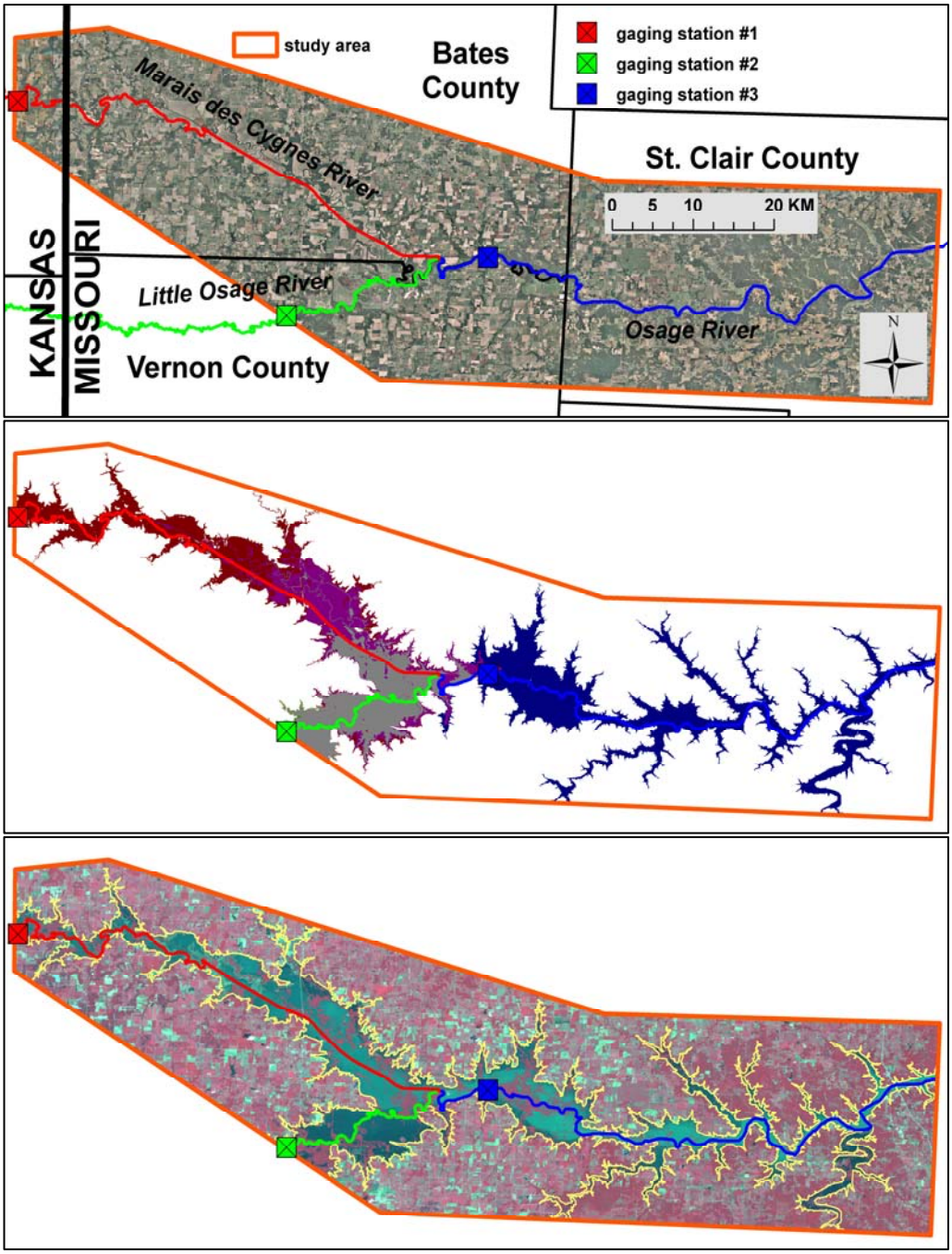

Figure 1-3. Pilot study area along the Marais des Cygnes, Little Osage, and Osage Rivers in Missouri. Floods crested in early July, several days before acquisition of the above Landsat 5 scene, which can be seen in the bottom graphic. Peak stage values were used from three USGS gaging stations as inputs to the FLDPLN model. The combined flood extent estimate for the three river segments, shown in red, blue, and green, is shown in the middle graphic. The yellow boundary in the bottom graphic corresponds to the model estimated flood extent. The estimated extent had an accuracy of 81.7%.

CHAPTER 2

QUALITY ASSESSMENT AND EVALUATION OF THE USGS NATONAL ELEVATION DATASET (NED) FOR FLOOD MODELING APPLICATIONS

Abstract

While riverine flooding is a natural and ecologically beneficial phenomenon, severe flood events continue to result in loss of life and property. Major flood events affecting Kansas in 2007 and Iowa in 2008 exposed the lack of timely, accurate information needed during major flood emergencies. Current initiatives at the Kansas Biological Survey aim to bridge the gap between the limited information that is presently available and what is needed to effectively respond to the next disaster. The focus of this effort is the development of a library of modeled flood inundation extents for major streams across the state that can be accessed in near real-time to provide valuable information to disaster responders. Modeling floods is an effective way to improve preparedness and to more expeditiously and effectively respond to widespread flood events, particularly if real-time and predicted flood extent maps can be integrate with critical infrastructure and population information in a GIS environment. Flood models often rely on elevation data with undocumented uncertainties. This study examines the USGS National Elevation Dataset (NED) and evaluates the effects of errors in the elevation data on flood inundation extent estimation. By comparing NED datasets to survey and LiDAR derived data, a measure of error is associated with the data that can be used to communicate uncertainties and improve decision-making. In addition, HAZUS and FLDPLN flood models are used to highlight the variability in mapped flood extent between model runs using LiDAR-derived NED data and pre-LiDAR NED data.

Terms and Abbreviations

[**GPSBM**] National Geodetic Survey GPS-on-benchmark control points

[FEMA] Federal Emergency Management Agency

[**FLDPLN**] FLDPLN model used to derive a library of inundation extents

[**HAZUS**] FEMA HAZUS-MH flood, earthquake and hurricane model

[**KLCP 05**] 2005 Kansas Land Cover Patterns, Level 1

[**NED3L**]1/9 arcsecond (~3 m) NED data derived from the 2m LiDAR data by the USGS

[**NED10**] 1/3 arc second (~ 10 m) NED elevation data **not** updated with the LiDAR data

[**NED10L**]1/3 arc second NED (~ 10 m) elevation data updated with 2006 LiDAR data

[NED30] 1/3 arc second NED (~30 m) elevation data **not** updated with LiDAR data

[NED30L] 1 arc second NED (~30 m) elevation data updated with 2006 LiDAR data

[NFIP] National Flood Insurance Program

[LIDAR2] 2m horizontal resolution LiDAR data for Douglas County, Kansas

Units and measures

Stream discharge (flow): given in cubic feet per second (cfs), discharge is a measure of the volume of water flowing though a vertical plane oriented perpendicular to the direction of stream flow. Often referred to as a measured quantity, it is actually

calculated from a set of measured velocities along a stream channel cross section. When calculated for a range of river levels and combined with an adequate historical baseline of stage data (see below), discharge can be plotted on a logarithmic scale to develop a flood frequency regression equation to estimate the return period of a given magnitude flood event.

River stage: a measured quantity that relates the water surface elevation at a monitored point on a stream (e.g. at a stream gage) to an arbitrary reference datum with a known elevation. The reference datum is usually chosen to be below the streambed to avoid negative stage values. With datum and stage information, the water surface elevation at the gage location can be determined for any given stage.

Depth to flood (DTF): the output of the FLDPLN model developed by Kastens (2008) relating the minimum flood depth required to inundate a non-stream pixel from a reference stream pixel. In some circumstances the DTF can be used as a proxy for stage.

Flood frequency: Refers to a flood level that has a specified percent chance of being equaled or exceeded in any given year. For example, a 100-year flood theoretically occurs **on average** once every 100 years and thus has a 1-percent chance of occurring in a given year.

http://ks.water.usgs.gov/waterwatch/flood/definition.html

Introduction

In the summer of 2007 persistent and intense rainfall caused extensive, record flooding over a twenty-county area of southeast Kansas (Vardi 2007) (Figure 2-1). The flooding was so extensive and widespread that emergency management personnel were challenged by their inability to produce even crude maps of estimated flood extents over such a large area. In the days and weeks following flood crest, a variety of *ad hoc* methods were used by various local, state, and federal disaster response support personnel, including post-flood satellite image classification, to produce a number of geospatial flood extent estimates to use for response and recovery coordination and planning. The flood extent layers produced were a patchwork of incomplete, often inaccurate, and sometimes conflicting information. This event prompted the author and colleagues at the Kansas Biological Survey (KBS) to explore the development of more effective geospatial tools and datasets that could be used during future disaster response efforts.

As the utility of GIS for coordination of disaster response and facilitation situational awareness is increasingly recognized (Schmitt et al. 2007), developing supporting datasets that complement existing information and decision support tools is more valued (Mansourian et al. 2006). Indeed, this complex environment of disaster preparedness and response drives both application and data development. Recent advances in both computational capacity and geospatial applications development have created new opportunities for research and application development for flood preparedness and response (Sagun et al. 2009).

However, because much of this data and application development is new in terms of approach, scale, and implementation, there is often trepidation by funding agencies regarding commitment of limited resources to novel techniques. One such novel technique under development at KBS is the FLDPLN model (Kastens 2008), which can be used for production of flood inundation libraries that can be accessed during flood events to produce real-time flood extent estimates using only river stage as an input. (A library consists of a set of GIS layers for each stream segment that relates stream stage to a "depth to flood" (DTF) value that can be used to map estimated flood extent for a given stage.)

A pilot project was conducted for stretches of the Marais des Cygnes, Little Osage, and Osage Rivers in western Missouri. The results showed good correspondence between flood extent predicted by the FLDPLN model, which was calibrated to USGS gage data, and actual flooding that was mapped using Landsat imagery acquired at or near flood crest during the 2007 event, with an overall accuracy of 81.7%. The only inputs required to generate the FLDPLN-modeled flood extent were the 1 arc second NED DEM (30-meter) and USGS stage crest data corresponding to the 2007 flood event for three gaging stations. The reference flood extent was digitized from the Landsat imagery by the author. To avoid any confirmation bias, the author did not have access to the model results until after the digitization was completed. These results provided the impetus to further develop the flood mapping application.

During subsequent efforts to secure funding to develop a library of inundation extents for major streams in eastern Kansas using the FLDPLN model, two primary questions emerged: 1) is the 1/3 arc second (10m) National Elevation Dataset (NED)

adequate for inundation library development, which is addressed in this study, and 2) is the FLDPLN model an appropriate tool for developing the inundation library, which is addressed in a separate study.

Value of Flood Mapping for Preparedness and Response

Flood extent layers are far more than simple visual aids used to produce maps that aid emergency management personnel. When combined with existing geospatial information such as roads, population, built structures, property values, critical infrastructure, and hazardous materials in a GIS environment, they can identify structures and population at, help route supplies and personnel, aid decision making on where to preposition temporary shelters, give early estimates of likely flood losses, and more (Zerger and Wealands 2004). However, due to the computationally and labor intensive nature of flood inundation extent mapping, the appropriate time to develop flood inundation layers is long *before* they are needed.

Existing Flood Mapping Resources

The Federal Emergency Management Agency's (FEMA) National Flood insurance Program (NFIP) sponsors the creation of flood insurance rate maps (FIRMS) that identify zones of flood risk based on expected flood frequency. These are used to administer a federally secured flood insurance program in participating communities (FEMA 2003). Flood zones are used by communities to guide development and limit construction of structures in areas at greatest risk of flooding. Areas designated as "Zone A" have, based in USGS regression equations for stream flow, a ≥1% annual chance of

inundation, and thus represent the theoretical 100-year floodplain, and. Areas of outside of Zone A have, theoretically, <1% annual chance of flooding, and lower elevation areas within the 100-year floodplain generally have >1% of flooding. But from a disaster response perspective, the only flood boundary that is important is the one corresponding to the event at hand, which may be a 5000-year event or a 50-year event, or possibly even a wide range of flood frequency events on multiple streams over multiple watersheds. Consequently, the "Zone A" boundaries have limited utility for disaster response.

With the rise in LiDAR data availability, the National Weather Service (NWS) has begun a program to develop libraries of inundation extents for select sites around the county (NWS 2010). The specifications for this program require elevation data that are capable of supporting development of 2-foot contours, and most LiDAR-derived elevation data are produced to meet this specification. These extent libraries are usually limited to stream segments within one to two miles of USGS or NWS stream gages. For areas that are mapped, this is a valuable response and planning tool, but the covered area represents only a small fraction of the total flood-prone stream miles across the country. Although no sites have been mapped in Kansas, there are only about 13 sites that meet the stringent NWS criteria for supporting data and site criticality, which if mapped would be approximately 26 to 52 stream miles out of thousands across the state.

Sources of uncertainty

Uncertainties involved in flood mapping exist at virtually every step of the mapping process. While this is true of most general modeling applications, it is

important to be aware of these uncertainties, have a sense of their magnitude, and be aware of how they might affect modeled results.

Hydrologic modeling estimates the timing and magnitude of stream discharge (flow rate) based on watershed and rainfall parameters. This component of flood modeling is subject to a number of uncertainties, including assumptions about 1) watershed characteristics; 2) storm precipitation dynamics, 3) infiltration, and 4) antecedent conditions (Singh 1997). Each of these parameters has associated uncertainties, also. Implementation of flood extent libraries using predicted stage does rely on hydrologic models, but stage forecasts are issued by the NWS and evaluation of them is beyond the scope of this study.

Streamflow is calculated by measuring flow velocity at a number of points along a stream cross section, following standard protocols, for a range of river stages and combining them with surveyed cross section information to produce an estimated flow volume, usually reported in cubic feet per second (cfs). From these data a stage-discharge relationship can be modeled to produce a general stage-discharge lookup table for any stage. For typical conditions, streamflow value errors can range from 3% to 19%, and as high as 42% in the least favorable cases (Harmel et al. 2009).

Flood frequency is commonly used as a tool to guide design and development decisions by examining historical stream flows to determine areas that are likely to flood with a specified minimum frequency, often the 100-year flood. The most commonly used specifications for determining flood frequency are outlined in Bulletin No.17B authored by the Interagency Advisory Committee on Water Data ((IACWD) 1982), which recommends using a Log-Pearson Type III probability distribution (Merwade et al.

2008b). This analysis relies on historical stream flow records, and often these records have a baseline shorter than the average recurrence interval for the design storm of interest. More recent work suggests that this method needs to be updated to a hybrid approach that includes paleoflood data, when available, and also uses an iterative least squares regression in a pooled regression technique (England et al. 2003, Griffis and Stedinger 2007a, Griffis and Stedinger 2007b). In addition to the uncertainty of these techniques themselves, other factors contributing to modeling errors include selection of data series, assumptions about probability distributions, climate trends, land use changes, years where no floods have occurred, and missing data must be considered (Merwade et al. 2008b). Regional flood frequency analysis where no flow data exist relies on hydrologic models that use watershed characteristics and rainfall records to develop estimated flood frequencies. There is significant error associated with these approaches, like those used in the National Streamflow Statistics, which range from 15% to more than 100% (Ries and Atkins 2007).

Because terrain data represent the 3-dimensional surface over which flood waters flow, terrain data quality has a direct affect on flood extent estimates. It affects hydrologic model discharge values (Brasington and Richards 1998, Valeo and Moin 2000, Hancock 2005, Kenward et al. 2000), water surface elevations derived from flood models (Marks and Bates 2000, Casas et al. 2006), and the estimated horizontal extent of flood inundation (Tate et al. 2002, Wang and Zheng 2005, Merwade et al. 2008a, Merwade et al. 2008b). There is a wide range of uncertainties associated with elevation datasets, such as those pertaining to source data, interpolation techniques, cell resolution, data fusion, hydrologic conditioning, and others (Merwade et al. 2008b). The potential

cumulative influence of these uncertainties and the uncertainties associated with streamflow, flood frequency, hydrologic modeling, and hydraulic modeling point to the need to develop an approach that integrates an uncertainty analysis into mapped flood extent estimates (Smemoe et al. 2004, Crosetto et al. 2000, Merwade et al. 2008b, Weichel et al. 2007). Although it is beyond the scope of this study to examine each of these in detail, the affect of elevation data quality on flood extent estimation is the focal point.

Available Elevation Data

This study focuses specifically on evaluation of the National Elevation Dataset data. The 1/3 arc second NED (also referred to as the 10-meter NED) is the most accurate and current dataset used for flood mapping that is freely available for the entire state of Kansas. The source data for the NED vary (Gesch 2007), but for Kansas the two primary sources are: 1) cartographic contours and mapped hydrography, source material for which dates from 1933 through 1996 (Figure 2-2), and 2) LiDAR, which presently accounts for less that 10% of the state, although there are efforts underway to update additional areas of the state with LiDAR-derived data (Figure 2-3). For the foreseeable future, it is likely that additional LiDAR coverage will be achieved in piecemeal fashion through a series of *ad hoc* initiatives supported by coalitions of local, state, and federal agencies as funding becomes available. The result of this approach will be an ever changing patchwork of moderate and high quality elevation data. Therefore it is important to assess and communicate the accuracy and applicability of the NED for flood model applications.

Objective

This study addresses the following questions: what is the utility and what are the limitations of the currently available elevation data for Kansas with regard to flood modeling.

Previous work

The most significant NED evaluation done to date has been performed by Dean Gesch of the United States Geological Survey (USGS). Most notably, Gesch (2007) used National Geodetic Survey GPS on benchmark points to show that the overall absolute vertical accuracy of the 1/3 arc second NED is 2.44 meters (RMSE), with a relative vertical accuracy of 1.64 meters, both of which are significantly better than the often quoted, and USGS stated, accuracy of ± 7 meters (USGS 2010). Gesch has also done work in identifying topographic changes by comparing the NED to the Shuttle Radar Topography Mission (SRTM) data (Gesch 2006).

Recent work specifically related to the variability of model outputs using different terrain source data has been done on two river reaches, one in North Carolina and one in Texas (Cook and Merwade 2009). The authors evaluated discrepancies between modeled results for multiple elevation data sets, which include 1 arc second NED, 1/3 arc second NED, LiDAR, and integration of surveyed cross-sections with all three aforementioned data set. Two models, HEC-RAS 4.0 and FESWMS-2DH 3.1.5, were run using all six topographic data sets. Results were evaluated to determine the effect of horizontal resolution and vertical accuracy on flood extent mapping, as well as highlight the

discrepancies between these two models at varying resolutions and vertical accuracies. In general, the flood extents mapped using the FESWMS-2DH model were smaller compared to the HEC-RAS results, and flood area tended to shrink with finer horizontal resolution and greater vertical accuracy. There were no empirical flood data available, therefore evaluation of modeled flood extent accuracy was not possible.

Mason et al. (2009) used ERS-1 synthetic aperture radar (SAR) data, acquired during a 5-year (i.e. 20% chance per year) flood event in Oxford, England, fused with LiDAR elevation data and modeled flood extent of the LISFLOOD-FP to evaluate the use of the height-based probability statistic versus the F-statistic (Bates and De Roo 2000), a performance-based measure of areal extent mapped. The height-based statistic, using an active contour model for the fused SAR/LiDAR data as the reference value, which effectively extracts elevation values at the waterline as determined by the SAR imagery, was found to offer less uncertainty in the flood map than the F-statistic when evaluating the LISFLOOD-FP model. It is worth noting that SAR imagery, as opposed to imagery from optically based sensors, has the advantages of acquisition by day or night, in all weather conditions, and is able to penetrate tree canopies. This makes it an ideal reference against which to evaluate modeled flood event, and a tool to calibrate models. Although this is an interesting and valuable approach, it requires both high accuracy elevation data and SAR imagery during a flood event.

FLDPLN Model

Kastens (2008) developed the FLDPLN model, a static model that relies entirely on topographic data. After standard fill, flow direction, and flow accumulation

procedures are applied to a DEM, this model utilizes an iterative two-step, backfill and spillover procedure that is seeded with stream pixels derived from the flow accumulation layer. In essence, each stream pixel is flooded to a specified depth (iteration * step size), so that all upstream, connected pixels, as specified by the corresponding flow direction layer, are assigned a depth-to-flood (DTF) reflecting elevation differences between the stream pixel in question and the indentified flooded pixels. This is followed by a spillover step that address discontinuities created by flow divides and allows for the creation of new floodwater flow paths. These steps are repeated in small vertical step size increments to create a DTF map from which a library of inundation extents can be derived.

Study Area and Data

Douglas County, Kansas was selected for the study area because appropriate elevation data were available to perform the NED elevation data analysis. The primary data requirements for this analysis were the availability of 1/3 arc second NED data (the source data for which is *not* LiDAR data (NED10)) 2 m LiDAR data (LIDAR2) with vertical accuracy significantly greater than the NED10 data, and 1/3 arc second NED data derived from the LIDAR2 data (Figure 2-4).

High accuracy, high precision reference elevation points within the study area were needed to evaluate the accuracy of the elevation datasets against a common reference. Because the primary study area, Douglas County, has only five National Geodetic Survey (NGS) GPS-on-benchmark points (GPSBMs), GPSBMs in Shawnee and Jefferson Counties were also incorporated into the analysis, yielding a total of 15

points (Figure 2-5). All three counties are completely covered by the 2006 LiDAR acquisition. Although a larger number of reference points would be desirable, it was beyond the scope of this project to conduct additional field surveys.

The Kansas and Wakarusa Rivers, which cross the county from west to east and respectively frame the city of Lawrence to the north and south, respectively, fall in the range of moderate to large streams that are subject to slow-rise riverine flooding, which is the focus of flood extent libraries under development at KBS. This combination of data availability and representative streams makes this area appropriate for evaluation of the NED for flood modeling (Figure 2-6).

Methods

The utility and limitations of the currently available elevation data for Kansas with regard to flood modeling were assessed through the following tasks:

1) Assess the quality of existing LiDAR-derived datasets within the study area,
2) Assess the quality of the NED10 dataset, using the NED10L as the reference,
3) Evaluate the impact of data quality on modeled flood extents.

The procedures used to perform each of these tasks are outlined below

Accuracy assessment using GPSBMs

Accuracy assessment of elevation data relies on the use of reference elevation data of higher accuracy (NDEP 2004). Although the existing LiDAR data for Kansas were produced to meet FEMA specifications, independent evaluation of these data was conducted for this study. The GPSBMs, which are high precision reference points used

to compute the geoid, served as a best available common measure of accuracy for all of the other elevation data sets that were evaluated, with vertical accuracy of ± 2.4 cm at the 95% confidence (Roman et al. 2009). The 2009 GPSBMs for the continental US were downloaded from the NGS website (NGS 2010) in an Excel spreadsheet and imported into an ESRI shapefile. Points outside of Douglas, Jefferson, and Shawnee Counties were removed, leaving 15 points within the study area (Figure 2-5).

In 2006, a LiDAR acquisition campaign that was funded by a consortium of local, state, and federal stakeholders was conducted along the Kansas River corridor, extending from Johnson and Wyandotte Counties on the eastern border of Kansas toward the west approximately 120 miles to Riley County (Figure 2-3). LiDAR data for five counties and several additional adjacent, contiguous areas were collected. Of the suite of project data deliverables, in this study the bare-earth 2-meter horizontal resolution DEM (LIDAR2) was downloaded from the State of Kansas Data Access and Support Center (www.kanssgis.org) for evaluation. The published accuracy of the LIDAR2 data, extracted from the metadata, follows:

> *"Logical Consistency Report:* This dataset was compiled to meet FEMA specifications. The collection specifications are this - 1.4 meter average point spacing, Vertical Bare earth 18.5 cm RMS @ 95% confidence, 15 cm RMS @ 90% confidence, Vertical in Vegetation 37 cm RMS @ 95% confidence. Horizontal 1 meter RMS @ 95% confidence. Uses automated and manual filtering for LIDAR products with the following minimum performance for bare earth models - 90% of artifacts or more removed depending on terrain and

vegetation; 95% of outliers removed; 95% of all vegetation removed; 98% of all buildings removed."

As part of the USGS ongoing effort to update the NED with the most current, best available data, the LIDAR2 data have been resampled and used to update the NED 1/9 arcsecond (NED3L), 1/3 arcsecond (NED10L), and the 1 arcsecond (NED30L) elevation data (ned.usgs.gov)(Gesch 2007). The NED10 and NED30 were also evaluated using the GPSBMs (described below). In addition to the LiDAR derived NED data, pre-LiDAR 1/3 arcsecond and 1 arcsecond NED data (NED10 and NED30, respectively) for the study were also evaluated. All NED datasets were downloaded from the USGS Seamless Data Distribution System (seamless.usgs.gov/).

For each elevation dataset (2mL, NED3L, NED10L, NED30L, NED10, and NED30), values for DEM cells corresponding to the GPSBM locations were extracted using Hawth's Tools (www.spatialecology.com/) in ArcGIS (Table 2-1). The extracted values were differenced from the reference GPSBM point vales to determine individual errors (Table 2-2) and calculate summary statistics for each elevation dataset (Table 2-3). High resolution aerial imagery from multiple dates, including USGS DOQQ (1m), USDA FSA NAIP (1-2m), and Douglas County (6in) imagery (www.kansasgis.org) were used to evaluate each location to determine if there was cause for point rejection.

Horizontal positional accuracy assessment of DEMs is inherently difficult due to the lack of distinct, identifiable topographic features in the landscape (NDEP 2004). Inaccuracies in horizontal positioning can affect the vertical accuracies, which are exacerbated in high slope areas. Horizontal accuracy assessments were beyond the scope

of this project and were not performed. However, throughout this study the assumption was made that no significant horizontal inaccuracies exist in the data.

NED10 accuracy assessment

Although approximately 10% of Kansas has high-quality LiDAR elevation data (Figure 2-3) that has been or will soon be integrated into the NED10L (with additional projects in the planning phase), it is likely that the existing NED10 data will be the best available data for flood modeling applications for years to come for many parts of the state. For this reason it is important to have an understanding of the both the accuracy of the data and corresponding implications for flood modeling applications beyond the FEMA NFIP.

Because the NED10L values served as the reference for evaluation of the NED10 in this study, the number of reference samples was not limited by budget or time for collection, as is often the case with accuracy assessments that use surveyed point data. Therefore, a simple random sampling approach was used to leverage the abundance of reference data in the NED10L to yield a robust assessment of the NED10 accuracy. A set of 3000 random points was generated covering the study area (Figure 2-7). This approach yielded sample sizes for each land cover type that were proportional to their representation in the Kansas Land Cover Patterns 2005 (KLCP05) data. After masking out points that fell outside of Douglas County (n = 231) and removing points that fell on areas classified as water (n = 109), which were removed because water surface elevation are not considered static features), a total of 2660 points remained for the accuracy assessment.

Separate accuracy assessments were conducted for five different land use and land cover classes: 1) urban, which is an aggregate of the five level-2 urban classes in the KLCP05 (n = 163), 2) cropland (n = 597), 3) grassland (n = 1282), 4) woodland (n = 557), and 5) an overall assessment that includes the Conservation Reserve Program grasslands (n = 51) and the "other" (n = 7) classes, for a total of 2660 points, with summary statistics reported in Table 2-4. FEMA specifications for LiDAR data accuracy assessment call for evaluation of at least 20 points in each of three major landcover classes, totaling no less than 60 points. Clearly, the number of samples is sufficient to meet this quality assessment standard.

Errors as a function of terrain condition were also examined by plotting the error for each sample point against elevation, aspect, slope, and local relief (Gesch 2007). For these analyses, elevation, slope, aspect, and local relief (range of DEM cell values within 90m radius of each sample point) were taken or derived from the NED10L data using standard ArcGIS geoprocessing tools. A visual inspection of the error plots was performed in an attempt to identify systematic errors.

Model flood extent comparison for 50 yr and 100 yr discharge

To evaluate and quantify the impact that discrepancies between the NED10 and NED10L have on flood extent estimation, HAZUS (described below) and FLDPLN analyses (Kastens 2008) were conducted and compared for the 50 and 100 year discharges for segments of the Wakarusa River and the Kansas River in Douglas County (Figure 2-6). These discharges were selected because they represent major floods within the range that would require coordinated response by state emergency managers and are

commonly referenced magnitudes. Each river segment was compared for modeled flood extent of corresponding discharges for each model between the NED10 and NED10L.

The HAZUS modeling was conducted first so that the 50 and 100 yr discharges determined by the HAZUS hydrologic analysis could be used to determine the comparable DTF values needed for the FLDPLN analysis. The HAZUS-MH software comes with all data required to perform a level 1 analysis, except for the DEM data that are supplied by the user (NED10 and NED10L for this study). A HAZUS level 1 analysis is performed with minimal user inputs, and proceeds as follows:

1) the study region is defined
2) the user supplies DEM data for the study area
3) the minimum catchment area is defined by the user (70 sq miles for this study)
4) HAZUS performs the standard hydro-processing steps of DEM filling, flow-direction determination, flow-accumulation, and generation of stream segments based on the specified minimum specified catchment size
5) the user creates a scenario by selecting stream segments for analysis
6) the user initiates a hydrologic analysis of the study area during which HAZUS derives discharge rating tables for 2, 20, 50, 100, 200, and 500 year discharges for each stream segment using USGS regression equations and rainfall data that are supplied with the software
7) the user specifies discharge values for each stream segment, or chooses one or multiple flow frequency analysis to be performed by HAZUS to delineate the flood extent for the specified conditions (the 50 and 100 yr discharges were chosen for this study).

The HAZUS output consists of a flood extent polygon and a flood depth grid for the specified discharge or return period. There are additional analysis options available that utilize census or user supplied data to transform flood depth grids into damage and loss estimates that can be used for planning and response, but they were not used for this study.

HAZUS analysis was conducted for the Kansas River segment which enters the study area to the west of Lecompton and meanders through the Kansas River Valley in and east south-easterly direction until exiting the study area to the east of Eudora. The discharge values produced by the HAZUS hydrologic analysis were 201,747 and 275,650 cfs for the 50 and 100 year events, respectively. HAZUS analysis was conducted for the Wakarusa River segment, which extends from Shawnee County on the western edge of Douglas County, through Clinton Reservoir to its confluence with the Kansas River at Eudora to the west. Discharge values produced by the HAZUS hydrologic analysis were 33,218 and 40,671 cfs for the 50 and 100 year events, respectively.

Because the FLDPLN model requires stage values instead of discharge values, a method was needed to translate the discharges used by HAZUS into stage values. The 50 and 100 yr discharges (Table 2-5) for each segment were taken from the HAZUS flood frequency-discharge tables. The discharge values were then cross-referenced with stage-discharge tables for the Lecompton (USGS 06891000) and Wakarusa (USGS 06891500) gages that were acquired from the USGS (waterdata.usgs.gov). For the Kansas River, stage values for the modeled discharges were taken directly from the stage-discharge tables, which are shown graphically in Figure 2-8. The stage values in the table are reported in 1/100 ft increments, ranging from 1.33 to 30.5 ft for the Kansas River, and

flow values are given to three significant digits, ranging from 450 to 484,000 cfs. The stage values were translated into DTF values for the FLDPLN model by adding the stage values of 25.2 and 26.9 for the 50 and 100 yr stage, respectively, to the gage datum value of 821.8 ft (NAVD88), then subtracting from that value the "filled" NED10 or NED10L stream pixel elevation values, 826.3 ft and 823.8, respectively, for the gage location (Table 2-5).

The Wakarusa River gage stage-discharge table values range from 3.94 to 32.88 ft, and flow values range from 0.5 to 32700 cfs, shown graphically in Figure 2-9. Because the maximum discharge given in the table is below the 50 and 100 yr discharges modeled by HAZUS (33,281 and 40,671 cfs, respectively) a 4th order polynomial was fit to the data points in the table:

$$y = 0.3253x^4 - 19.43x^3 + 405.89x^2 - 3170.1x + 8186.4 \qquad \text{Eq. (1)}$$

Eq.(1) was used to calculate the stage values of 33.0 and 34.0 feet used in the DTF calculation. The DTF calculations were completed in the same manner as they were for the Kansas River values, with results shown in Table 2-5. Using the appropriate DTF values, the corresponding flood extents were extracted from the FLDPLN database.

For each of the flood extent polygons produced above, the flood extent polygon was coded for source data by adding a new field to the attribute table (F_stat_cod), which was then populated with a "1" for flood extent polygons produced with the NED10 and a "2" for flood extent polygons produced with the NED10L data. The polygons for corresponding model and return period/stages were unioned, another field was added

(F_stat_sum) to the attribute table, and the two coded F_stat_cod fields produced by the union were added to calculate the F_stat_sum value that represents one of three unique co-occurrence conditions: "1" representing areas only flooded with the NED10 DEM, "2" representing areas flooded only in the NED10L DEM, and "3" representing areas flooded by both. Area sums calculated for each value were used to calculate the level of correspondence using the F-statistic (Bates and De Roo 2000, Cook and Merwade 2009, Kastens 2008, Horritt and Bates 2001, Tayefi et al. 2007)

$$F = 100 * (A_{op}/(A_o+A_p-A_{op})) \quad \text{Eq. (2)}$$

where A_o: observed area of inundation (model A)

A_p: predicted area of inundation (model B)

A_{op}: area that is both observed and predicted as inundated.

F-statistic values for each case were summarized and compared (Table 2-6). Because a comparative analysis between models is performed in Chapter 3 of this study for a separate study area, no attempt was made to evaluate or compare model performance between models.

Results

Accuracy assessment of NED10 against GPSBMs

Although 15 GPSBMs were initially selected as reference data for accuracy assessment of the DEM datasets (Table 2-1), upon closer inspection three points were rejected. Stations "Valencia" and "N346" had been destroyed during highway

construction subsequent to their inclusion in the NGS GPS-on-benchmark dataset. Valencia, located west of Topeka along Interstate 70, was positioned at the upper fringe of a road cut that had been expanded during a major road improvement project earlier this decade. Station N346, located on the east side of Topeka, was destroyed during a major renovation of the east Topeka turnpike interchange. The Golden station was rejected because it is located on a highway overpass that is not represented in any of the DEMs. It was the great disparity between these GPSBM elevation values and the DEM values relative to the close correspondence of the other 12 that prompted this high level of scrutiny (Table 2-2). One other point was rejected, KAN1A, but only for the NED30 analysis. A review of the site indicated that the NED30 discrepancy of 4.31 m was likely due to earthwork that had been performed in the area between the source data collection and the establishment of the benchmark. It was decided that this type of anomalous error was atypical and would skew the analysis results.

For all remaining points the error statistics were computed and are reported in Table 2-3. With the exception of the "B 276 RESET" and the "KAN1B" points, no individual LiDAR-derived error for any dataset exceeded 1 m. The "B 276 RESET" benchmark presents a unique setting that is likely the cause for the apparent error, and serves as an opportunity to more closely examine the underlying assumptions and uncertainties of elevation data production. Figure 2-10 shows an *in situ* photograph of the benchmark. A site visit revealed that the benchmark is set in the sill of a concrete culvert at the bottom of a drainage ditch surrounded by locally steep and variable terrain. While actual point location elevation values are very accurate (shown in yellow in Figure 2-10), the LiDAR return values are variable in the immediate vicinity (shown in green)

due to the uneven terrain. The gray blocks in the background of Figure 2-10 represent the footprint of the LIDAR2 DEM cells with the cell values shown in white. When the LIDAR2 cells are reprojected and resampled to fit the NED3L geographic coordinate standards (the native projection of the LIDAR2 data is UTM Zone15N), the elevation values are further degraded in resulting cells, and there is no practical way to determine which and in what proportion LIDAR2 cell values contribute to particular NED3L cell. Depending on the origin chosen during this process, the contributing cell may be centered on the GPSBM, get most of their value from the ravine bottom, or from the side slope and road. Ultimately, the small-scale terrain variability at this location introduces additional uncertainty into the NED3L value.

As the data are resampled to generate the NED10L, then again for the NED30L, these factors continue to alter the cell value represented at this, and every other location. In the last two downsampling steps, NED3L to NED10L and NED10L to NED30L, the contributing cells are nested in resultant cells, so one NED10 cell comprises nine underlying NED3L, and one NED30L comprises nine NED10L cells (81 NED3L cells). For flood modeling, the important feature, though, is that while there is some degradation of vertical accuracy, it is small and measurable as evidenced by the summary statistics in Table 2-3. This can be seen graphically in Figure 2-11, which shows a 2500 m cross section profile taken from the Wakarusa River Valley south of Lawrence for all DEMs except the NED30, which was withheld so focus could be brought to the NED10 data and the LiDAR derived products. Even though the LiDAR derived DEMs are degraded substantially in horizontal resolution, they are only degraded slightly in vertical accuracy, and very minimally in the flatter terrain that characterizes most of the floodplain. It is

reasonable to conclude, then, that even with coarse resolution LiDAR derived NED data, a flood model, depending on its method of implementation, would be better able to represent probable flooding using a NED30L dataset than a NED10 dataset. From a computational efficiency standpoint, if channel widths are sufficiently large to have representation, it may indeed be preferable to use a coarser resolution LiDAR derived DEM for larger areas, particularly for iterative, raster based algorithms like the FLDPLN model.

NED10 accuracy assessment

In general, it was expected that accuracy of the NED10 data would decrease for landcover classes with increased vegetation density and height, that the errors would be normally distributed, and that some outliers would exist where significant terrain modification had taken place since the date of the NED10 source data. With nearly 3000 reference points, scrutiny at the level of the GPSBM analysis was not possible. The summary statistics, however, show an approximately normally distributed sample set that is representative of the overall population (Table 2-4). It is interesting that the minimum value for each cover class is greater in magnitude than the corresponding maximum, except for grassland, which is nearly equal. Also, the mean for each evaluation is slightly less than zero, or about 10% of the RMSE for cropland and grassland and around 20% for urban and woodland. This negative bias indicates that on average the NED10L values were slightly greater than the NED10 values consistently across all cover types, and more so on the two cover types that have significant vertical features. The significance of this

bias is not clear, and it does not have obvious implications for flood modeling given the overall error and uncertainty of flood model inputs and results.

As was expected, the RMSE for woodland (1.87 m) and urban (1.60 m) is slightly higher than for grassland (1.42 m) and cropland (1.39 m) which is why the generally accepted accuracy standards for elevation data are categorized by cover type (NDEP 2004). The exact standard varies by cover class, target specification, and standard-setting body, but an example from the FEMA LiDAR standard is given in the LIDAR2 metadata above: "Vertical Bare earth 18.5 cm RMS @ 95% confidence, 15 cm RMS @ 90% confidence, Vertical in Vegetation 37 cm RMS @ 95% confidence." The overall absolute vertical RMSE for the NED10 in Douglas County of 1.51 m is significantly lower than the 2.44 m figure reported by Gesch (2007) for the nationwide NED, which was evaluated using over 13,000 GPSBMs, and much lower than the often cited ± 7 m accuracy of the NED, which is actually a production goal, not an accuracy statistic (Gesch 2007).

There are two slight anomalies in the error plots for landscape factors, one in the elevation plot and one in the aspect plot, that are detectable visually. In the lower elevations of the elevation plot (Figure 2-12), roughly in the 245-265 m elevation range, there are several striations in the data indicating that NED10 data errors within narrow elevation ranges trend from approximately -2 m to +2 m from higher to lower elevations. Closer inspection revealed that these patches of trending error occur within the Kansas River floodplain and appear to correspond to alluvial deposition features. It is possible that scouring and redeposition of floodplain soils may have occurred during the major floods of 1951, which would be consistent with the vintage of the NED10 source data for

this area (1950-1951, Figure 2-4). Because these errors occur within the floodplain and their magnitude range is several meters, these errors could impact modeled flood extents in these areas.

The second anomaly, observed in the aspect plot (Figure 2-13), shows a slight negative bias in error for the northern aspect that trends to unbiased near the southern aspect. A 3rd-order polynomial is plotted in Figure 2-13 to highlight this trend. The cause for this trend could not be determined, and given its relatively small magnitude relative to the overall error, it is not likely to greatly impact flood extent estimation. Other than these examples, the errors do not appear to be correlated with any of the landscape parameters and appear to be approximately normally distributed about the zero-error axis. Neither the error vs. slope (Figure 2-14) nor error vs. local relief (Figure 2-15) show any obvious anomalies, asymmetries, or trending.

Model flood extent comparison for 50 and 100yr discharge

Figure 2-11 illustrates one example of disparity in a cross sectional profile between the elevation values of the NED10 and NED10L datasets. When modeling flood extent, these disparities can yield inconsistent calculated flood surface elevation values and flood depth values, and differences in mapped flood extents. By comparing mapped flood extents between the NED10 and NED10L using the same model for the same simulated flood event, the potential impact of elevation errors can be examined.

Comparing equivalent flood events modeled using the NED10 and NED10L datasets, the 100 yr flood (275,650 cfs) modeled by HAZUS for the Kansas River segment showed 1204 ha flooded with the NED10L data that were not flooded with the

NED10 data, while the NED10 showed only 181 ha of flooding that were not flooded with the NED10L data. 13,329 ha were flooded by both, yielding an F-statistic of 90.6, the highest of all modeled results (Table 2-6, Figure 2-16). The 50 yr HAZUS flood (201,737 cfs) showed nearly equal overall area flooded, with 865 ha flooded using the NED10L data that were not flooded with the NED10 data, and 992 ha were flooded with the NED10 data that were not flooded with the NED10L data. 10,521 ha were flooded using both datasets. The F-statistic from this comparison was 85.0.

The 100 yr flood (DTF of 24.9 and 22.5 ft for NED10L and NED10, respectively) modeled by FLDPLN for the Kansas River segment showed 912 ha flooded with the NED10L data that were not flooded with the NED10 data, while the NED10 showed 514 ha of flooding that were not flooded with the NED10L data. 4,613 ha were flooded by both, yielding an F-statistic of 76.4 (Table 2-6, Figure 2-17). The 50 yr FLDPLN flood (DTF of 23.2 and 20.8 ft for NED10L and NED10, respectively), showed comparable overall flooded area between both datasets, with 801 ha flooded with the NED10L data that were not flooded with the NED10 data. 604 ha of flooded with the NED10 data that were not flooded with the NED10L data. 3,637 ha were flooded by both, giving an F-statistic of 72.1.

The 100 yr flood (40,671 cfs) modeled by HAZUS for the Wakarusa River segment showed 356 ha flooded with the NED10L data that were not flooded with the NED10 data, while the NED10 showed only 58 ha of flooding that were not flooded with the NED10L data. 2,179 ha were flooded by both, yielding an F-statistic of 84.0 (Table 2-6, Figure 2-18). The 50 yr HAZUS flood (33,218 cfs) showed 426 ha flooded with the NED10L data that were not flooded with the NED10 data, while the NED10 showed 111

ha of flooding that were not flooded with the NED10L data. 1,909 ha were flooded by both, yielding an F-statistic of 78.0.

The 100 yr flood (DTF of 25.0 and 28.6 ft for NED10L and NED10, respectively) modeled by FLDPLN for the Wakarusa River segment showed 33 ha flooded with the NED10L data that were not flooded with the NED10 data, and the NED10 showed 1006 ha of flooding that were not flooded with the NED10L data. 2,328 ha were flooded by both, yielding an F-statistic of 69.1 (Table 2-6, Figure 2-19). The 50 yr FLDPLN flood (DTF of 24.0 and 27.6 ft for NED10L and NED10, respectively) showed nearly 38 ha flooded with the NED10L data that were not flooded with the NED10 data, and the NED10 showed 1132 ha of flooding that were not flooded with the NED10L data. 2,328 ha were flooded by both, yielding the lowest F-statistic of 64.4.

In general, these results show that the flood models are significantly affected by the input elevation data and that the models are not equivalently sensitive to disparities among data sets. There are likely two major factors that contribute to inconsistencies between modeled results. First, the differences in cross sectional profile between the elevation data sources, as illustrated in Figure 2-11, can lead to different water surface elevations. Second, the terrain surface that is intersected by the modeled flood water surfaces are different and yield correspondingly different flood extent estimates as well as different flood depth estimates, which are important for risk and damage assessment tools like those included with HAZUS.

Conclusions

The elevation accuracy assessment of the NED datasets against the NGS GPSBMs showed that the LiDAR data have sufficiently high accuracy to be used as reference data for evaluation of the NED10 data. Although the 12 GPSBM reference points did not represent a full range of landscape and land cover conditions, the analysis did point to the retention of vertical accuracy in downsampled NED3L, NED10L, and NED30L datasets, which has positive implications for the use of lower resolution DEM datasets for flood modeling and has the potential to significantly reduce file sizes and computational workload. Even the NED10 and NED30 showed RMSEs of 0.93 and 1.26 m, respectively, in this analysis, which was better than expected, albeit for a small sample size.

The NED10 accuracy assessment, which had 2,660 sample points, showed and overall RMSE of 1.51 m, which is better than the 2.44 m error reported by Gesch (2007) for the nationwide NED10 using over 13,000 GPSBM reference points. As expected, the errors in the urban and woodland classes were slightly higher than the grassland and cropland classes because of the influence of the higher manmade and vegetative vertical features in the urban and woodland classes. The 1.51 m overall error equates to 4.95 ft, almost exactly ½ of the 10 ft contour interval upon which the NED10 data are based, and in line with the general accuracy rule of thumb for elevation contours themselves. There was no interesting relationship found between NED10 elevation error and the landscape characteristics of elevation, slope, aspect, or local relief. A slight trending was detected in the error vs. aspect plot, but its cause is not obvious, and it would appear to have only marginal implications for flood modeling due to its small magnitude. Some slight

anomalies were detected in the error vs. elevation plot that appear to be artifacts of alluvial transport during major floods, possibly even the floods of 1951 (which pre-date levee construction in the study area). These discrepancies are more likely to impact flood extent estimates due to their larger range of magnitude and occurrence in flood-prone areas, particularly for moderate level floods characterized by overbank flow but under what is generally considered major flood stage.

Ultimately, testing for disparity in model flood extent outputs between otherwise equivalent model inputs for separate elevation source inputs, at a minimum, can show a potential for flood information inaccuracies. Examination of modeled 100 and 50 yr flood events for segments of the Kansas and Wakarusa Rivers showed a significant potential for discrepancies on both rivers for the HAZUS and FLDPLN models. In all cases, larger floods showed greater flood extent correspondence between elevation datasets, and the HAZUS model flood extents showed overall better correspondence than the FLDPLN model flood extents. The FLDPLN model, then, appears to be more sensitive to discrepancies in elevation inputs, at least for the four cases examined here. There is insufficient information from this analysis, however, to draw any conclusions regarding the accuracy of either model.

It is worth noting, however, that the HAZUS model shows considerable flooding in north Lawrence, which is protected by levees that were represented in both the NED10 (accurate levee elevation data were "burned" into the NED10) and the NED10L (Figure 2-16). This flooding occurred at both the 50 and 100 yr flood levels. Neither of these flood levels should produce significant flooding in this area. The cause of the flooding is not clear, but it may be related to the projection of the DEMs by HAZUS from

geographic coordinates to UTM coordinates. This may, in effect, be breaching the levees during the resampling. Alternatively, HAZUS may simply be overestimating the water surface elevations.

Overall, this analysis showed that elevation data quality can have a significant impact on modeled flood extent, even for the NED10 with an RMSE of 1.51 m (4.95 ft) in the study area. When considering that the difference in stage between the 100 and 50 yr events for the Kansas and Wakarusa Rivers was only 1.7 ft and 1.0 ft, respectively, the significance of these errors becomes more apparent. The data do, however, show that these errors become less significant for higher flood stages. This is important because floods of greater magnitude have greater potential to cause damage and are more likely to require large, coordinated response efforts.

Tables

Table 2-1. Elevation values corresponding to GPSBM locations. Red values denote those that were rejected. All units are meters.

Station Name	Reject	BCP	2mL	NED3L	NED10L	NED10	NED30L	NED30	Comment
KAN1 A		282.36	282.20	281.83	282.30	281.31	282.13	278.04	Excl. for NED30
KAN1 B		286.34	286.31	285.85	286.06	288.55	287.48	287.49	
N 346	x	305.68	302.17	302.28	301.18	303.51	301.19	302.41	Not recoverable
GOLDEN	x	300.28	294.47	294.48	294.43	294.81	295.17	297.52	On Overpass
VALENCIA	x	324.89	321.10	322.75	320.62	325.06	319.79	323.45	Not recoverable
AP STA B		266.08	266.10	266.19	266.40	265.49	266.75	267.09	
KANWAKA		344.41	344.47	344.41	344.48	343.30	344.44	342.89	
Y 368		275.48	275.34	275.29	275.74	275.73	275.77	276.13	
C 367		270.31	270.31	270.39	270.03	271.63	270.03	271.27	
N 367		279.67	279.53	279.39	279.53	280.01	279.39	280.72	
C 371		303.11	303.21	303.27	303.04	303.18	302.99	304.43	
B 276 RESET		248.83	248.50	250.13	248.82	249.25	249.66	248.42	
LLOYD		252.60	252.62	252.64	252.47	253.35	252.49	251.14	
VALENCIA 2		325.39	325.41	325.43	325.10	325.22	324.93	327.88	
LLOYD AZ MK		252.87	252.88	252.70	252.67	253.16	252.87	252.78	

Table 2-2. Elevation value differences between GPSBMs and DEMs (GPSBM - DEM). Red values denote those that were rejected. All units are meters.

Station Name	Reject	BCP	2mL	NED3L	NED10L	NED10	NED30L	NED30	Comment
KAN1 A		-	0.16	0.53	0.06	1.05	0.23	4.31	Excl. for NED30
KAN1 B		-	0.03	0.49	0.28	-2.21	-1.14	-1.15	
N 346	x	-	3.51	3.40	4.50	2.17	4.49	3.27	Not recoverable
GOLDEN	x	-	5.81	5.80	5.85	5.46	5.11	2.75	On Overpass
VALENCIA	x	-	3.79	2.14	4.27	-0.17	5.10	1.44	Not recoverable
AP STA B		-	-0.03	-0.12	-0.33	0.58	-0.68	-1.02	
KANWAKA		-	-0.07	-0.01	-0.07	1.11	-0.04	1.52	
Y 368		-	0.14	0.18	-0.26	-0.25	-0.29	-0.65	
C 367		-	0.00	-0.08	0.28	-1.32	0.28	-0.96	
N 367		-	0.14	0.28	0.14	-0.34	0.27	-1.05	
C 371		-	-0.10	-0.16	0.07	-0.07	0.12	-1.32	
B 276 RESET		-	0.33	-1.29	0.01	-0.42	-0.83	0.41	
LLOYD		-	-0.02	-0.04	0.13	-0.74	0.11	1.46	
VALENCIA 2		-	-0.03	-0.04	0.29	0.17	0.45	-2.49	
LLOYD AZ MK		-	-0.02	0.16	0.19	-0.30	-0.01	0.09	

Table 2-3. Summary accuracy statistics for elevation data. All units are meters.

	Minimum	Maximum	Mean	Standard Deviation	RMSE	NMAS (90%)	NSSDA (95%)	n
2mL	0.33	-0.10	0.05	0.12	0.13	0.21	0.25	12
NED3L	0.53	-1.29	-0.01	0.47	0.45	0.73	0.87	12
NED10L	0.29	-0.33	0.06	0.20	0.20	0.34	0.40	12
NED10	1.11	-2.21	-0.23	0.94	0.93	1.53	1.82	12
NED30L	0.45	-1.14	-0.13	0.50	0.50	0.82	0.97	12
NED30	1.52	-2.49	-0.47	1.81	1.26	2.07	2.47	11

Table 2-4. Accuracy statistics for the NED10, referenced to the NED10L, by land use and cover type. Two classes, CRP (n=54) and "other" (n=7) were not evaluated individually, but are included in the overall summary statistic calculations. All units are meters.

	Minimum	Maximum	Mean	Standard Deviation	RMSE	NMAS (90%)	NSSDA (95%)	n
Overall	-11.77	9.88	-0.16	1.51	1.52	2.50	2.98	2660
Urban	-8.55	4.11	-0.38	1.56	1.60	2.63	3.14	163
Cropland	-10.65	9.01	-0.12	1.39	1.39	2.29	2.73	597
Grassland	-9.30	9.88	-0.12	1.42	1.43	2.35	2.80	1282
Woodland	-11.77	7.38	-0.30	1.84	1.87	3.07	3.66	557

Table 2-5. Discharges for the 50 and 100yr flood events, as calculated by HAZUS. Corresponding stage values were derived from USGS lookup tables for USGS gage sites (Figures 2-9 and 2-9)). DTF values used with the FLDPLN model were derived by differencing the NED values for the nearest steam pixel corresponding to gage sites from the sum of the gage datum and stage.

	Discharge (cfs)	Stage (ft)	NED10 (ft)	NED10L (ft)	Datum (ft)	DTF-NED10 (ft)	DTF-NED10L (ft)
Wakarusa - 50yr	33,218	33.0	804.6	808.2	799.3	27.6	24.0
Wakarusa - 100yr	40,671	34.0	804.6	808.2	799.3	28.6	25.0
Kansas - 50yr	201,747	25.2	826.3	823.8	821.8	20.8	23.2
Kansas- 100yr	275,650	26.9	826.3	823.8	821.8	22.5	24.9

Table 2-6. Correspondence of equivalent modeled flood events between datasets. Correspondence codes are: 1) flooded in NED10 but not in NED10L (disagreed), 2) flooded in NED10L but not in NED10 (disagreed), 3) flooded in NED10 and NED10L (agreed). The F-statistic is a measure of the agreement as a percentage of the overall area flooded in both source data scenarios.

Kansas River **Model-Return Period**	**Correspondence Type** 1	2	3	**F-Statistic**
HAZUS - 100yr	181	1204	13329	90.6
HAZUS - 50yr	992	865	10521	85.0
FLDPLN - 100yr	514	912	4613	76.4
FLDPLN- 50yr	604	801	3637	72.1
Wakarusa River **Model-Return Period**				
HAZUS - 100yr	58	356	2179	84.0
HAZUS - 50yr	111	426	1909	78.0
FLDPLN - 100yr	1006	33	2328	69.1
FLDPLN- 50yr	1132	38	2117	64.4

Figures

Figure 2-2. Aerial photographs taken during the peak flooding in Montgomery County in July of 2007. The top two photos show oil release from a refinery in Coffeyville, which flowed south in the Verdigris River into Oklahoma. (www.kansasgis.org)

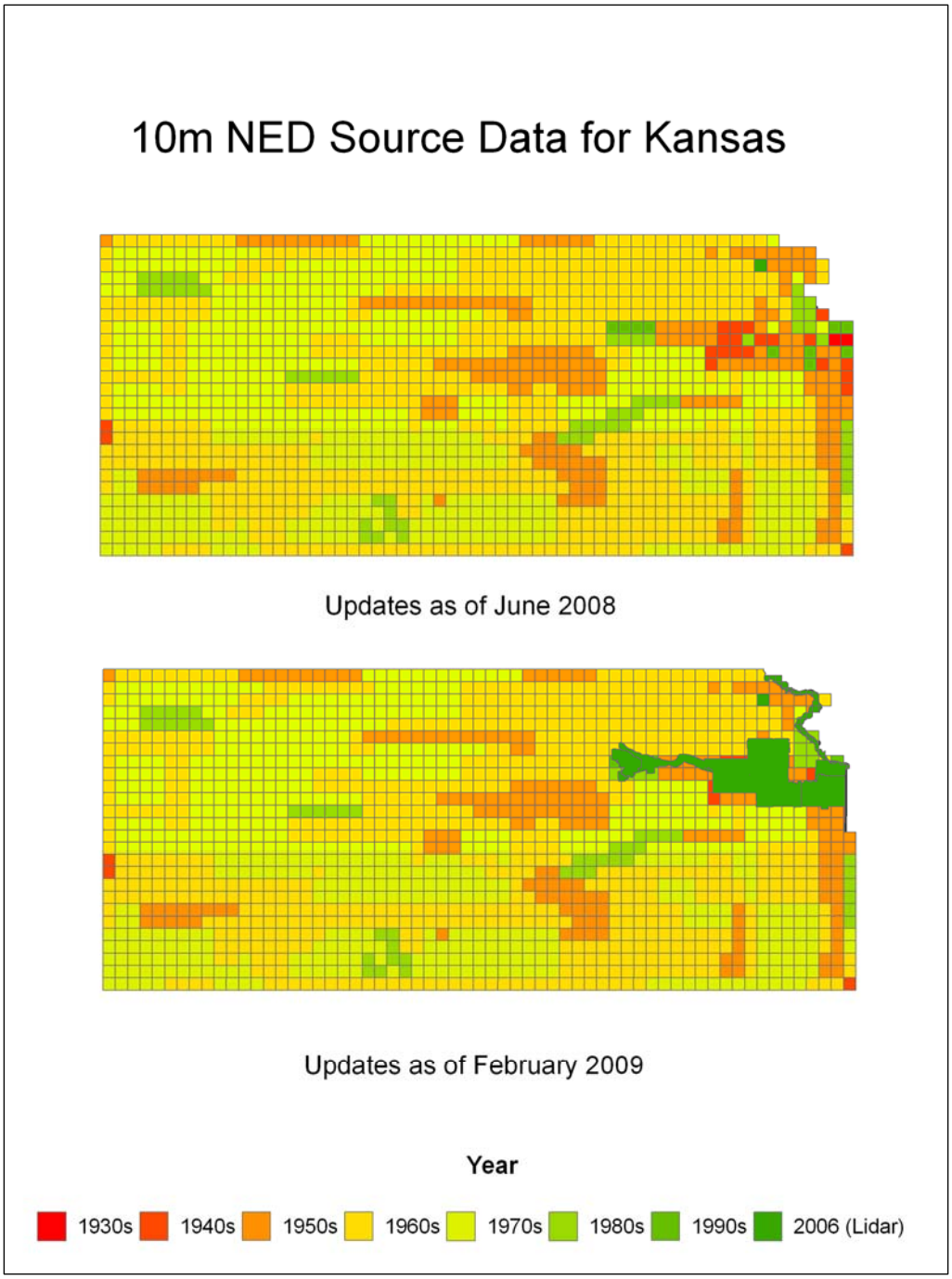

Figure 2-3. Kansas National Elevation Dataset (NED) source data dates, grouped by decade. In 2006 a consortium of stakeholders at the state and local level coordinated LiDAR data acquisition along the Kansas River corridor. These higher resolution and higher precision data were eventually incorporated into the NED.

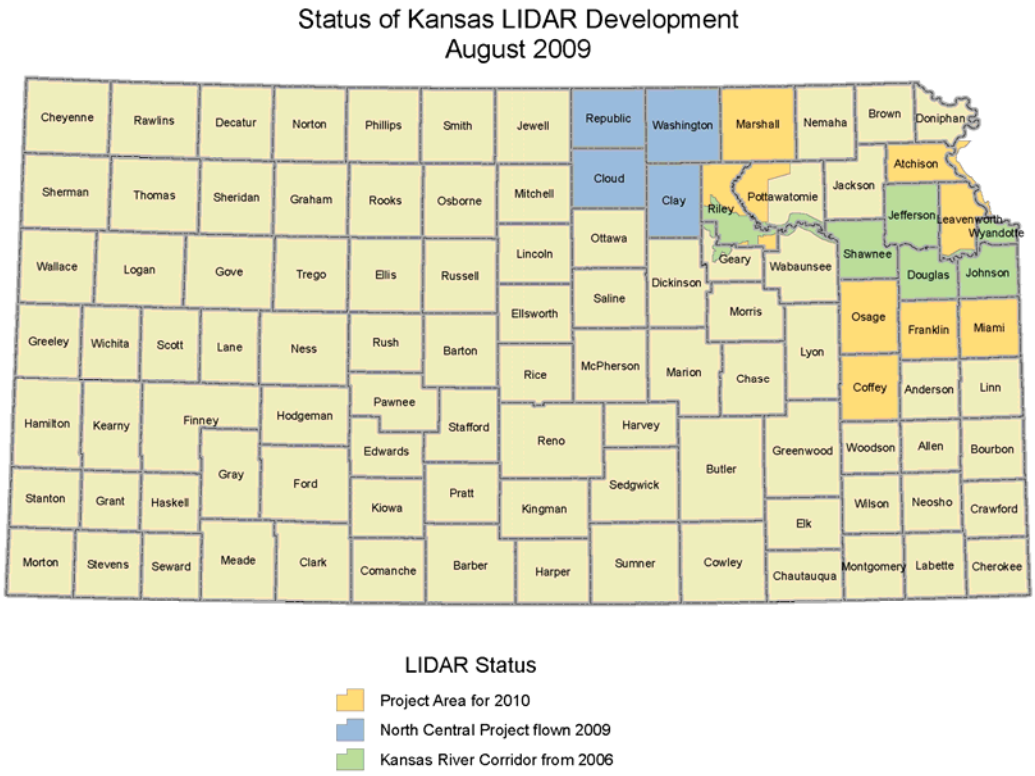

Figure 2-4. Current coverage and planned LiDAR acquisitions by the State of Kansas (www.da.ks.gov/gis/) . Sedgwick County has LiDAR coverage that was funded by the county and the city of Wichita. Montgomery, Cowley, and Sumner Counties are also scheduled to purchase LiDAR data with federal funds.

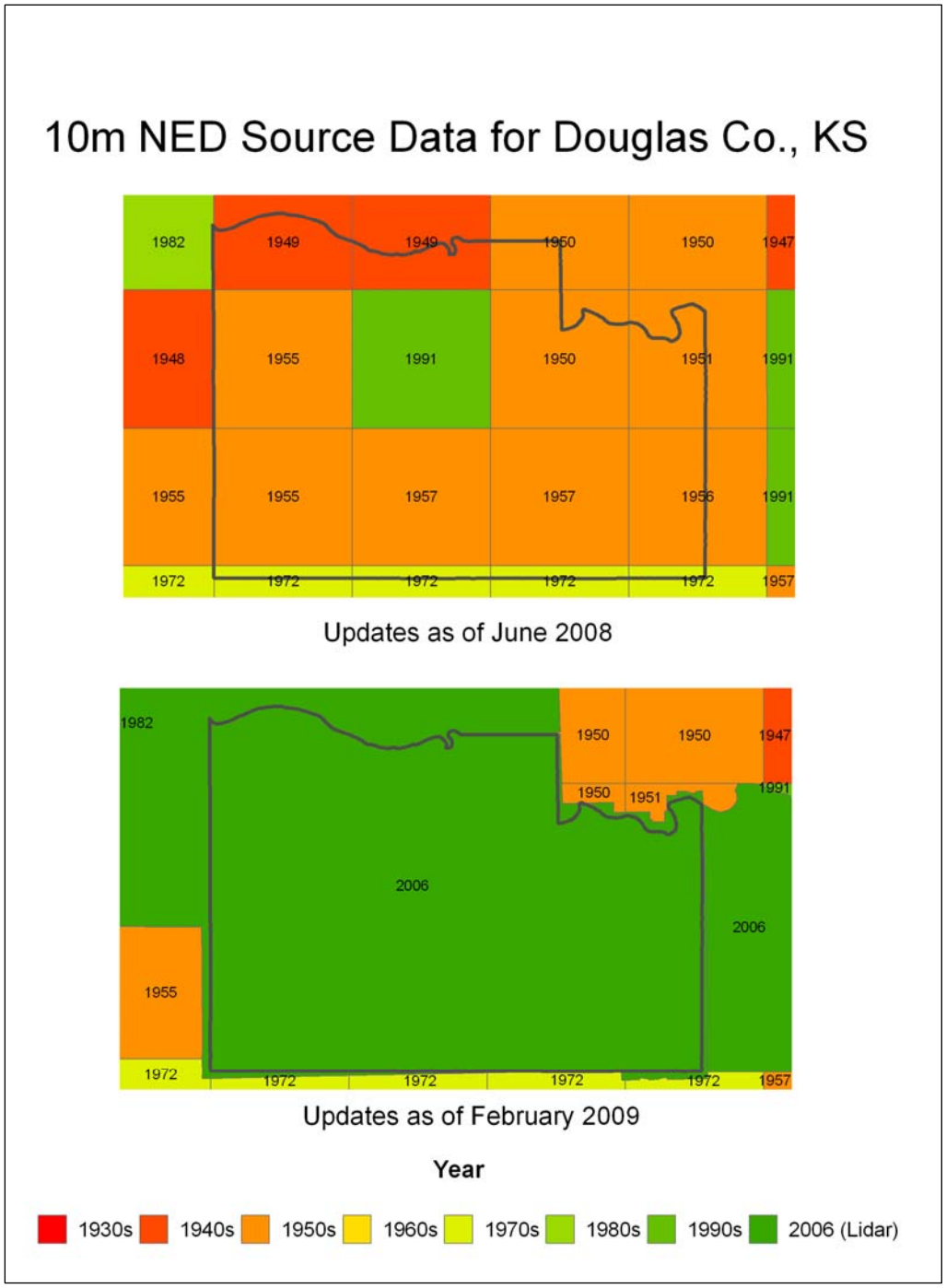

Figure 2-5. Douglas County National Elevation Dataset (NED) source data dates, grouped by decade.

Figure 2-6. Location of NGS GPSBMs within the Kansas River corridor LiDAR coverage. A total of 15 points (two of the points are close together, so their map symbols overlap) were used for evaluation of elevation datasets in this study. Three points were ultimately rejected. Two of the three points had been destroyed during recent highway construction and one is located on a highway overpass, which is not representing in the DEMs.

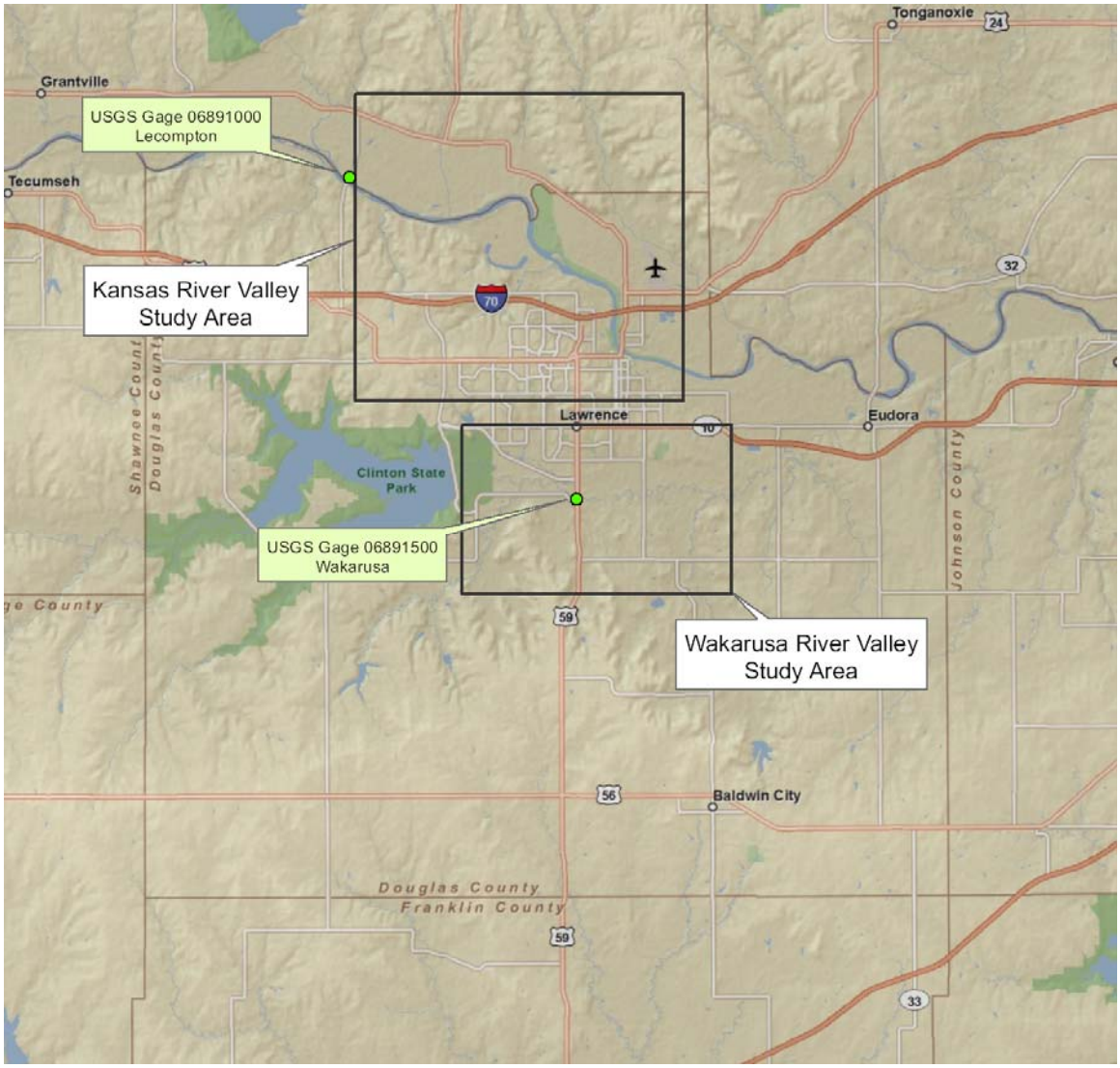

Figure 2-7. Kansas and Wakarusa River Valley study areas. The effect of elevation data quality on HAZUS and FLDPLN flood models output was evaluated on stream segments of the Kansas and Wakarusa Rivers. The USGS gage stage-discharge tables were used to translate discharge values generated by HAZUS for the 50 and 100 yr storm events into stage values to calculate DTF values used for the FLDPLN model.

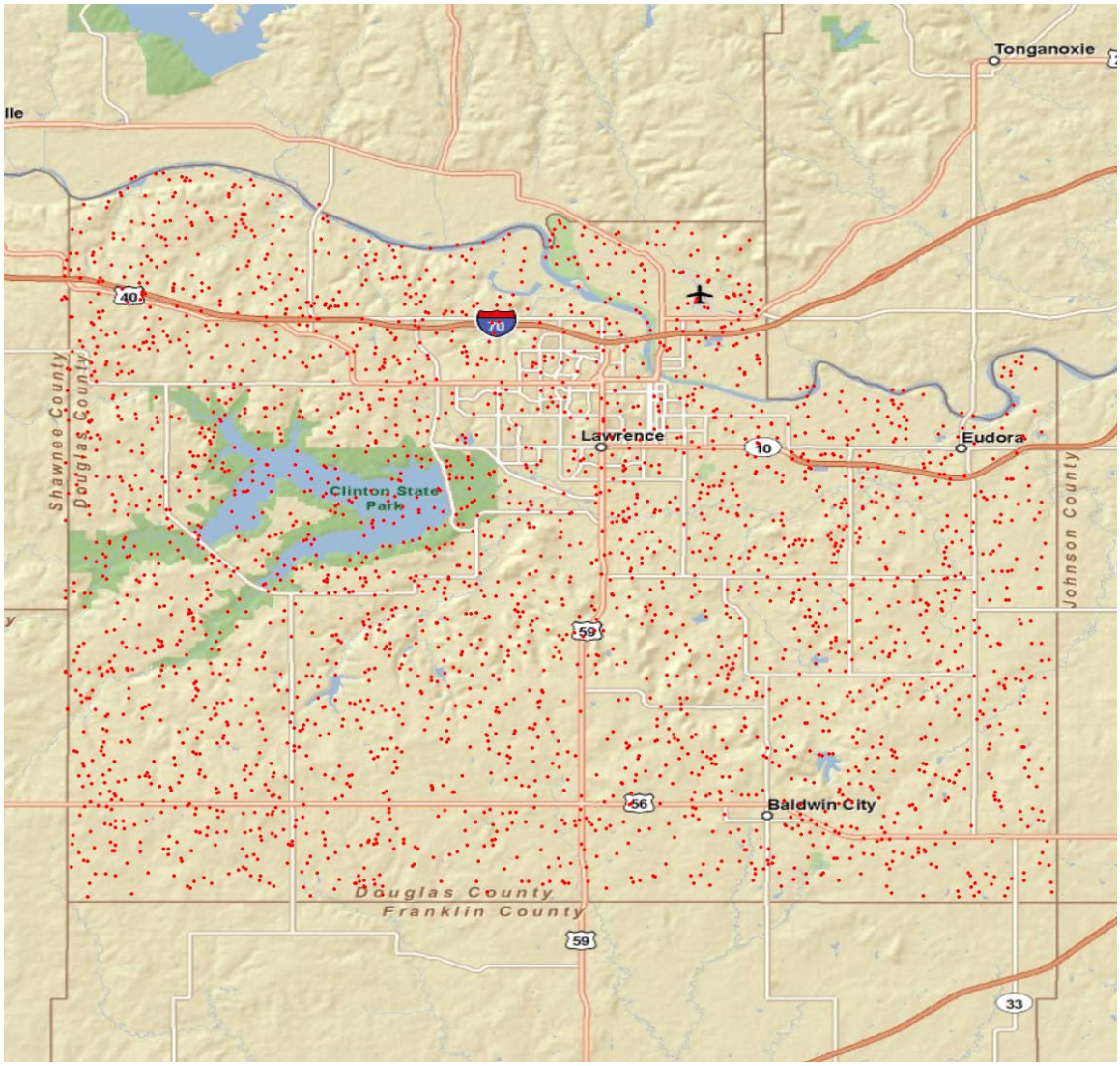

Figure 2-8. Randomly selected points used for evaluation the NED10 data. 3000 points were initially generated. Points that fell on areas classified as water in the KLCP05 were eliminated, along with a few points that fell outside county boundary. Table 2-4 gives counts and error statics by cover class, as well as overall summary statistics for the NED10 using the NED10L as a higher accuracy reference.

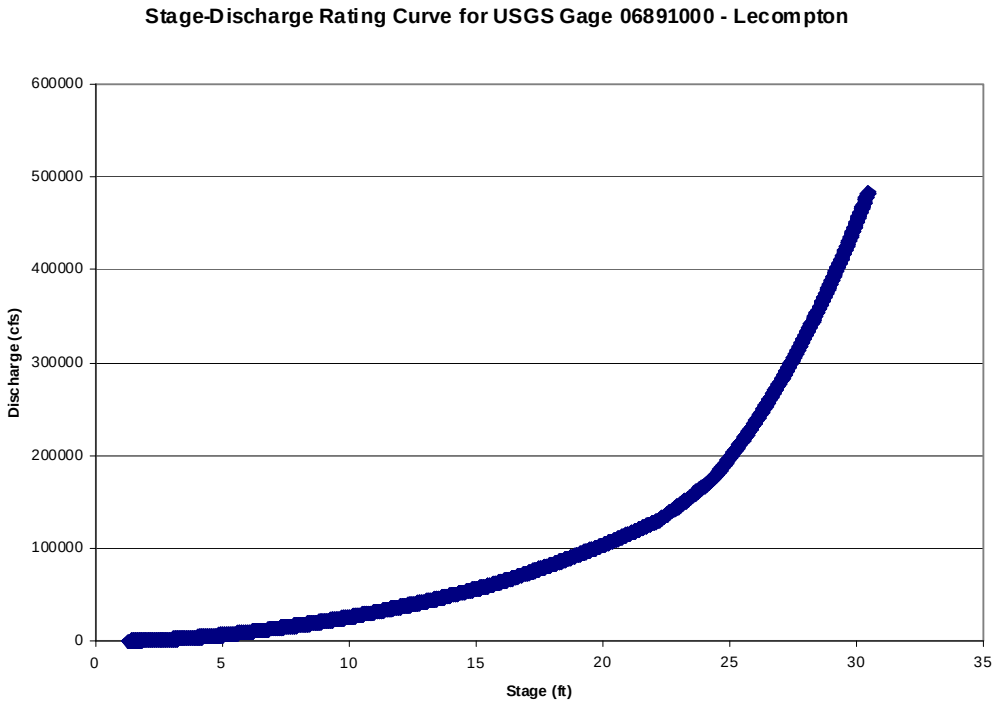

Figure 2-8. Plot of the stage-discharge values (blue) available for the USGS Lecompton gage. 50 and 100 yr discharge values generated by HAZUS were cross-referenced with this table to calculate DTF values used by the FLDPLN model.

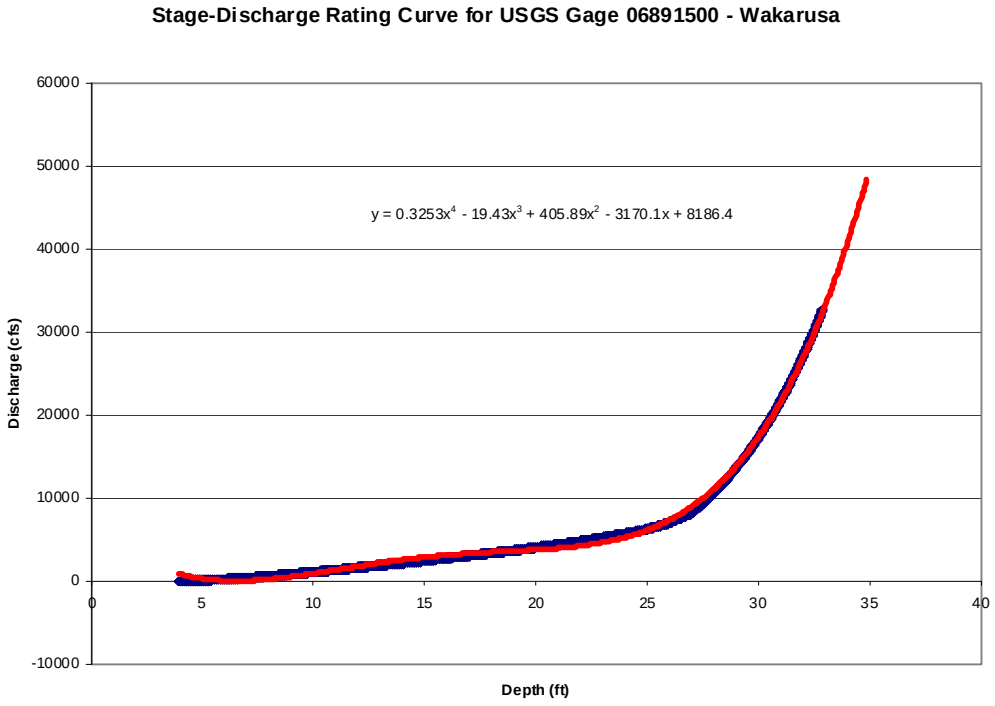

Figure 2-9. Plot of the stage-discharge values (blue) available for the USGS Wakarusa gage. 50 and 100 yr discharge values generated by HAZUS were greater that the largest values in the table, so a 4th-order best-fit polynomial trend line (red) was created in Excel and used to estimate the appropriate stage values used to calculate DTF values for the FLDPLN model.

Figure 2-10. GPSBM "B276 Reset", located in Lawrence, KS, is shown in the photo above. As an example of the inherent difficulty in using a point elevation (represented in yellow in the bottom graphic by "B276 Reset"), 2 meter DEM cells are show above in gray with corresponding values in white. The green asterisks represent the location and values of the LiDAR returns from which the DEM values are derived. A LiDAR vendor would likely not use this GPSBM as a checkpoint because of the uneven ground surrounding the checkpoint.

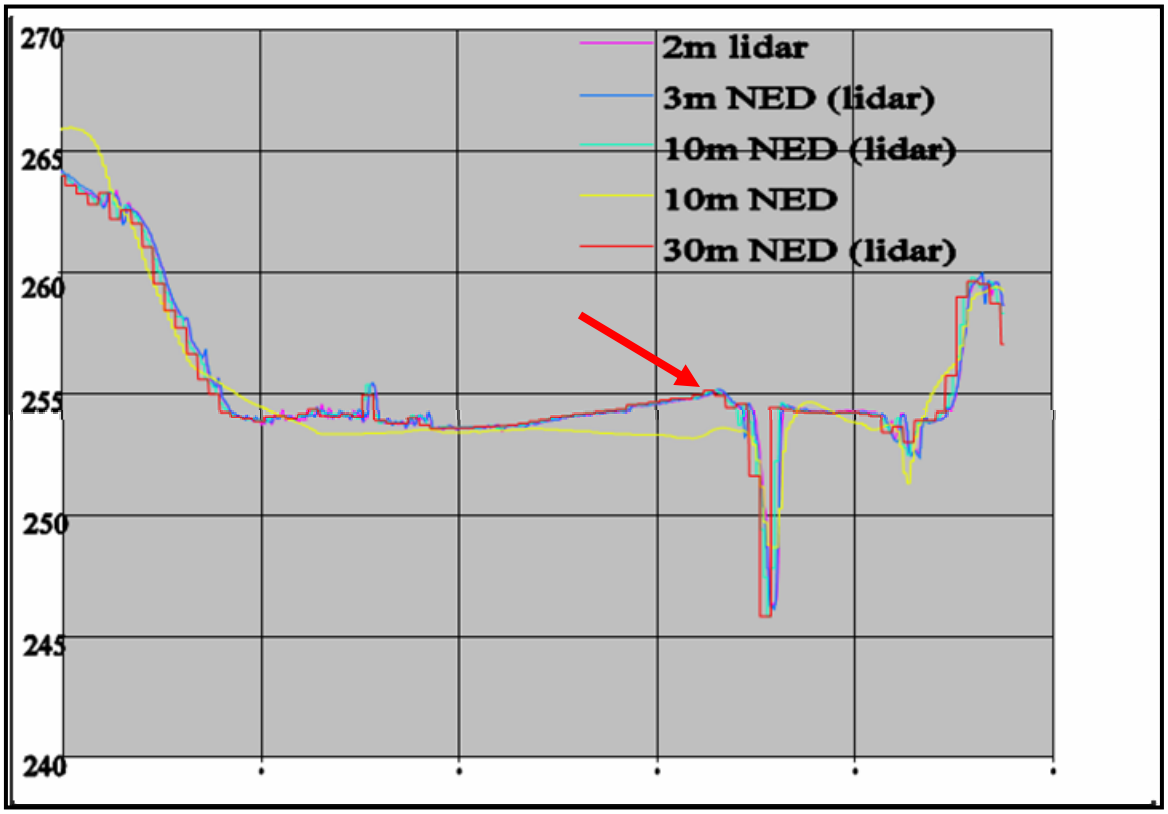

Figure 2-11. This cross-section profile, which represents an approximately 2500 m profile across the Wakarusa River valley south of Lawrence, shows elevation discrepancies between NED10 and LiDAR derived elevation datasets. The steep valley to the right represents the actual river channel. The valley walls are the steep features on the far right and far left of the plot. The yellow line represents the NED10 data and is noticeably distinct from the other lines, which are all derived from the same LiDAR data and correspond very closely with one another. The red arrow points to a natural levee that is represented in all of the LiDAR datasets, but is absent in the NED10 data. A simplistic example illustrates the significance of this discrepancy: if the actual water surface elevation were 253 m, for instance, modeling with the NED10 data would show extensive flooding on to the left of the channel, whereas models using any of the LiDAR data should not indicate flooding there. (The horizontal and vertical axes are not on the same scale; the vertical axes are exaggerated relative to the horizontal)

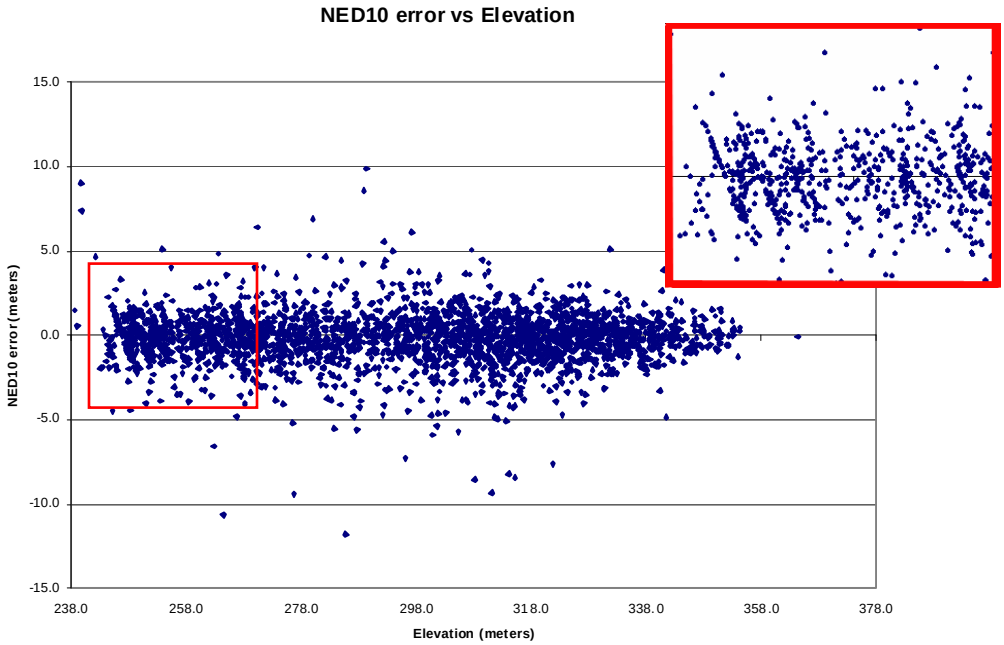

Figure 2-12. Plot of the NED10 error vs. elevation. Local, linear trending features can be seen in the lower elevations (red box and inset), which represent points in floodplain areas. These may be due to scouring and deposition during major floods that occurred between the respective elevation data source dates.

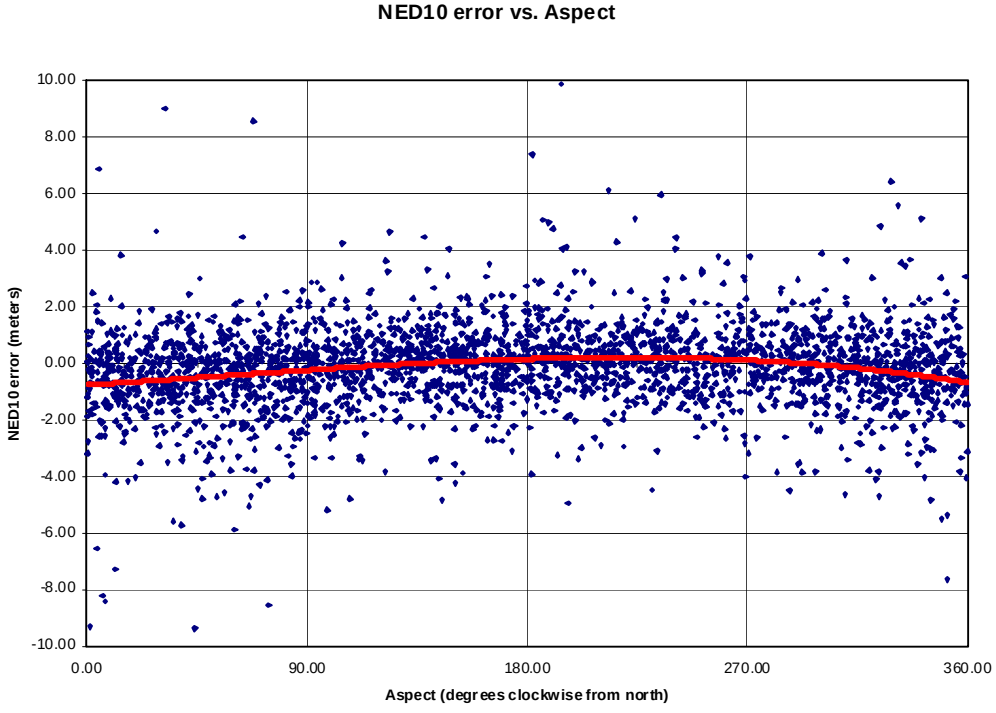

Figure 2-13. Plot of the NED10 error vs. aspect. A best-fit, 3rd order polynomial trendline (red) highlights the slight systematic error present in the data.

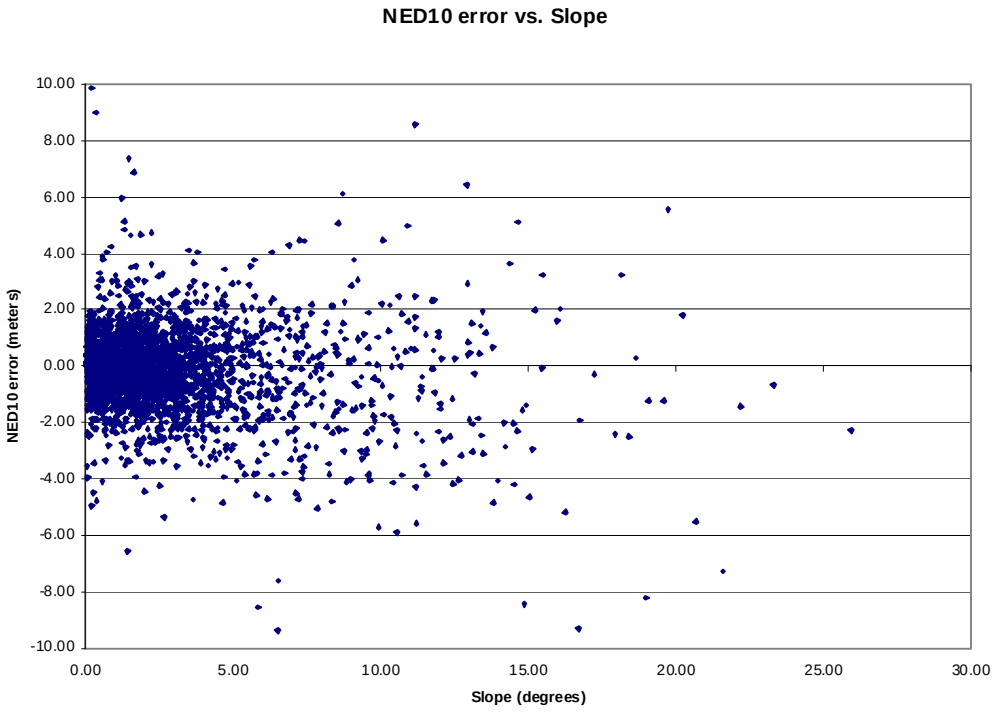

Figure 2-14. Plot of the NED10 error vs. slope.

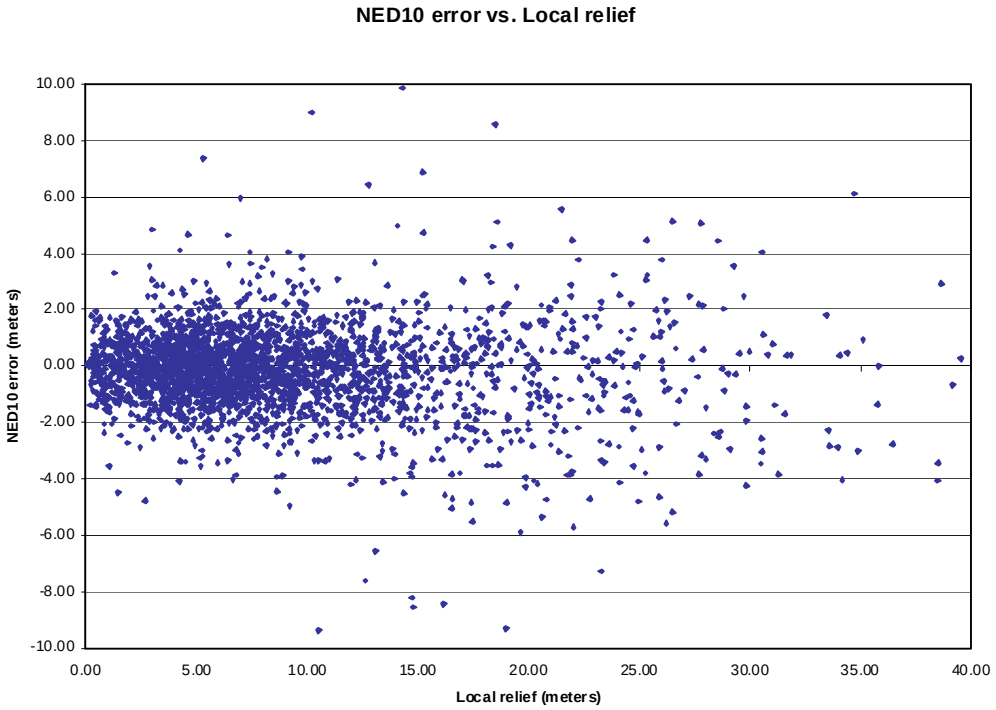

Figure 2-15. Plot of the NED10 error vs. local relief (elevation value range [maximum-minimum] within a 90 m radius).

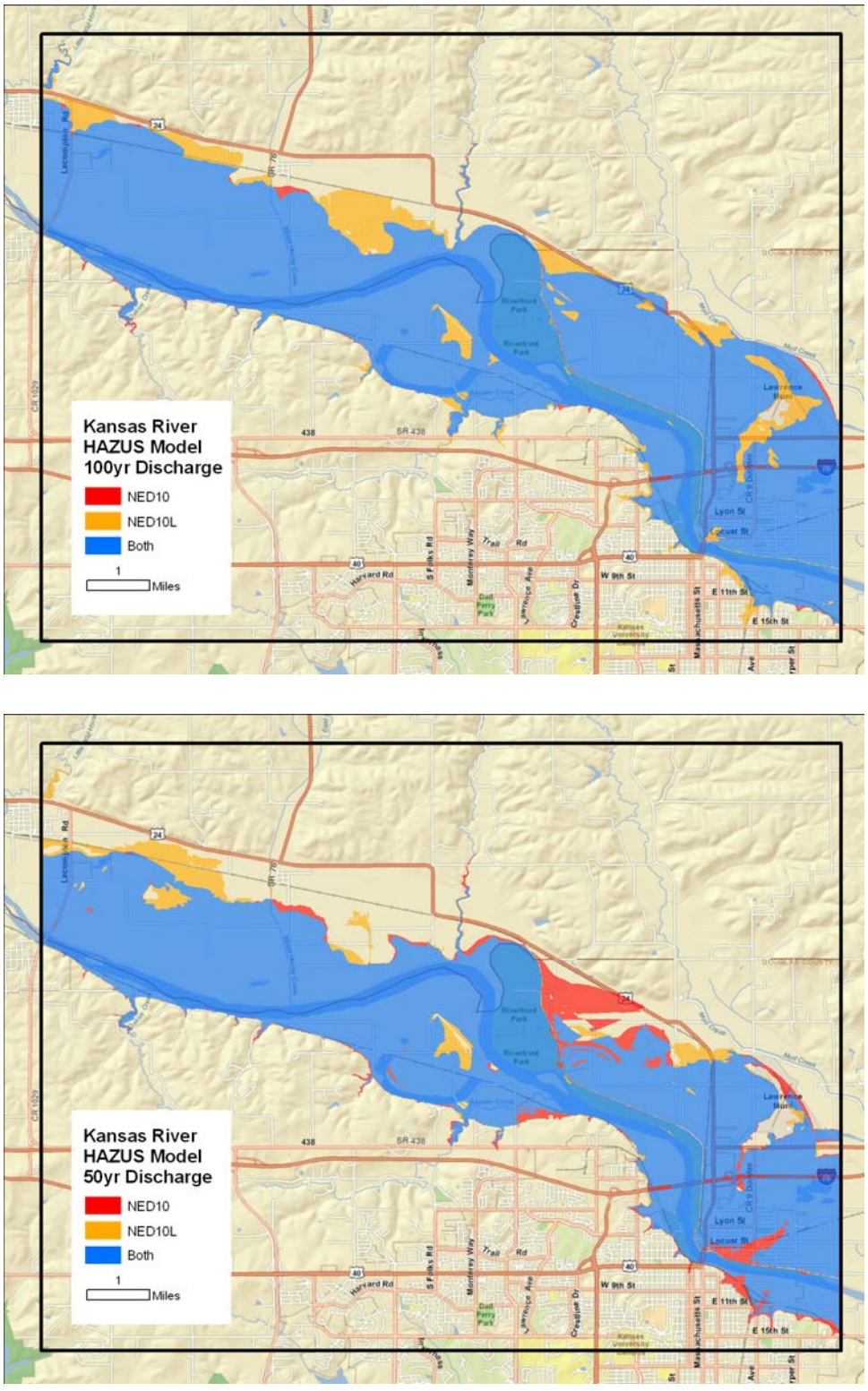

Figure 2-16. HAZUS model correspondence for the Kansas River study area.

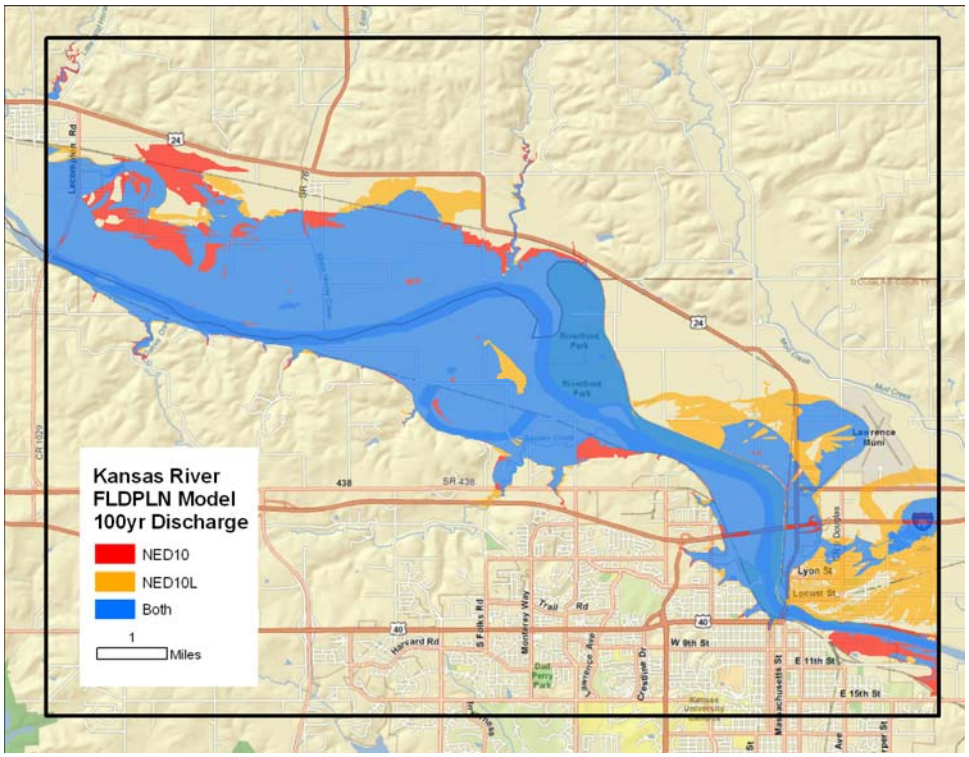

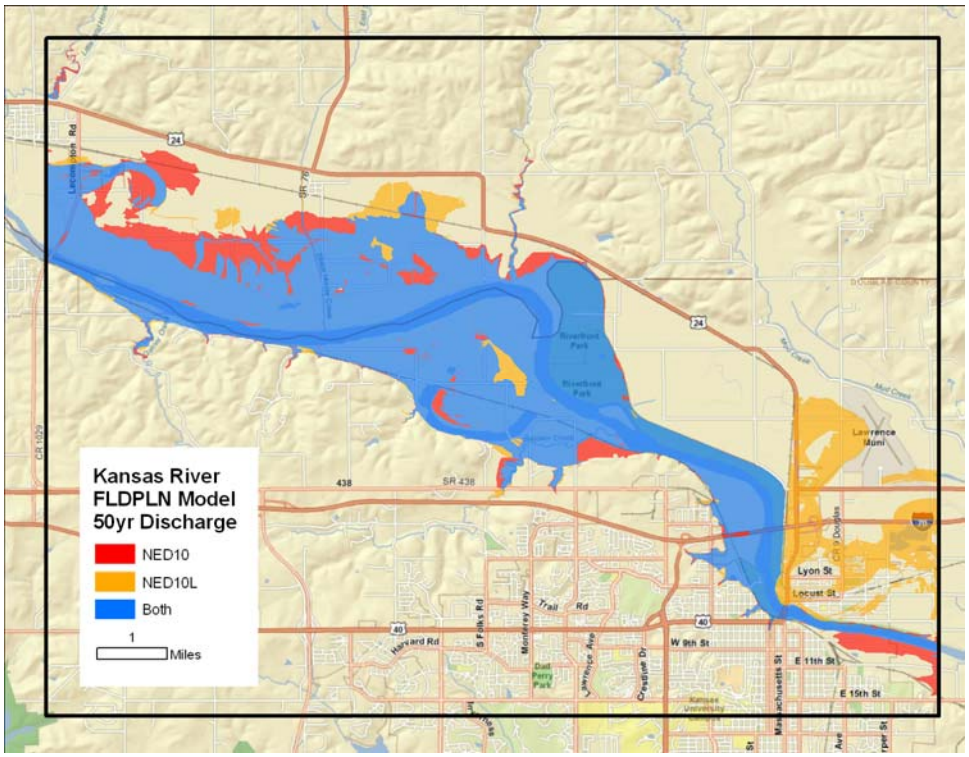

Figure 2-17. FLDPLN model correspondence for the Kansas River study area.

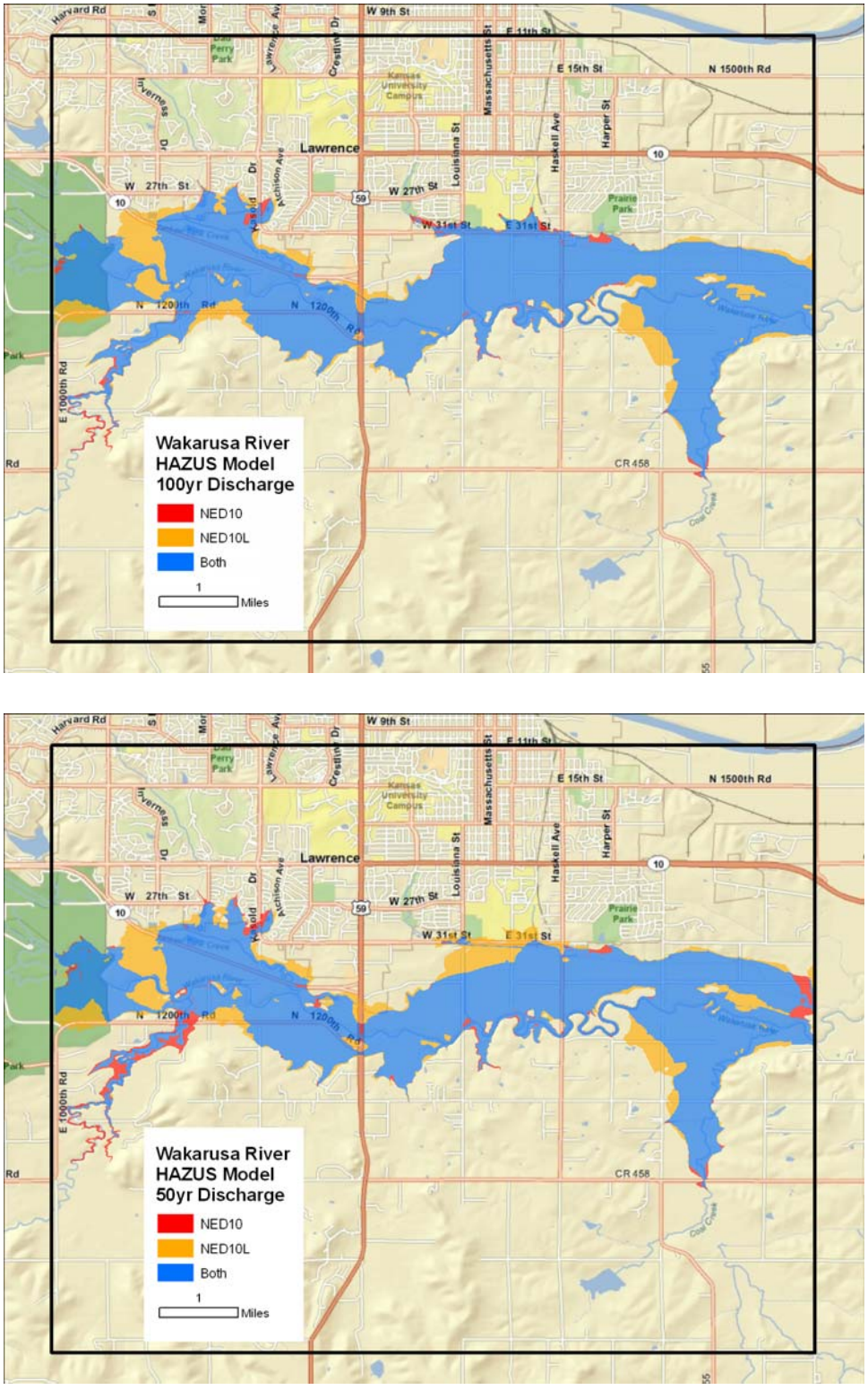

Figure 2-18. HAZUS model correspondence for the Wakarusa River study area.

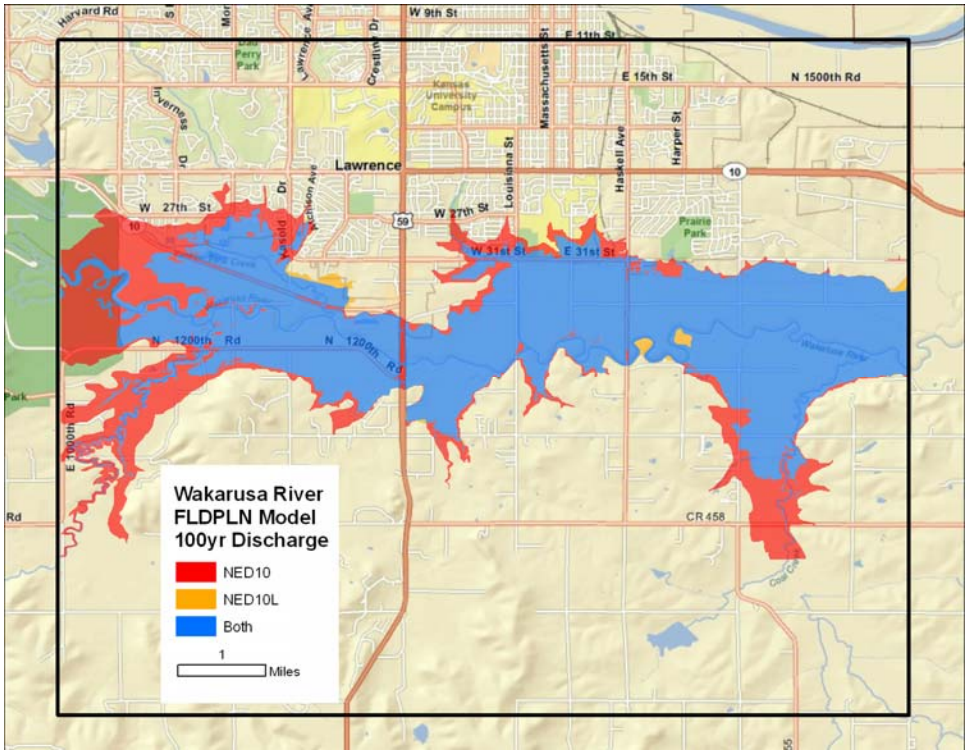

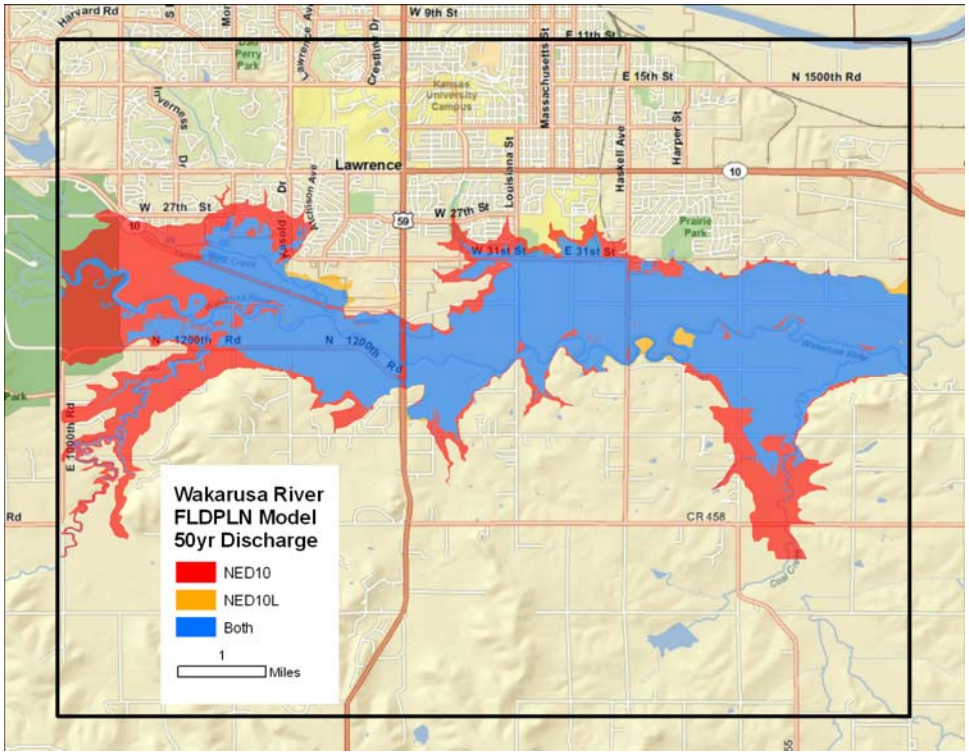

Figure 2-19. FLDPLN model correspondence for the Wakarusa River study area.

Reference Cited

(IACWD), I. A. C. o. W. D. 1982. Guidelines for determining flood flow frequency. In *Bulletin 17B of the Hydrology Subcommittee*.

Bates, P. D. & A. P. J. De Roo (2000) A simple raster-based model for flood inundation simulation. *Journal of Hydrology,* 236**,** 54-77.

Brasington, J. & K. Richards (1998) Interactions between model predictions, parameters and DTM scales for TOPMODEL. *Computers & Geosciences,* 24**,** 299-314.

Casas, A., G. Benito, V. R. Thorndycraft & M. Rico (2006) The topographic data source of digital terrain models as a key element in the accuracy of hydraulic flood modelling. *Earth Surface Processes and Landforms,* 31**,** 444-456.

Cook, A. & V. Merwade (2009) Effect of topographic data, geometric configuration and modeling approach on flood inundation mapping. *Journal of Hydrology,* 377**,** 131-142.

Crosetto, M., S. Tarantola & A. Saltelli (2000) Sensitivity and uncertainty analysis in spatial modelling based on GIS. *Agriculture, Ecosystems & Environment,* 81**,** 71-79.

England, J. F., R. D. Jarrett & J. D. Salas (2003) Data-based comparisons of moments estimators using historical and paleoflood data. *Journal of Hydrology,* 278**,** 172-196.

FEMA. 2003. Guidelines and Specifications for Flood Hazard Mapping Partners.

Gesch, D. B. 2006. An inventory and assessment of significant topographic changes in the United States. xvii, 217 leaves. Geography Dept., South Dakota State University, 2006.

---. 2007. Chapter 4 – The National Elevation Dataset. In *Digital Elevation Model Technologies and Applications: The DEM Users Manual,* ed. D. Maune, 99-118. Bethesda, Maryland: American Society for Photogrammetry and Remote Sensing.

Griffis, V. W. & J. R. Stedinger (2007a) The use of GLS regression in regional hydrologic analyses. *Journal of Hydrology,* 344**,** 82-95.

--- (2007b) Evolution of Flood Frequency Analysis with Bulletin 17. *Journal of Hydrologic Engineering,* 12**,** 283-297.

Hancock, G. R. (2005) The use of digital elevation models in the identification and characterization of catchments over different grid scales. *Hydrological Processes,* 19**,** 1727-1749.

Harmel, R. D., D. R. Smith, K. W. King & R. M. Slade (2009) Estimating storm discharge and water quality data uncertainty: A software tool for monitoring and modeling applications. *Environmental Modeling & Software,* 24**,** 832-842.

Horritt, M. S. & P. D. Bates (2001) Effects of spatial resolution on a raster based model of flood flow. *Journal of Hydrology,* 253**,** 239-249.

Kastens, J. H. 2008. Some New Devolopments On Two Separate Topoics: Statistical Cross Validation and Floodplain Mapping. In *Mathematics*, 191. Lawrence: The University of Kansas.

Kenward, T., D. P. Lettenmaier, E. F. Wood & E. Fielding (2000) Effects of Digital Elevation Model Accuracy on Hydrologic Predictions. *Remote Sensing of Environment,* 74**,** 432-444.

Mansourian, A., A. Rajabifard, M. J. Valadan Zoej & I. Williamson (2006) Using SDI and web-based system to facilitate disaster management. *Computers & Geosciences,* 32**,** 303-315.
Marks, K. & P. Bates (2000) Integration of high-resolution topographic data with floodplain flow models. *Hydrological Processes,* 14**,** 2109-2122.
Merwade, V., A. Cook & J. Coonrod (2008a) GIS techniques for creating river terrain models for hydrodynamic modeling and flood inundation mapping. *Environmental Modelling & Software,* 23**,** 1300-1311.
Merwade, V., F. Olivera, M. Arabi & S. Edleman (2008b) Uncertainty in Flood Inundation Mapping: Current Issues and Future Directions. *Journal of Hydrologic Engineering,* 13**,** 608-620.
NDEP. 2004. Guidelines for Digital Elevation Data, Version 1.0. In *National Digital Elevation Program (NDEP)*.
NGS. 2010. GPS On Bench Marks (GPSBM) Used To Make GEOID09; http://www.ngs.noaa.gov/GEOID/GPSonBM09/.
NWS. 2010. Advanced Hydrologic Prediction Service; http://www.weather.gov/ahps/inundation.php.
Ries, K. G. & J. B. Atkins. 2007. *The National streamflow statistics program : a computer program for estimating streamflow statistics for ungaged sites*. Reston, Va.: U.S. Department of the Interior, U.S. Geological Survey.
Roman, D. R., Y. M. Wang, J. Saleh & X. Li. 2009. National Geoid Height Models for the United States: USGG2009 and GEOID09. In *ACSM-MARLS-UCLS-WFPS Conference*.
Sagun, A., D. Bouchlaghem & C. J. Anumba (2009) A scenario-based study on information flow and collaboration patterns in disaster management. *Disasters,* 33**,** 214-238.
Schmitt, T., C. National Research, R. R. Ramesh & E. Jon. 2007. *Improving Disaster Management: The Role of IT in Mitigation, Preparedness, Response, and Recovery*. National Academy Press.
Singh, V. P. (1997) Effect of spatial and temporal variability in rainfall and watershed characteristics on stream flow hydrograph. *Hydrological Processes,* 11**,** 1649-1669.
Smemoe, C., J. Nelson & A. Zundel. 2004. Risk Analysis Using Spatial Data in Flood Damage Reduction Studies. 262-262. Salt Lake City, Utah, USA: ASCE.
Tate, E. C., D. R. Maidment, F. Olivera & D. J. Anderson (2002) Creating a Terrain Model for Floodplain Mapping. *Journal of Hydrologic Engineering,* 7**,** 100-108.
Tayefi, V., S. N. Lane, R. J. Hardy & D. Yu (2007) A comparison of one- and two-dimensional approaches to modelling flood inundation over complex upland floodplains. *Hydrological Processes,* 21**,** 3190-3202.
USGS. 2010. National Elevation Dataset (NED) 1/3 Arc Second; http://seamless.usgs.gov/products/3arc.php.
Valeo, C. & S. M. A. Moin (2000) Variable source area modelling in urbanizing watersheds. *Journal of Hydrology,* 228**,** 68-81.
Vardi, N. (2007) Slick. *Forbes,* 180**,** 50-50.

Wang, Y. & T. Zheng (2005) Comparison of Light Detection and Ranging and National Elevation Dataset Digital Elevation Model on Floodplains of North Carolina. *Natural Hazards Review,* 6**,** 34-40.

Weichel, T., F. Pappenberger & K. Schulz (2007) Sensitivity and uncertainty in flood inundation modelling; concept of an analysis framework. *Advances in Geosciences,* 11**,** 31-36.

Zerger, A. & S. Wealands (2004) Beyond Modelling: Linking Models with GIS for Flood Risk Management. *Natural Hazards,* 33**,** 191-208.

CHAPTER 3

A CASE STUDY: FLOOD MODEL COMPARISONS AND EVALUATIONS USING EMPRICAL DATA FROM THE 2007 SOUTHEAST KANSAS FLOOD

Abstract

In the summer of 2007 severe flooding impacted a 20-county region of southeast Kansas. Flooding occurred on all major streams in the region, many at record levels. Response to the disaster was hampered by the inability of emergency managers and responders to map inundated areas. Developing a library of modeled flood extents for communities over a range of potential flood levels can offer a resource that is easily accessed and, when combined with addition geospatial data, can provide valuable information that can be used to guide critical, time dependent decision making. In response to the 2007 flood events, the Kansas Biological Survey (KBS) has developed a segmented library of inundation extents (SLIE) with the FLDPLN model, developed at KBS, that can be accessed quickly during future events. In this study, flood surface elevations from a USACE post-flood high water mark survey and flood boundary points extracted from ASTER satellite imagery and high resolution aerial imagery are compared to flood surface elevations modeled with FEMA's HAZUS-MH, USACE's HEC-RAS model, and the FLDPLN model. In addition, a range of river stages and corresponding flood extents were modeled with the FLDPLN model and compared to modeled extents produced by HAZUS-MH and HEC-RAS. While a variety of uncertainties are present in all of these data (both empirical data from the flood event and modeled flood extents), the analyses garnered from this unique opportunity where empirical data are available for model evaluation serve as a reference point for both applications development and reliability under real-world conditions.

Abbreviations

[FEMA] Federal Emergency Management Agency

[FLDPLN] FLDPLN ("Floodplain") model used to derived a library of inundation extents

[HAZUS] FEMA HAZUS-MH flood, earthquake and hurricane model

[NED10] 1/3 arc second USGS National Elevation Dataset

[NFIP] National Flood Insurance Program

[SAR] Synthetic Aperture Radar

Terms

Stream discharge (flow): given in cubic feet per second (**cfs**), discharge is a measure of the volume of water flowing though a vertical plane oriented perpendicular to the direction of stream flow. Often referred to as a measured quantity, it is actually calculated from a set of measured velocities across the stream channel. When calculated for a range of river levels and combined with an adequate baseline of stage data (see below), discharge can be plotted on a logarithmic scale to develop a flood frequency regression equation to estimate the return period of a given magnitude flood event.

River stage: a measured quantity that relates the water surface elevation at a monitored point on a stream (stream gage) to a pre-specified reference datum with a known elevation. The reference datum is usually chosen to be below the stream channel to avoid negative stage values. With the datum and stage information, the water surface elevation at the gage location can be determined for any stage.

Depth to flood (DTF): the output of the FLDPLN model developed by Kastens (2008) relating the minimum flood depth required to inundate a non-stream pixel from a reference stream pixel. In some circumstances the DTF can be used as a proxy for stage.

Introduction

Riverine flooding occurs throughout the United States and causes billions of dollars in damage annually (Pielke 2002). Even with programs like the FEMA National Flood Insurance Program (NFIP) in place, potential loss of property and life continues to be a significant concern in many communities (National Research Council (U.S.). Committee on FEMA Flood Maps. et al. 2009). While much research effort has been applied to understanding the hydrologic and hydrodynamic processes that govern the recurrence intervals, timing, magnitude, and dynamics of flood events, for many communities there is very little information concerning the potential impact of future local flood events. One of the most effective ways to enhance flood preparedness and response is to model flood events. This is one of the primary activities of the NFIP's Map Modernization Program (Map Mod) (National Research Council (U.S.). Committee on FEMA Flood Maps. et al. 2009). The most common map product of the NFIP is known as the 100-year floodplain, commonly referred to as "the" floodplain. More accurately, it is the 1-percent-annual-chance floodplain. Although the area comprised by the arbitrary 100-year floodplain is useful for determining flood risk, particularly for insurance purposes, at best it has only a 1% chance of coinciding with an actual flood event within a given year. A more comprehensive approach for disaster response is to develop a library of inundation extents for a range of river stages that covers an expected range of events from low flow to above-record levels (Bales and Wagner 2009). During an actual flood event, appropriate inundation extent estimate maps can be created based on actual and predicted river levels.

In the summer of 2007, severe flooding triggered federal disaster declarations for twenty counties in southeast Kansas. Inadequate information relating both the real-time and predicted river stage to actual spatial flood extents hampered response efforts and contributed to the unintentional release of 90,000 gallons of crude oil into the Verdigris River as flood waters inundated an oil refinery in Coffeyville, Kansas (Vardi 2007)(Figure 3-1). It was over seven days after flood crest that ASTER (Figure 3-2) and Landsat satellite imagery was acquired and available to map the inundation extent over most of the flooded area. Inherent limitations of optical remotely sensed imagery (Voigt et al. 2007) and the paucity of any additional timely information led the author and colleagues to investigate the application of the FLDPLN model (Kastens 2008), which was developed at the Kansas Biological Survey, for production of flood inundation libraries that could be accessed during flood events to produce real-time flood extent estimates with only flood stage as the input variable. (A library consists of a set or GIS layers for each stream segment that relates stream stage to a "depth to flood" (DTF) value that can be used to map estimated flood extent for a given stage.)

A pilot project was conducted for stretches of the Marais de Cygnes, Little Osage, and Osage Rivers in western Missouri. The results showed good correspondence between flood extent predicted by the FLDPLN model, which was calibrated to USGS gage data, and actual flooding that was mapped using Landsat imagery acquired at or near flood crest during the 2007 event (Figure 3-3), with an overall accuracy of 81.7%. The only inputs required to generate the FLDPLN-modeled flood extent were the 1 arc second NED DEM (30-meter) and USGS stage crest data corresponding to the 2007 flood event for three gaging stations. The reference flood extent was digitized from the Landsat imagery by the author. To avoid

any confirmation bias, the author did not have access to the model results until after the digitization was completed. These results provided the impetus to further develop the flood mapping application.

During subsequent efforts to secure funding to develop a library of inundation extents for major streams in eastern Kansas using the FLDPLN model, two primary questions emerged: 1) is the 1/3 arc second (10m) National Elevation Dataset (NED) adequate for inundation library development, which is addressed in a separate study, and 2) is the FLDPLN model an appropriate tool for developing the inundation library, which is addressed in this study.

Existing Flood Mapping Resources

The FEMA NFIP sponsors the creation of flood insurance rate maps (FIRMS), that identify zones of flood risk based on USGS regression equations for stream flow (flood) frequency, which are used to administer a federally backed flood insurance program in participating communities. These flood zones are used by communities to guide development and limit construction of structures in areas at greatest risk to flooding. Areas designated as "zone A" are considered the 100-year floodplain, and as mentioned above, have a 1% annual chance of inundation. But from a disaster response perspective, the only flood boundary that is important is the one corresponding to the event at hand, which may be a 5000-year event or a 50-year event, or more likely any of an entire range of flood frequencies on multiple streams over multiple watersheds. Consequently, the A-zone boundaries have little relevance for disaster response. Furthermore, in many areas of Kansas FIRMS have not even been developed.

As new, higher accuracy elevation data have become available, the National Weather Service (NWS) has begun a program to develop libraries of inundation extents for a handful of sites around the county (NWS 2010). The specifications for this program require elevation data that are capable of supporting development of 2-foot contours, which qualifies most LiDAR derived elevation data. However, these extent libraries are usually limited to stream reaches within one or two miles of a USGS or NWS stream gage. For the mapped areas this is a valuable response and planning tool, but represents only a fraction of a percent of the flood prone streams across the country. Although Kansas does not have any of these sites, based on a preliminary analysis conducted by KBS, there only about 13 sites currently that meet the NWS criteria, which if mapped would be approximately 26-52 stream miles out of thousands across the state.

Sources of modeling uncertainty

Uncertainties involved in flood mapping exist at virtually every part of the mapping process. While this is true of all modeling efforts that use measured, calculated, interpolated, and extrapolated data, it is important to recognize these uncertainties, have a sense of their magnitude, and be aware of how they might affect modeled results.

Hydrologic models attempt to estimate the timing and magnitude of stream flow based on watershed and rainfall parameters. This component of flood modeling is subject to a number of uncertainties, primarily: 1) watershed characteristics, 2) storm precipitation dynamics, 3) infiltration, and 4) antecedent conditions (Singh 1997). Each of these has associated uncertainties, also. The inundation mapping under consideration in this study, however, does not rely on this variety of hydrologic modeling for real-time flood estimation,

but does implicitly though flood forecast levels issued by the NWS that use rain forecast and hydrologic models to forecast steam flow.

Streamflow is calculated by measuring flow velocity along a stream cross section, following standard protocols, for a range of river stages and combining them with surveyed cross section information to produce and estimated flow volume, usually reported in cubic feet per second (cfs). From these data a stage discharge relationship can be calculated to produce a stage-discharge lookup table for any stage. For typical conditions, streamflow value errors can range from 3% to 19%, and as high as 42% in the least favorable cases (Harmel et al. 2009).

Flood frequency is commonly used as a tool to guide design and development decisions by examining historical stream flows to determine areas that are likely to flood with a specified minimum frequency, often the 100-year flood. The most commonly used specifications for determining flood frequency are outlined in Bulletin No.17B authored by the Interagency Advisory Committee on Water Data ((IACWD) 1982), which recommends using a Log-Pearson Type III probability distribution (Merwade et al. 2008b). This analysis relies on historical stream flow records, and often these records have a baseline shorter than the average recurrence interval for the design storm of interest. More recent work suggests that this method needs to be updated to a hybrid approach that includes paleoflood data, when available, and also uses an iterative least squares regression in a pooled regression technique (England et al. 2003, Griffis and Stedinger 2007a, Griffis and Stedinger 2007b). In addition to the uncertainty of these techniques themselves, other factors contributing to modeling errors include selection of data series, assumptions about probability distributions, climate trends, land use changes, years where no floods have occurred, and missing data

must be considered (Merwade et al. 2008b). Regional flood frequency analysis where no flow data exist relies on hydrologic models that use watershed characteristics and rainfall records to develop estimated flood frequencies. There is significant error associated with these approaches, like those used in the National Streamflow Statistics, which range from 15% to more than 100% (Ries and Atkins 2007).

Because terrain data represent the 3-dimensional surface over which flood waters flow, terrain data quality has a direct affect on flood extent estimates. It affects hydrologic model discharge values (Brasington and Richards 1998, Valeo and Moin 2000, Hancock 2005, Kenward et al. 2000), water surface elevations derived from flood models (Marks and Bates 2000, Casas et al. 2006), and the estimated horizontal extent of flood inundation (Tate et al. 2002, Wang and Zheng 2005, Merwade et al. 2008a, Merwade et al. 2008b). There is a wide range of uncertainties associated with elevation datasets, such as those pertaining to source data, interpolation techniques, cell resolution, data fusion, hydrologic conditioning, and others (Merwade et al. 2008b). The potential cumulative influence of these uncertainties and the uncertainties associated with streamflow, flood frequency, hydrologic modeling, and hydraulic modeling point to the need to develop an approach that integrates an uncertainty analysis into mapped flood extent estimates (Smemoe et al. 2004, Crosetto et al. 2000, Merwade et al. 2008b, Weichel et al. 2007).

Objective

In order to assess the needs and capabilities of current flood preparedness initiatives at KBS, this study addresses the following questions: what are the capabilities and limitations of the FLDPLN model for inundation estimation?

Previous work

Recent work specifically related to the variability of model outputs using different terrain source data has been done on two river reaches, one in North Carolina and one in Texas. The authors evaluate discrepancies between modeled results for multiple elevation data sets, which included 1 arc second NED, 1/3 arc second NED, LiDAR, and integration of surveyed cross-sections with all three aforementioned data sets (Cook and Merwade 2009). Two models, HEC-RAS 4.0 and FESWMS-2DH 3.1.5, were run using all six topographic data sets. Results were evaluated to determine the effect of horizontal resolution and vertical accuracy on flood extent mapping, as well as to highlight the discrepancies between these two models at varying resolutions and vertical accuracies. In general, the flood extents mapped using the FESWMS-2DH model were smaller compared to the HEC-RAS results, and flood area tended to be reduced with greater horizontal resolution and greater vertical accuracy. There were no empirical flood data available; therefore evaluation of modeled flood extent accuracy was not possible.

Mason et al. (2009) used ERS-1 synthetic aperture radar (SAR) data, acquired during a low level, 5-year flood event in Oxford, England, fused with LiDAR elevation data and modeled flood extent of the LISFLOOD-FP model to evaluate the use of the height-based probability statistic versus the F statistic (Bates and De Roo 2000), a performance-based measure of areal extent map accuracy. The height-base statistic, using an active contour model for the fused SAR/LiDAR data as the reference value, which effectively extracts elevation values at the waterline as determined by the SAR imagery, was found to offer reduced uncertainty in the flood map compared to the F-statistic when evaluating the LISFLOOD-FP based model. It is worth noting that SAR imagery, as opposed to optically

based sensors, has the advantages of acquisition by day or night, in all weather conditions, and is able to penetrate tree canopies. This makes it an ideal reference against which to evaluate modeled flood events, and to calibrate models. Although this is an interesting and valuable approach, it requires both high accuracy elevation data, like LiDAR, and SAR imagery of a flood event to be replicable.

Ad hoc flood mapping has been done with FEMA HAZUS-MH software at a local level, particularly in response to isolated flood events. KBS evaluations have shown that HAZUS modeling has a number of limitations that make it cumbersome and potentially unsuitable for inundation extent library production. These limitations include software instability, discontinuous flood depth value, insufficient stream buffer distances, difficulty handling backwater effects, and excessive user interaction for library development. Use of HAZUS is certainly appropriate for many applications (Scawthorn et al. 2006a, Gall et al. 2007), but for large area inundation extent library development it has many limitations.

As mentioned above, in a limited number of areas the National Weather Service has partnered with state and local cooperators to develop inundation libraries for river segments directly surrounding particular NWS and USGS gage locations (Merwade et al. 2008b). The library extents are limited to approximately one to two miles upstream and downstream from the gage location. As per NWS specifications, the development of these libraries requires the use of elevation data that will support 2-foot contours, generally LiDAR or photogrammetrically derived elevation, and the use of approved hydrodynamic flow models, such as HEC-RAS.

FLDPLN Model

Kastens (2008) developed the FLDPLN model, which is a static computational model that relies entirely on topographic data. After standard fill, flow direction, and flow accumulation procedures are applied to a DEM, this model utilizes a two-step, iterative backfill and spillover procedure that is seeded with stream pixels derived from the flow accumulation layer. In essence, each stream pixel is flooded to a specified depth, or increment size, and all pixels in the upstream watershed as specified by the corresponding flow direction layer, are classified as flooded if the reference pixel elevation value plus the step size value exceeds the boundary pixel value. This is followed by a spillover step, which addresses discontinuities created by flow divides. These steps are repeated in small increments to build a library of inundation extents. The following is a synopsis of the FLDPLN algorithm (from Kastens, 2008):

i) Initialize the depth-0 floodplain to be the stream segment. Initialize flood depth $h = dh$, for some depth increment dh.

ii) Use the topography and the gradient direction field to backfill flood outward from the floodplain boundary to depth h. Add these points to the current floodplain.

iii) Locate points on the current floodplain boundary where spillover flooding will occur. Determine the "spillover flood depth" for each spillover point.

iv) Use the gradient direction field to determine new floodwater routes originating from the spillover flood points. Halt each route when it returns to the main channel downstream, or when it returns to the current floodplain, or when it reaches the study area boundary, whichever comes

first.

v) Backfill flood each new floodwater route to its respective spillover flood depth.

vi) Add the newly flooded points to the current floodplain. Since these new points largely will have resulted from backfill flooding, it is possible that additional points will now be present on the floodplain boundary that require spillover flooding.

vii) Repeat steps *(iii)* – *(vi)* until the steady-state is reached (optional).

viii) Increase *h* if necessary, and go back to step *(ii)*.

Evaluation of the FLDPLN model is the primary focus of this study. As a relatively novel modeling approach, it is important to evaluate the model's performance from a variety of perspectives, which are outlined below.

Study Area and Data

South-central Montgomery County, Kansas, was selected for the study area. The primary requirements for this analysis are the availability of 1/3 arc second NED data (the NED source data vintage for Montgomery County ranges from 1959 to 1962), remotely sensed imagery that captures flood extents, other supporting ground reference data such as USACE high water mark (HWM) points from the 2007 event, and the availability of additional flood models with which to compare the FLDPLN model. The FEMA HAZUS model and the HEC-RAS model, which were prepared by URS Corporation under contract with FEMA, were used. One additional requirement was the availability of stream gages with stage data for the 2007 event and a stage-discharge table. There is one USGS river gage

and one NWS gage (Figure 3-4) within the study area, both of which provided reference data for the study.

The study area is an approximately 52 square mile area that encompasses the city of Coffeyville and the surrounding area along the Verdigris River (Figure 3-5), extending nine miles to the north and two miles to the south of the city to near the Oklahoma-Kansas border. The geometry of the study area bounding box represents the region for which flood model output was available for all three models used in the research. This area experienced severe flooding in 2007 and exemplifies the most severe flooding of that event.

Methods

The capabilities and limitations of the FLDPLN model for inundation estimation were assessed through the following tasks:

4) Compare FLDPLN, HEC-RAS, and HAZUS flood extent estimates with the F-statistic for hypothetical floods modeled at 5 ft stage increments based on USGS gage stage at Coffeyville, and for the 2007 flood event based on the NWS gage at Coffeyville.
5) Compare HWM elevation values to water surface elevation values for FLDPLN, HEC-RAS, and HAZUS model results for 2007 flood event.
6) Compare flood boundary elevation values obtained from post-flood ASTER and aerial imagery to water surface elevation values for FLDPLN, HEC-RAS, and HAZUS model results for 2007 flood event.

The procedures used to perform each one of these steps are outlined below.

Flood Model Inundation Extent Comparison

In the absence of empirical data against which to compare model results, it is insightful to compare results between models for the same, or appropriately similar, inputs. Although empirical flood data are used in the second and third tasks, those analyses account for only a single magnitude flood event. In order to examine the performance of the FLDPLN model relative to the HAZUS and HEC-RAS models, in the first task elevation data were prepared, input parameters for each model were determined, flood simulations were performed for each model using a range of flood stages, and the corresponding flood extent results were evaluated and compared.

The first data preparation step involved acquiring the NED10 elevation data from the USGS (ned.usgs.gov) and conditioning the DEM with the ArcHydro "fill", "flow direction", and "flow accumulation" procedures. In addition to being standard DEM processing steps for the models, because the FLDPLN model uses the stream channel derived from the filled DEM, the elevation value used to calculate the DTF corresponding to each simulated flood, described below, must come from the "filled" DEM.

Because the FLDPLN model requires a stage value to produce the appropriate flood extent, and HAZUS and HEC-RAS require discharge values, it was necessary to have at least one reference that could provide a stage-discharge relationship to supply inputs to all three models that represented the same set of hypothetical flood events. Although there are two stream gages within the study area on the Verdigris River, the gage that is just south of Coffeyville (USGS 07170990) has a stage-discharge table that is well documented and readily available. The stage-discharge table for the USGS Coffeyville gage (waterdata.usgs.gov), was downloaded and examined in Excel. Discharge values at 5 ft

increments were extracted from the table, ranging from 5 to 45 ft (Table 1, Figure 3-6). Stage values in the table are reported in 1/100 ft increments, ranging from 2.31 to 46.60 ft, and flow values are given to three significant digits, ranging from 1 to 400,000 cfs. The stage values were translated into DTF values for FLDPLN model input by adding the stage value (e.g. 10 ft) to the gage datum value of 675 ft (NAVD88), then subtracting that value from "filled" NED10 stream pixel elevation value (683.42 ft) for the gage location (Table 3-1). For example, at the 10 ft stage the DTF value would be 1.57 ft. The 5 ft stage was not used because the DTF value of -3.44 ft, which means that 5 ft stage is lower than the water surface elevation represented in the DEM and not represented in the FLDPLN model output, hence, only stage values from 10 to 45 feet were modeled.

For each model, the appropriate discharge values, ranging from 919 cfs to 320,000 cfs, were applied in successive model runs for each 5 ft stage increment (Table 3-1). The HEC-RAS and HAZUS outputs consist of both a flood depth grid and a flood boundary polygon. In the case of the FLPLN model, the appropriate DTF values were used to extract the appropriate pixel set and the raster outputs from the FLDPLN model were converted to polygons for the analysis. The full 0 to 15 m DTM raster from which the custom extents are extracted is shown in Figure 3-7. The eight flood stages modeled for each of the three models yielded a total of 24 separate flood extent polygons (three for each stage). The Shape_Area field for each flood extent polygon layer was updated using the "Calculate Geometry" field operator. For each polygon attribute table a "code" field was added and given the values 1, 2, and 4 for FLDPLN, HEC-RAS, and HAZUS layers, respectively. In the next step the three layers corresponding to each stage were "unioned" in ArcGIS. A code_sum field was then added and populated with the sum of the code fields, one for each

contributing layer. The result was 7 possible sums, 1,2,3,4,5,6,7, representing the 7 unique model occurrence conditions of the union polygons (Table 3-2). The results were assembled in an Excel spreadsheet for analysis.

The total area mapped for each code_sum was used to evaluate correspondence between model pairs, and also between all models. The formula used to calculate this measure, known as the F-statistic (Bates and De Roo 2000, Cook and Merwade 2009, Kastens 2008, Horritt and Bates 2001, Tayefi et al. 2007), is:

$$F = 100 * (A_{op}/(A_o+A_p-A_{op})) \quad \text{Eq. (1)}$$

where A_o: observed area of inundation (model A)

A_p: predicted area of inundation (model B)

A_{op}: area that is both observed and predicted as inundated.

The calculation for three models is achieved using the following equation:

$$F = 100 * (A_{op}/(A_o+A_p + A_q -A_{op})) \quad \text{Eq. (2)}$$

where A_q: predicted area of inundation of model C

A_{op}: now also requires the intersection of model C

The above steps were also applied to produce modeled inundation extents and depth grids for the 2007 flood using archived crest stage data collected at the time of the flooding. These results were used in the two tasks described below. The only difference between the two procedures was the use of the NWS gage stage value to identify the appropriate DTF

value for the FLDPLN model and the corresponding peak discharge of 169,000 cfs used for the HEC-RAS and HAZUS models. The NWS gage data were used for the 2007 modeling both because the historic data for this gage were more readily available and the NWS is more centered in the study area making it a more appropriate gage to use for actual flood response efforts in the study area.

High Water Mark Comparison

Within a month of the 2007 flood event, high water mark elevation data were collected by URS Corporation under contract with USACE (FEMA 2008). Altogether, 213 points were collected along five major streams, the Verdigris, Neosho, Fall, Marmaton, and Little Osage Rivers, and of those 13 were within the study area boundary along the Verdigris River (Figure 3-5). High water marks were identified on a variety of objects (utility poles, trees, buildings, signs, culverts, etc.) and surveyed to 0.25 foot vertical and 10 foot horizontal accuracy with a 95% confidence level. Examples of ground level photographs of HWM location are shown in Figure 3-8. For this study the final HWM data were acquired from the FEMA Region 7 office in Kansas City and were delivered via DVD in ESRI shapefile format. The data contained horizontal coordinates and elevation value fields, both NAV29 and NAVD88 datums, representing the flood's highest water surface elevation during the 2007 event those points..

Hawth's Tools' (www.spatialecology.com) "intersect point tool" (IPT) was then used to extract land surface elevation values from the NED10 dataset for each of the HWM points. The IPT appends the extracted values in a new column in the feature attribute table of the HWM layer. The next step involved extracting flood depth and DTF values from the

HAZUS flood depth, HEC-RAS flood depth, and FLDPLN DTF layers, which were derived as described in the first task, for each of the HWM locations. Again the IPT was used to perform this function and additional fields were appended to the attribute table with each operation. One point did not return a flood depth value from the HAZUS flood depth layer because the model did not indicate flooding at that location. A manual query was performed with the "information query tool" in ArcGIS for the elevation value of the closest HAZUS flood boundary pixel. This value was then differenced with the elevation value from the NED10 corresponding to the HWM point and entered into the attribute table as a negative flood depth.

For each point, flood surface elevations were calculated from the corresponding NED10 elevation and flood depth or DTF values. For the HAZUS and HEC-RAS models, the flood depth value was added to the NED10 value. For the FLDPLN model, the extracted DTF value was subtracted from the 10.41m DTF value applied to the model to create the 2007 flood extent. This difference represents the flood depth at the HWM point. Each derived flood surface elevation was then subtracted from the corresponding HWM value to determine the water surface elevation error for each model at each point. Error statistics were calculated from these results.

Image Derived Flood Boundary Comparison

While the final error analysis of the image derived flood boundary elevations is the same as for the HWM data, the method used to derive the elevation values was quite different. Both methods use a water surface elevation as the reference to test model results, but in general, HWMs are located within the interior of the actual flood extent and modeled

flood surface elevation values are calculated from flood depths, whereas image-derived flood boundary elevation value analysis uses zero depth, "shoreline" values for both reference and modeled data. There were two primary steps involved: 1) identify flood boundary locations on satellite and aerial imagery to derive the ground reference shoreline elevation data, 2) snap the identified point to the closest modeled flood boundary for each model to derive the modeled shoreline elevation data.

Two image sources were used in the first step to derive the reference data: 1) ASTER satellite imagery acquired on July 6th, 2007, and 2) 1-foot natural color aerial imagery acquired on approximately July 10th, 2007. The ASTER data have a 15m horizontal resolution with 3 spectral bands - green, red, and near-infrared. The aerial imagery was acquired within 3-4 days of the ASTER image, although no exact date information could be determined. A graduate research assistant was tasked with digitizing points along the flood boundary that could reasonably be identified as such. This was a subjective determination to some extent, but for each point there was some indicator, usually the boundary of visible vegetation damage in otherwise homogeneous grass or crop fields, that signified the flood boundary. Separate point layers were created for the ASTER and aerial image derived points. For each flood boundary point, the IPT was used to extract the corresponding NED10 elevation value.

The second step required horizontal snapping of the points to the closest flood boundary for each modeled flood extent. All flood boundary polygons were converted to polylines to satisfy the requirements the Hawth's tools "snap points to line tool" (SPLT). The SPLT was then used, with a maximum distance tolerance of 5000 ft, to reposition points to the closest corresponding modeled flood "shoreline". Visual inspection of point

proximities to boundary lines indicated that most points would either snap to a boundary that was nearby, or snap laterally, perpendicular to the flow direction, which would yield an appropriate elevation value (the movement could be thought of as moving along a cross-section line as opposed to up or downstream). Because the modeled flood extent boundaries were clipped in some locations at the study area boundary, points that snapped to this clipped boundary were eliminated because they did not represent zero-depth flood boundary locations. This process yielded with 260 and 200 reference points (Figure 3-5) derived the aerial and ASTER imagery, respectively, and separate layers for analysis of each model/image-source combination, 6 layers in all.

The IPT was then used on each layer to extract the corresponding NED10 value at the previously identified, modeled flood extent boundary points. The image point elevation value was subtracted from the elevation value for the snapped location for that point, which shows the difference between the image-derived shoreline elevation and the modeled shoreline elevation. This value represents the vertical overestimate or underestimate of the modeled flood surface elevation. The 6 point attribute tables were assembled in an Exel file for analysis in the same manner described above for the HWMs.

Results

Flood Model Inundation Extent Comparison

The inundation extent comparison showed the greatest correspondence with major flood stages, reaching as high at 91.4% at the 45 ft stage between the FLDPLN model and HEC-RAS, 83.4% between FLDPLN and HAZUS, 78.2% between HEC-RAS and HAZUS, and an overall correspondence of 77.2% (Table 3-3). Correspondence at the 10 ft stage was

below 40% for all comparisons, and actually dipped slightly at the 15 ft stage, then continued to increase with each increment thereafter (Figure 3-9). Interestingly, the 25 ft stage F-statistic value was virtually identical between model pairs at 46%, but with only 30% correspondence among all three models. It was at this stage the FLDPLN model and HEC-RAS transitioned from the worst corresponding pair to the best. Figure 3-10 shows that HEC-RAS consistently models more flooding at all stages. Below the 25 ft stage the FLDPLN model significantly trails HEC-RAS in overall area flooded, and falls slightly behind HAZUS. Just after the 25 ft stage the FLDPLN model overtakes HAZUS and begins to converge with HEC-RAS in overall are flooded.

It is not surprising that at low levels the correspondence is poor. Different thresholds for overbank flow, which vary depending on the model design and configuration (such as cross section placement), can result in one model showing large lateral flooding in low lying areas of the floodplain while another may still be confined to the stream banks in some areas. But, as Figure 3-11 indicates, as flood levels become higher these influences are minimized when flood waters spread laterally across the floodplain, and correspondence levels rise quickly, then begin to level off for stages consistent with major floods. As the low-slope floodplain transitions to steeper rises on the edge of the floodplain, the physical characteristics of the floodplain valley govern the convergence of flooded area correspondence.

The modeled 2007 flood offers a unique opportunity to evaluate the models with imagery acquired shortly after flood crest. The flood extents for all three models are shown in Figure 3-12. The 2007 comparison, which used 168,500 cfs for the discharge value for HAZUS and HEC-RAS and a 34.12 ft DTF value for the FLDPLN model, showed good

correspondence between HEC-RAS and FLDPLN models (91.6%), but significantly poorer correspondence between the other pairings and among all three, ranging from 78.7% between FLDPLN and HAZUS and 77.9% for HEC-RAS and HAZUS to 75.6% among all three. This, however, is consistent with trends shown for correspondence vs. flood stage in Table 3-3. One factor that may be affecting the HAZUS model performance is an apparent limit to the lateral distance that cross sections will extend. Discontinuities in flood depth reveal performance issues with the software. Figure 3-13 shows one example where flood boundary flood depths range from 3 to 11 ft. Unless there is a special circumstance like a sheer-faced bluff, flood boundaries should be approximately zero-depth. There are several implications of this type of error. From a planning and response perspective, this would require close scrutiny of all flood boundary pixels to identify areas that are mapped incorrectly when using the HAZUS model. *Ad hoc* means such as a local level-set operation may provide adequate results to guide limited manual correction to these discontinuities, but in a disaster situation that could lead to delayed response and lead to faulty decision making. In some sense, though, this also means that HAZUS has the potential to map better than indicated here, given that this "bug" is not a significant factor for some flood mapping scenarios.

Figure 3-14 shows a high resolution aerial image of a residential area in east Coffeyville that was inundated during the flood. The flood boundary lines show that the FLDPLN model performed the best at identifying the flood boundary, with HEC-RAS overestimating the flooding, and HAZUS underestimating. Point samples taken along the flood boundaries show that the HEC-RAS boundary is about 4.2 ft higher in elevation than the FLDPLN boundary, and the HAZUS boundary is about 1.3 ft lower. This shows a

greater than 5.5 ft range in flood surface elevations, which is significant in terms of potential flood impact, particularly in low slope areas, but it is consistent with the uncertainty of the underlying source data, the NED10.

High Water Mark Comparison

For the HWM error calculation, the modeled water surface elevation was subtracted from the reference water surface elevation, so positive values represent underestimates and negative values represent overestimates The surveyed HWM comparison revealed some anomalies in the modeled water surface elevations as well as some anomalies in the HWM data (Table 3-4). For example, Figure 3-15 shows HWM 07-V15 has a value of 723.22 and 07-V16 a value of 716.27, a difference of 6.94 ft. These two points, however, are only separated by 0.72 miles. This likely represents a greater gradient that can be explained under the physical circumstances, and is far greater then others with similar proximity. While obstructions can create backwater effects that raise the water surface elevation, this discrepancy is difficult to explain. Certainly there is some element of judgment that comes into play when determining what mark on a vertical object represents a high water mark. In view of these discrepancies, the reported accuracy of 0.25 ft is possibly misleading.

Steep vertical landforms can also lead to anomalies that don't represent the difference between actual and modeled flood surface elevations. Figures 3-16 and 3-17 show the position of HWM 07-V21 on a steep bluff on the western edge of the river valley. Horizontal positioning error may be either of the surveyed point itself or, more likely, the underlying NED10 or the HAZUS flood depth map, which is derived from the NED10, and is automatically reprojected by HAZUS during one its initial modeling procedures. Nearest

neighbor resampling is used, which also leads to anomalies and artifacts. The cautionary message is that reference data should be scrutinized for potential complications. The error in the flood surface elevation was calculated to be 16.9 ft (underestimate) at this location, which is almost certainly error attributable to horizontal alignment of data layers, not the model performance.

Where large errors do exist, in many cases they are likely due to issues like the one above. For the FLDPLN model, however, there may be additional factors. Because a single DTF value is determined from the gage stage, in regions farther from the reference stage the stage value is less reliable. This can lead to errors like the ones observed for HWM 07-V59, 07-V23, and 07-V22, which are -8.82, -7.36, and -12.45 ft, respectively. Conversely, for the rest of the points the FLDPLN model generally performs better than the models, with an RMSE of 3.15 ft and a median of 0.83, compared to RMSEs of 3.80 and 6.02 and median values of -3.21 and 3.13 ft for HEC-RAS and HAZUS, respectively. Summary statistics are given in Table 3-4 for all 13 HWM points and for the 10 where the FLDPLN model performance reflected the use of the most appropriate reference elevation value.

Overall, HAZUS performed the poorest in both sets, while HEC-RAS and FLDPLN performed comparably in the set of 10 points and both showed decreased performance with all 13 points, although the FLDPLN model more so with a drop in RMSE of 3.15 to 5.64 ft. One interesting point to note is that while HEC-RAS values are skewed toward overestimated flood surface elevations, and HAZUS toward underestimates, the FLDPLLN model remains the least biased with mean and median errors closer to 0. A more detailed analysis may reveal that the FLPLN model is better at representing a smooth water surface, which is likely due to the iterative, raster based backfill and spillover algorithm that is the

basis for the model. HAZUS and HEC-RAS both use a triangulated irregular networks (TIN) method for flood surface generation, which can produce unnatural, uneven surface representations that are transferred to the flood depth grids.

Image Derived Flood Boundary Comparison

The results for the image derived flood boundary point evaluation show some of the same uncertainty issues as above, with some points positioned on steep slopes where horizontal positioning inaccuracies can inflate reported vertical errors. However no attempt was made to remove points for any reason other than ones that snapped to boundaries resulting from truncated tributaries on the study area boundary, as indicated in the methods section. While point removal could be justified, it was decided that, rather than biasing the error, the analysis would be considered as a whole and potential sources of error acknowledged and left for later analysis if justified for specific applications.

While the aerial image point determinations were largely based on silt and mud visible on low lying vegetation, the ASTER imagery relied on apparent damage to vegetation that was visible primarily due to the inclusion of near-infrared (NIR) band in the imagery, which is particularly sensitive to vegetation health. Photosynthetically active plants reflect highly in the NIR, which means that healthy vegetation appears red in the false color composite representation of the ASTER imagery (Figure 3-12). While the horizontal resolution of the aerial imagery is significantly greater than that of the ASTER imagery, 1 ft compared to 15 m (which means that there approximately 2400 aerial image pixels to every ASTER pixel), the potential horizontal positioning uncertainty is not viewed as significant compared to the vertical uncertainty of the NED10. In other words, if the flood boundary

point were off by one ASTER pixel, the resulting difference in the extracted elevation values would not be significant compared to the inherent uncertainty of the elevation values of the NED10 data. It should be noted, however, that increased slope exacerbates the potential for larger errors attributable to this factor. With a flood of this magnitude, it is often the steep slopes of the valley walls that halt the lateral spread of flood waters, so the boundaries by their nature will often occur on steeper terrain during high flow conditions.

HAZUS performed better with the image-derived points than with the high water marks, and HEC-RAS and the FLDPLN model showed increased error (Table 3-5). For both reference data sets, HAZUS demonstrated nearly half the RMSE of the FLDPLN model, 5.32 and 10.46 ft for the aerial derived points, and 5.30 and 10.43 ft for ASTER, respectively. HEC-RAS fell in the middle with 8.30 ft and 7.53 ft RMSE for the aerial and ASTER comparisons, respectively. All three models showed tendencies for underestimating flood surface elevation when referenced to the aerial image points, while only HAZUS moved toward a slight underestimation for the ASTER reference.

The apparent overestimation tendencies of HEC-RAS and the FLDPLN model compared to HAZUS were surprising given the overall superior visual correspondence between the ASTER imagery and the other two models. This raises questions regarding the possibility of a visual interpretation bias with the image based approach. It would be worthwhile to make a more objective determination like SAR image classification flood boundaries and compare them to a similar set of image derived points to determine the magnitude of any bias, but no SAR data were available for this flood event.

Conclusions

The multiple stage model performance comparison raises as many questions as it answers. As expected, correspondence generally increases with increased stage, but low stages showed tremendous variability. This fact calls for closer examination of the models, and preferably the acquisition of low flood stage imagery for verification. Radar imagery, which is increasingly being used to map flooded areas during major disasters, may provide sources of empirical data. At present, the author is collaborating with counterparts at the University of Wisconsin on a project to evaluate the FLDPLN model as an image mask for radar image classification. Wisconsin experienced major flooding in 2008, as did Iowa, which prompted a wealth of data collection, both in terms of satellite imagery and post-flood assessments. As part of this effort, additional resources may be put toward comparisons similar to those made in this study. The motivation for the collaboration is to provide tools for use during disaster response in connection with activations of the International Charter "Space and Major Disasters" program, an agreement among ten member nations for "the coordinated use of space facilities in the event of natural or technological disasters" (http://www.disasterscharter.org).

An advantage to the high water mark analysis is that the reference elevations are higher quality compared to the NED10. It also allows an evaluation of HAZUS that does not consider the HAZUS flood boundary discontinuity problem. While the HWM analysis displayed the potential of the HAZUS model, it also under-represented the potential for error in the areal extent maps produced. The high water mark analysis showed that, at least for this major flood, the FLDPLN model performed well.

The flood imagery boundary point analysis highlighted complexities of compounding errors. Although the error statistics for both image sources, ASTER and aerial, were consistent with each model, without some truly *in situ* reference data, the results are difficult to interpret. The uncertainty of the visual interpretation approach to boundary identification, the equivalent uncertainty of both the reference point elevation values and the modeled boundary point elevation (the one extracted from the snapped reference points), and that of steep-sloped reference point locations, and the associated compounding of horizontal positional error on elevation values make it difficult to come to any firm conclusion regarding this approach. Although of limited sample size, the HWM data can serve as a reference regarding the impact of these errors because the HWM elevation is more reliable. No HWMs were zero depth (although 07-V23 is questionable), the average water depth was 4.8ft, ranging from 3.3 to 6.95 ft, and surveyed water surface elevation was certified to 0.25 ft. In terms of error reduction, this is a favorable dataset for accuracy assessment.

This study was not an exhaustive analysis of 2007 flood event, but it did address some of the open questions concerning flood modeling. LiDAR derived elevation data would certainly have improved the analysis, and may be possible in the near future with the scheduled acquisition of LiDAR for this area in the coming months. Emergency management personnel in Montgomery County have expressed interest in developing a library of inundation extents based on these LiDAR data, and the results presented here will be valuable for comparing model performance with improved elevation data.

Tables

Table 3-1. Stage-discharge values taken from the Table for USGS gage 07170990 used to produce flood extent estimates for a range of river levels with the HEC-RAS and HAZUS models. Equivalent DTF values, calculate from river channel elevation values, gage datum, and stage, are also shown. These values are used with the FLDPLN model.

Stage (ft)	DTF (ft)	Discharge (cfs)
5	-3.44	919
10	1.57	6,470
15	6.56	13,700
20	11.58	20,200
25	16.57	26,600
30	21.55	34,200
35	26.57	63,500
40	31.56	150,000
45	36.58	320,000

Table 3-2. Correspondence Key. The "Y" and "N" represent the "truth" value of whether a polygon in the "unioned" layer of all three model's flood extent polygons was flooded by that columns model, and the 0, 1,2, and 4 in parenthesis represent the value assigned to each model's flood extent polygon in the attribute table before the layers were "unioned." The sum of these values across each row is given in the Code_sum column, which represents all unique combinations of model correspondence between FLDPLN, HEC-RAS, and HAZUS. Figure 3-11 show s these correspondences mapped for stages 10 ft through 45 ft.

Model-Flood Status			
FLDPLN (1)	HEC-RAS (2)	HAZUS (4)	Code Sum
N (0)	N (0)	N (0)	**0**
N (0)	N (0)	Y (4)	**4**
N (0)	Y (2)	N (0)	**2**
N (0)	Y (2)	Y (4)	**6**
Y (1)	N (0)	N (0)	**1**
Y (1)	N (0)	Y (4)	**5**
Y (1)	Y (2)	N (0)	**3**
Y (1)	Y (2)	Y (4)	**7**

Table 3-3. F-statistic correspondence figures for each model pairing and between all models for each 5 ft river stage and for the 2007 flood. These results are also displayed graphically in Figure 3-9.

	Model Correspondence F-Statistic			
	FP-HR	FP-HZ	HR-HZ	All
10	19.1	38.3	36.9	15.9
15	12.4	24.4	35.2	9.8
20	16.2	27.7	37.0	12.2
25	45.9	46.7	46.5	30.0
30	71.0	47.1	50.9	40.3
35	83.4	63.8	63.5	59.0
40	90.3	78.7	77.4	74.4
45	91.4	83.4	78.2	77.2
07 Flood	91.6	78.7	77.8	75.6

Table 3-4. Reported high water mark elevations for the 2007 flood, calculated water surface elevations for the FLDPLN, HEC-RAS, and HAZUS models, and individual errors for each (all values are in feet).

					Difference (HWM-Model) (ft)		
HWM ID	**HWM Elev.**	**FSE HEC**	**FSE HAZ**	**FSE FLDPLN**	**HEC-RAS**	**HAZUS**	**FLDPLN**
07-V59	740.23	743.14	742.62	749.05	**-2.91**	**-2.39**	**-8.82**
07-V23	738.52	741.15	735.81	745.88	**-2.63**	**2.71**	**-7.36**
07-V22	737.05	741.04	737.80	749.41	**-3.99**	**-0.74**	**-12.35**
07-V21	731.07	732.78	714.17	730.31	**-1.71**	**16.90**	**0.76**
07-V20	728.79	729.65	722.86	721.61	**-0.86**	**5.93**	**7.18**
07-V19	725.32	729.65	724.19	721.61	**-4.33**	**1.13**	**3.71**
07-V18	723.60	727.40	724.90	721.61	**-3.81**	**-1.30**	**1.99**
07-V17	718.27	720.17	719.96	721.61	**-1.90**	**-1.69**	**-3.34**
07-V16	716.27	726.24	707.57	721.61	**-9.96**	**8.70**	**-5.34**
07-V15	723.22	725.83	719.67	721.61	**-2.62**	**3.54**	**1.61**
07-V14	721.26	725.75	720.29	721.63	**-4.49**	**0.97**	**-0.37**
07-V13	722.52	726.79	719.80	721.61	**-4.26**	**2.73**	**0.91**
07-V12	717.93	719.56	711.03	721.93	**-1.63**	**6.91**	**-4.00**

Table 3-5. Summary statistics for high water mark point analysis comparing modeled water surface elevations or the 2007 flood event using the FLDPLN, HEC-RAS, and HAZUS models. The 10 point statistics exclude the three northernmost points in the study area. This exclusion was done to determine if the FLDPLN model has better performance nearer to the reference gage location, which does appear to be the case.

	07-V12 thru 07-V21 (10 points) (ft)		
	HEC-RAS	HAZUS	FLDPLN
Mean	-3.56	4.38	0.31
Median	-3.21	3.13	0.83
StDev	2.61	5.57	3.77
RMSE	3.80	6.02	3.15

	All 13 HWM Points (ft)		
	HEC-RAS	HAZUS	FLDPLN
Mean	-3.47	3.34	-1.96
Median	-2.91	2.71	-0.37
StDev	2.28	5.32	5.51
RMSE	4.10	6.10	5.64

Table 3-6. Summary error statistics for the image-based high water mark (shoreline) analysis.

	Image Point Summary		
	Aerial (ft) (n=260)		
	HEC-RAS	HAZUS	FLDPLN
Mean	-6.55	-0.21	-6.05
Median	-5.66	-5.66	-4.95
St Dev	5.16	5.16	8.55
RMSE	8.30	5.32	10.46

	ASTER (ft) (n=200)		
	HEC-RAS	HAZUS	FLDPLN
Mean	-5.52	0.93	-5.37
Median	-5.32	1.69	-5.31
St Dev	5.13	5.31	8.86
RMSE	7.53	5.30	10.34

Figures

Figure 3-9. Aerial photographs taken during the peak flooding in Montgomery County in July of 2007. The top two photos show oil release from a refinery in Coffeyville, which flowed south in the Verdigris River into Oklahoma. (www.kansasgis.org)

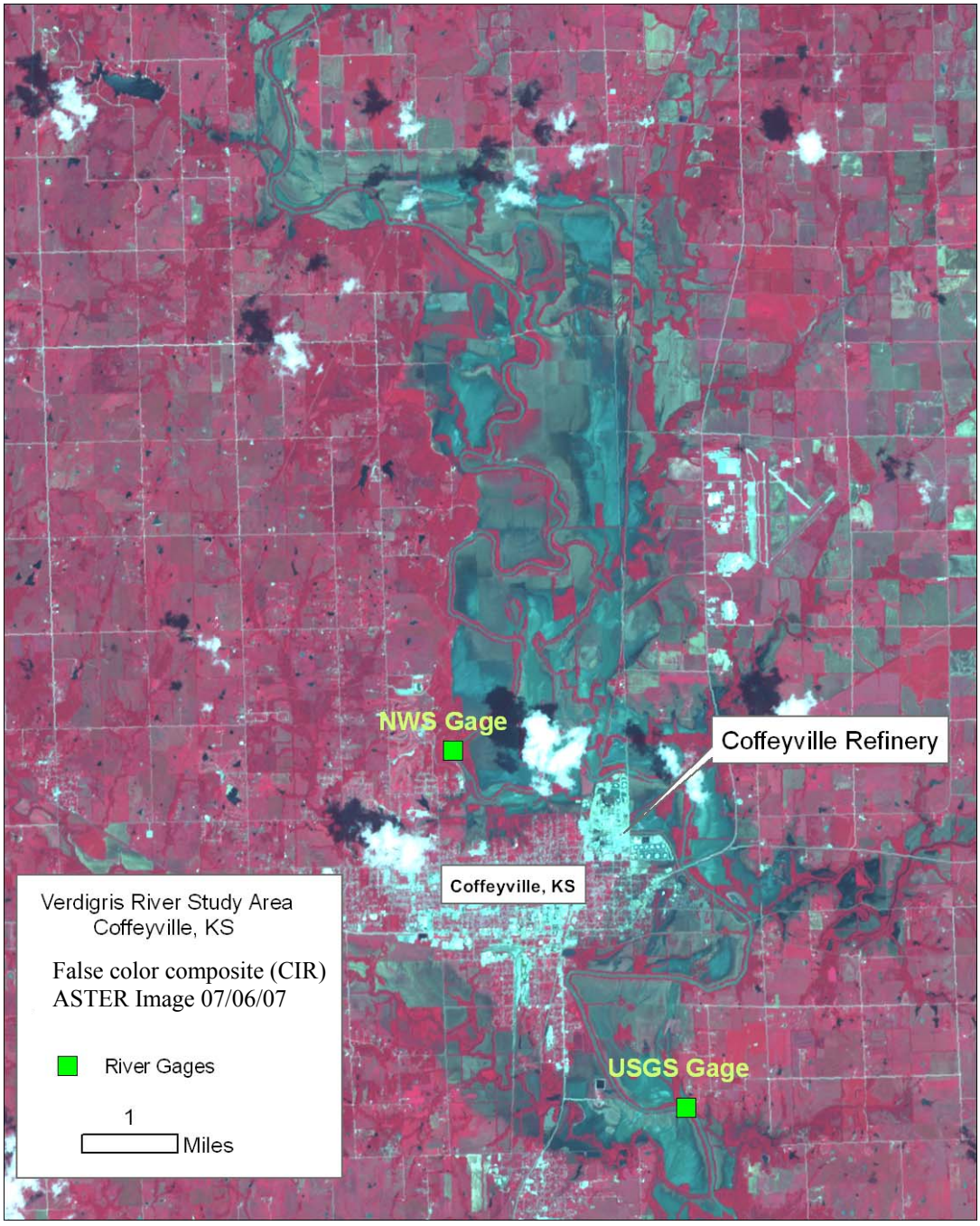

Figure 3-2. ASTER flood image. The base image is a color infrared, 15m resolution ASTER image acquired on July 6th, 2007, four days after flood crest. Dark areas along the Verdigris River are either standing water still pooled in the floodplain, or areas denuded of vegetation by flood waters. Brighter red areas within the flood zone are woodland canopies that are minimally impacted by flood waters.

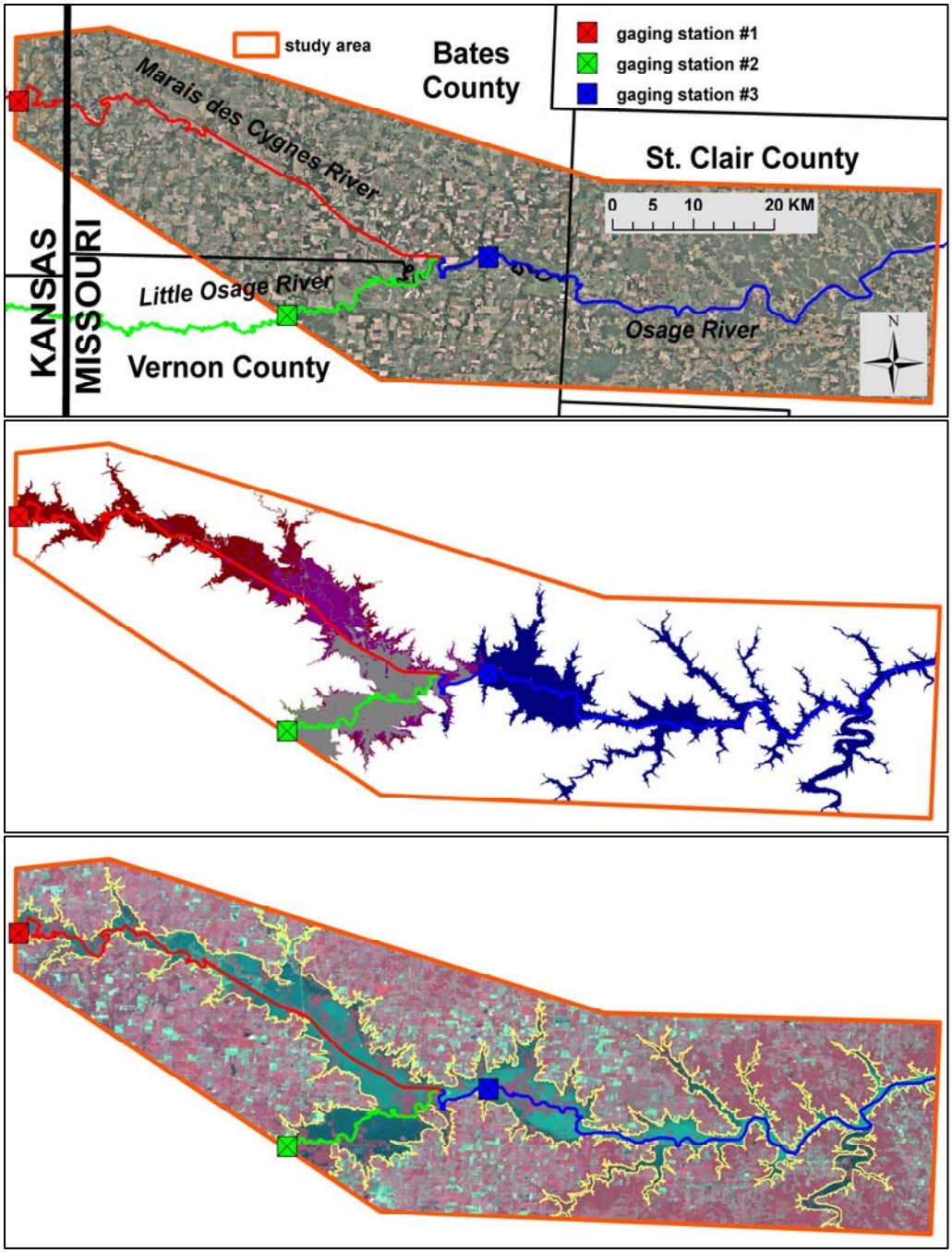

Figure 3-3. Pilot study area along the Marais des Cygnes, Little Osage, and Osage Rivers in Missouri. Floods crested in early July, several days before acquisition of the Landsat 5 scene, which can be seen in the bottom graphic. Peak stage values were used from three USGS gaging stations as inputs to the FLDPLN model. The combined flood extent estimate for the three river segments, shown in red, blue, and green, is shown in the middle graphic. The yellow boundary in the bottom graphic corresponds to the model estimated flood extent. The estimated extent had an accuracy of 81.7%.

Figure 3-4. NWS staff gage at Coffeyville- three views.
http://www.crh.noaa.gov/ahps2/hydrograph.php?wfo=ict&gage=cfvk1

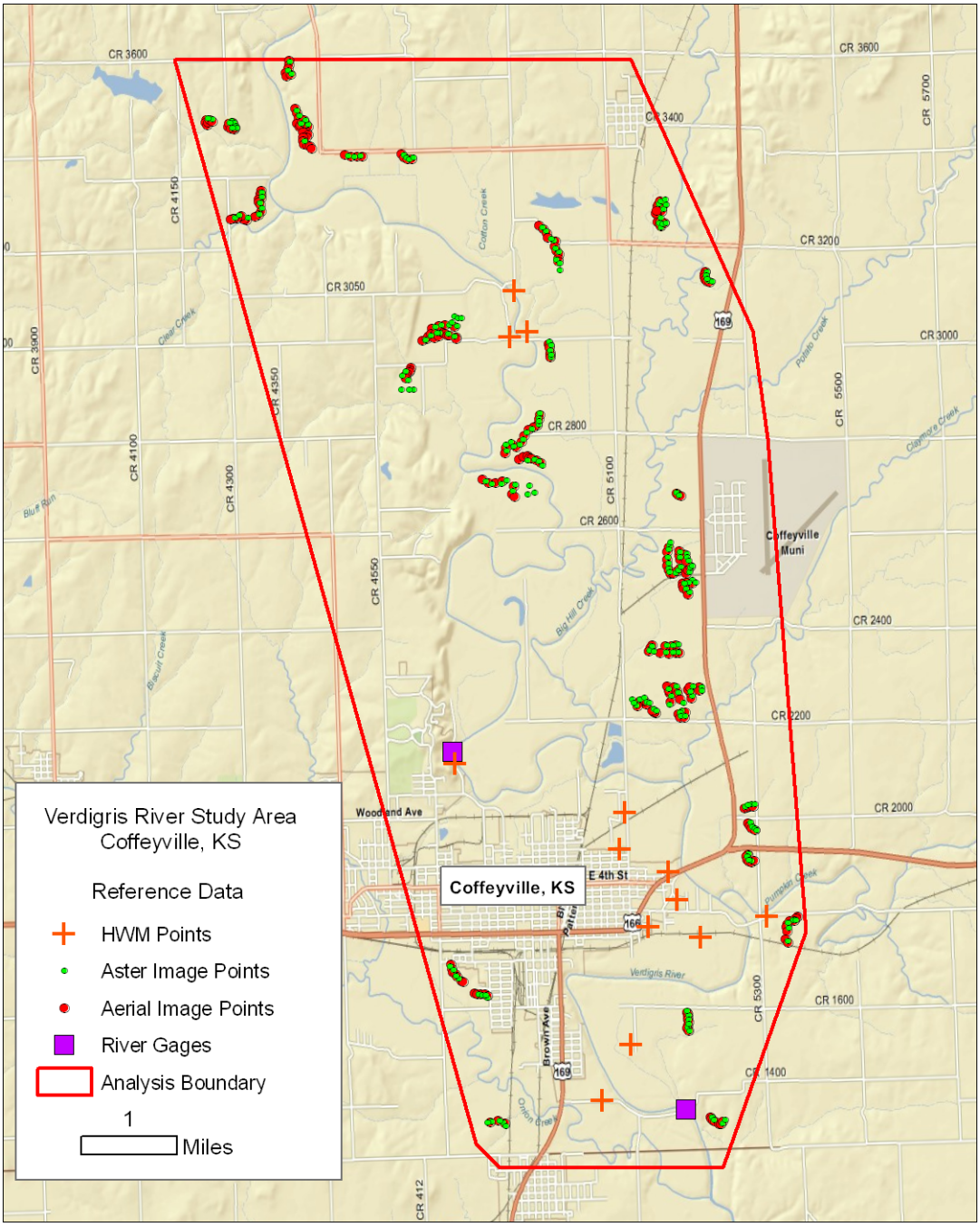

Figure 3-5. Verdigris River study area. Also shown are the NWS and USGS gage station locations, the 13 high water mark point locations surveyed after the 2007 flood, and the ASTER and aerial imagery based high water point locations.

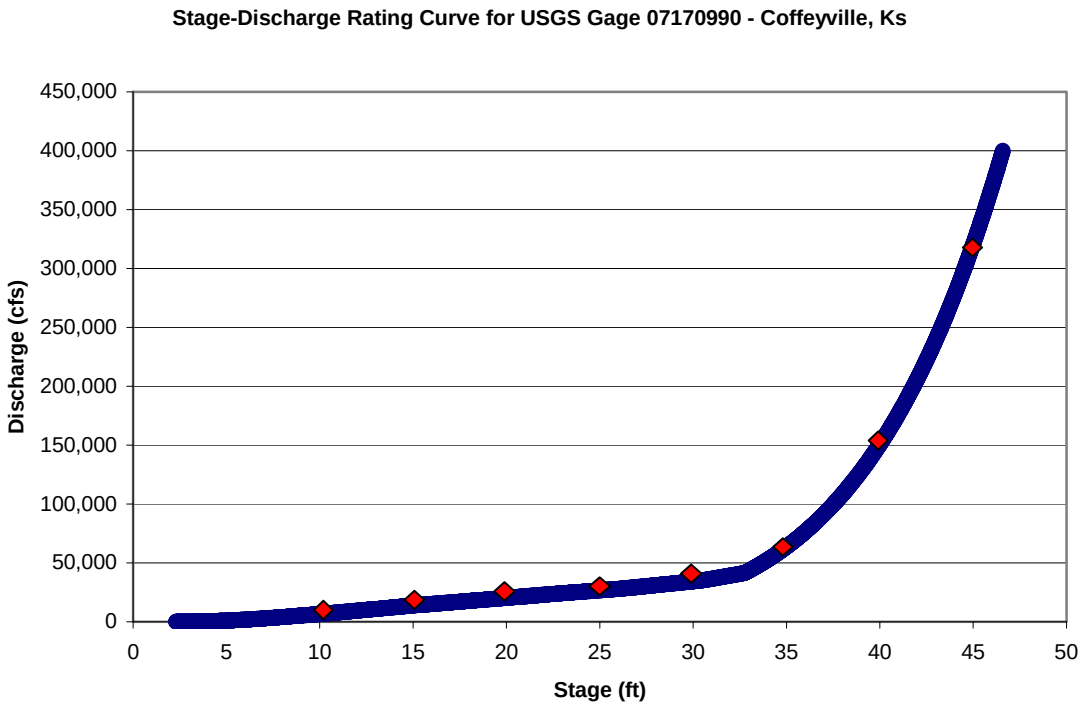

Figure 3-6. Plot of stage-discharge values for USGS gage 07170990. The red triangles represent discharges used (also shown in Table 3-1) for modeled flood extent comparisons.

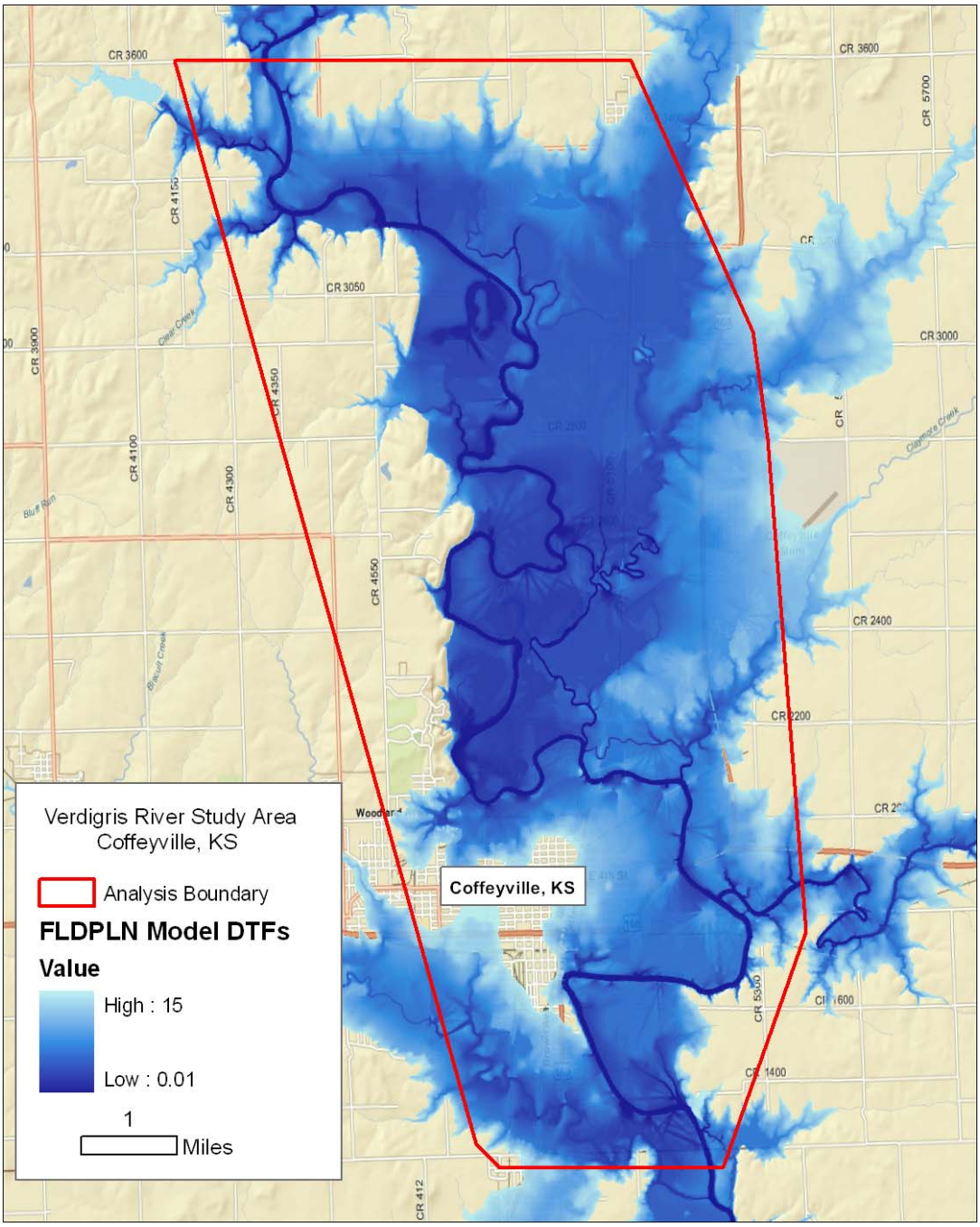

Figure 3-7. FLDPLN model raster DTF output for the 0 to 15 m flood within the study area. In a disaster response situation, custom flood extent maps can be produced by selecting DTF values at or below those corresponding to current or predicted flood stage.

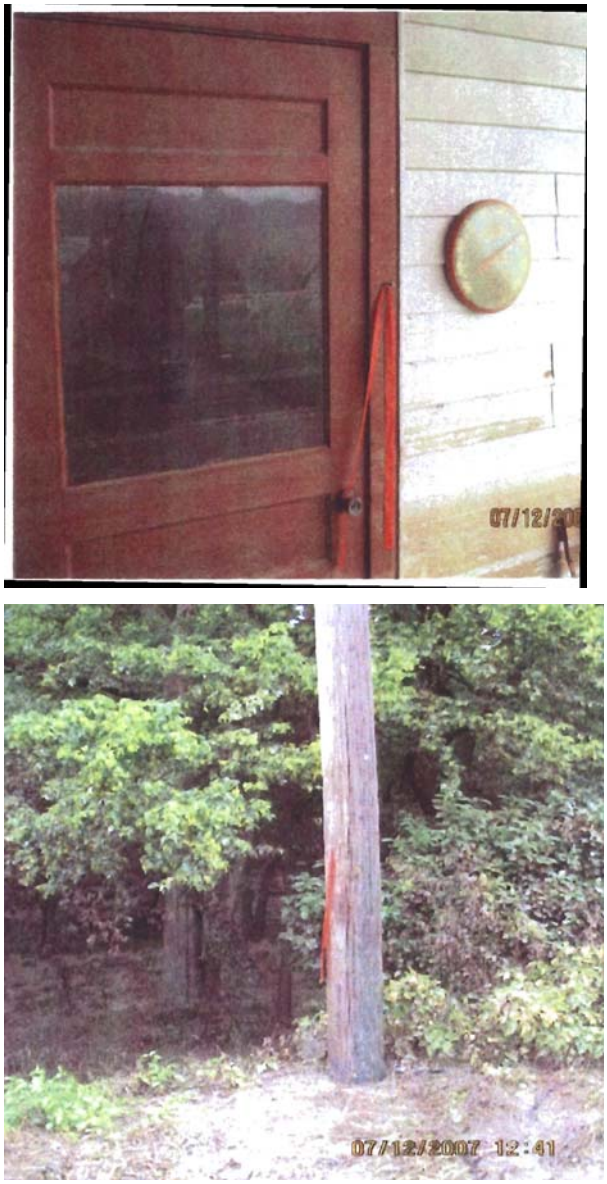

Figure 3-8. HWM *in situ* photos. Two examples of locations from which high water marks were surveyed after the 2007 flood, one on the side of a home and the other on a utility pole (USACE, 2007).

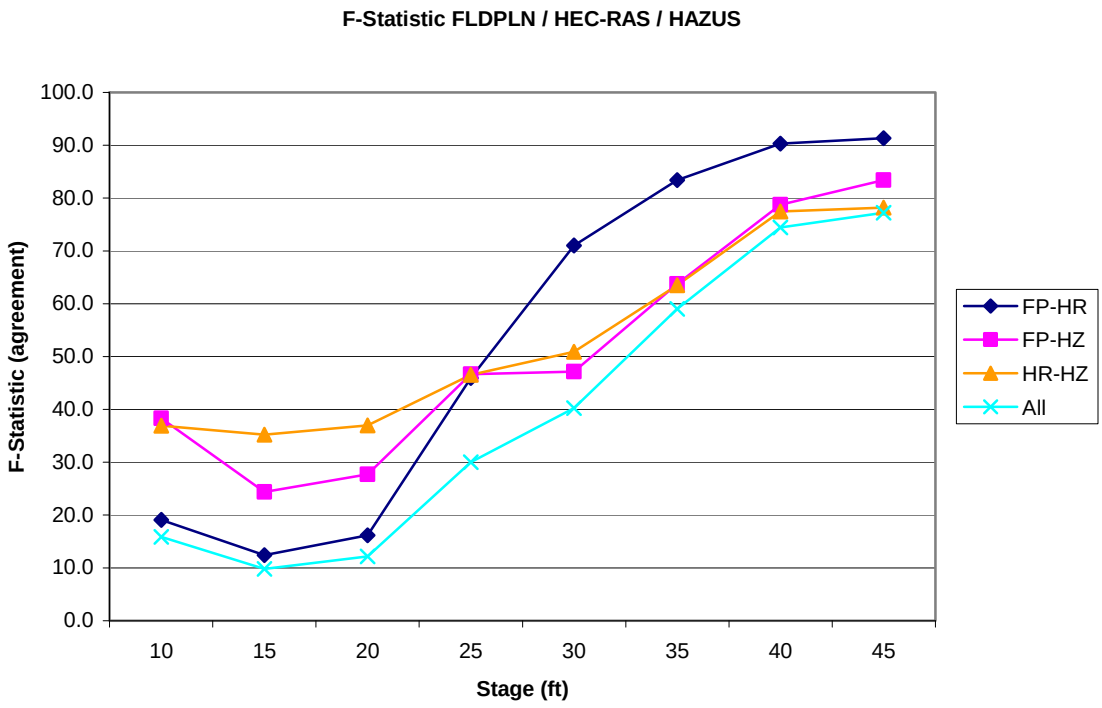

Figure 3-9. F-statistic vs. stage for all model pairings and between all models.

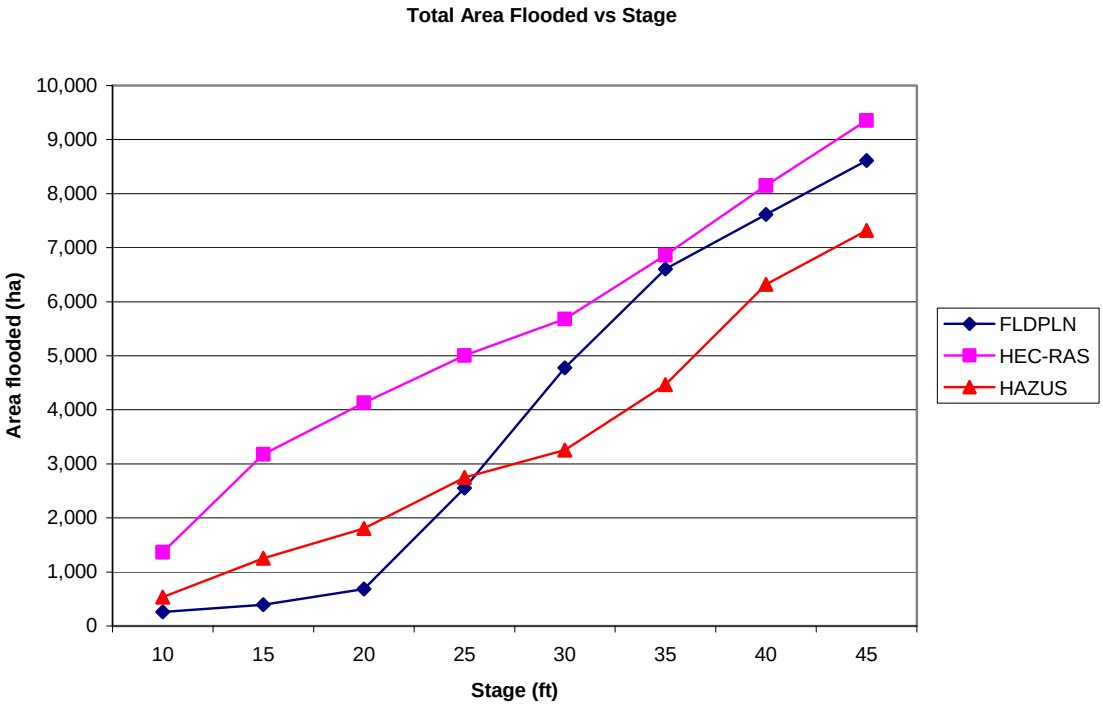

Figure 3-10. Total area flooded with each model vs. stage.

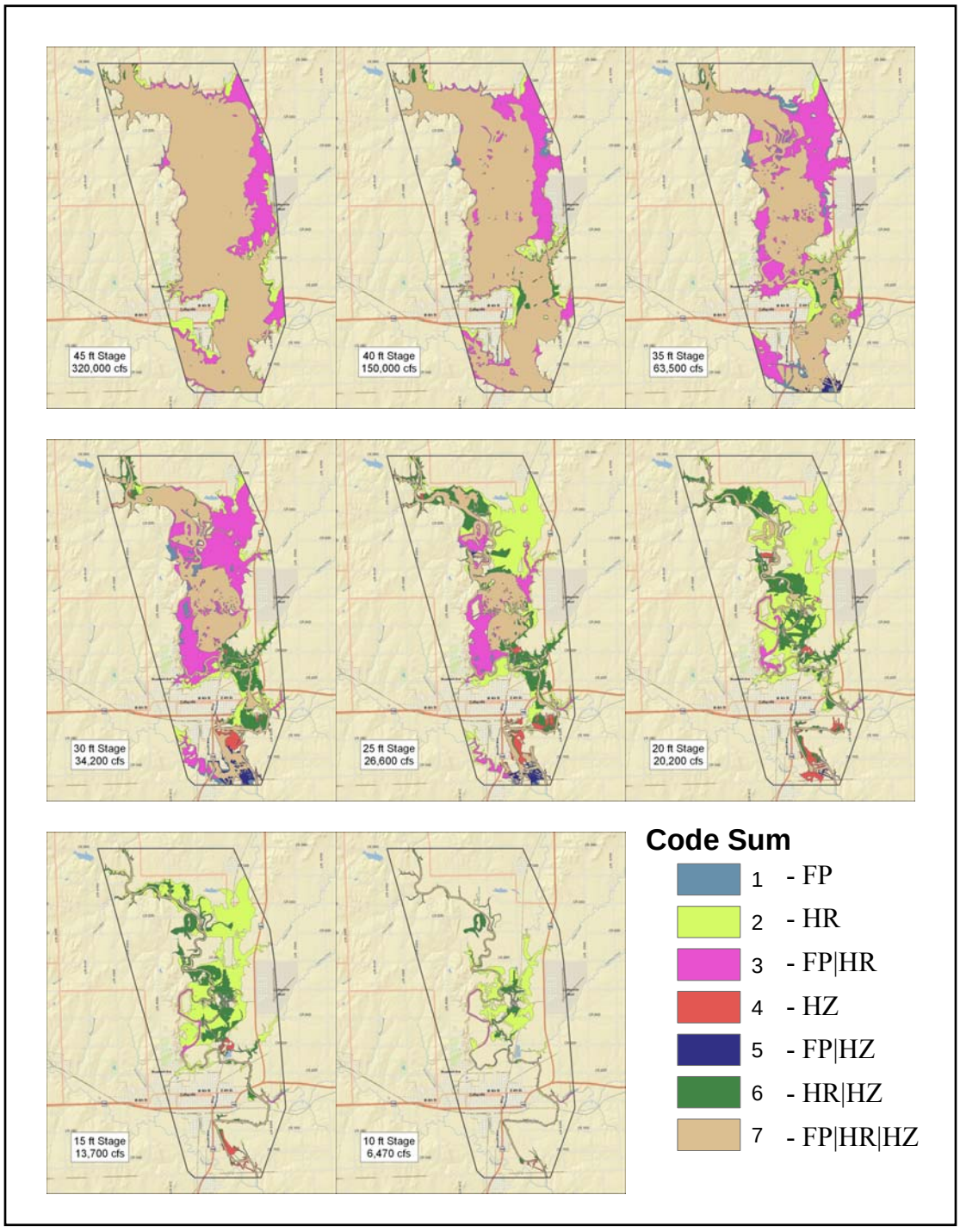

Figure 3-11. Flood extent correspondence between the FLDPLN (FP), HEC-RAS (HR), and HAZUS (HZ) models for the eight modeled flood stages. The Code Sum legend provides a key to the correspondence combination shown in the maps, the derivation of which is shown in Table 3-1.

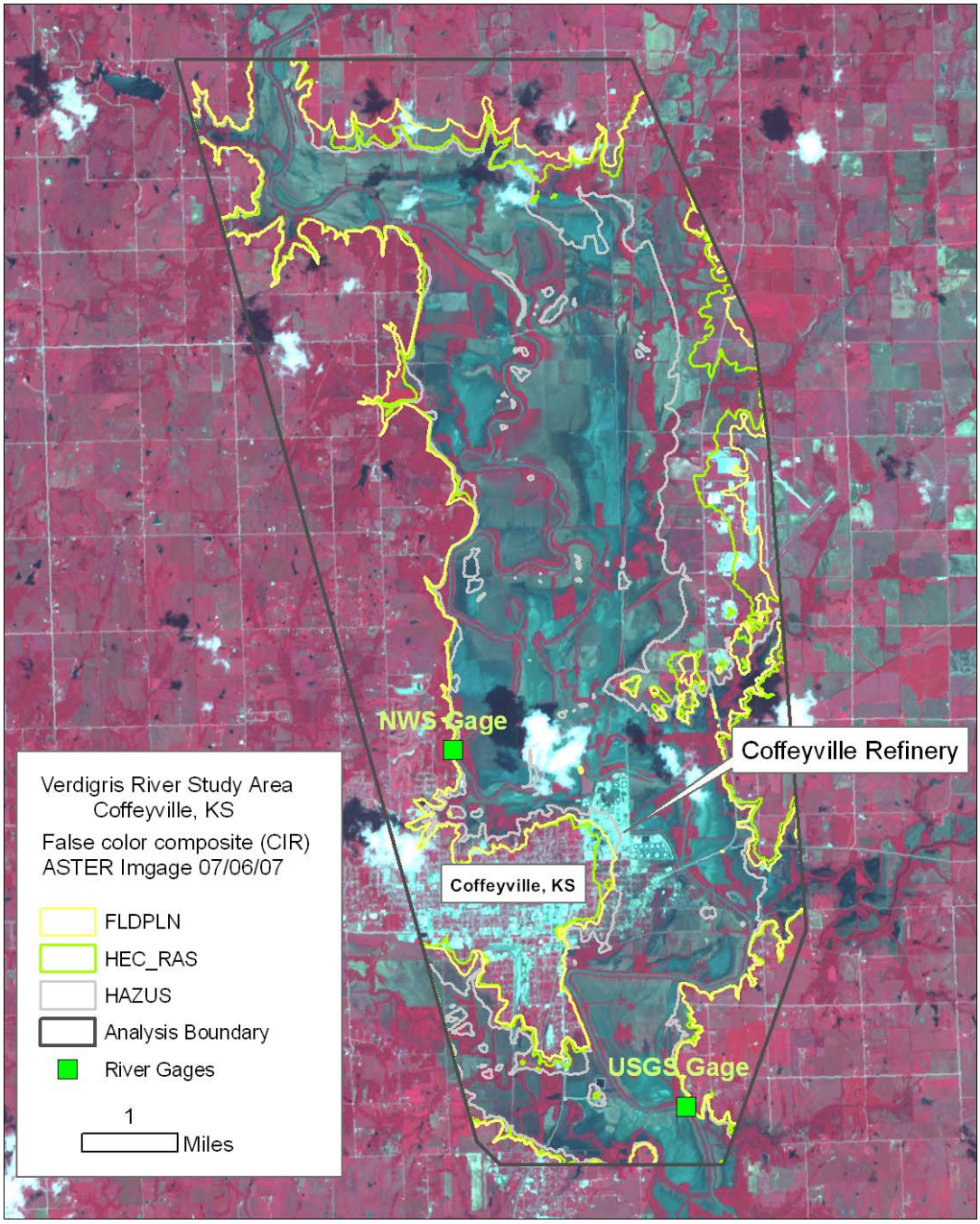

Figure e 3-12. Modeled flood extents for HEC-RAS, HAZUS and the FLDPLN model representing each model's estimated flood extent for the corresponding peak discharge of 186.000 cfs

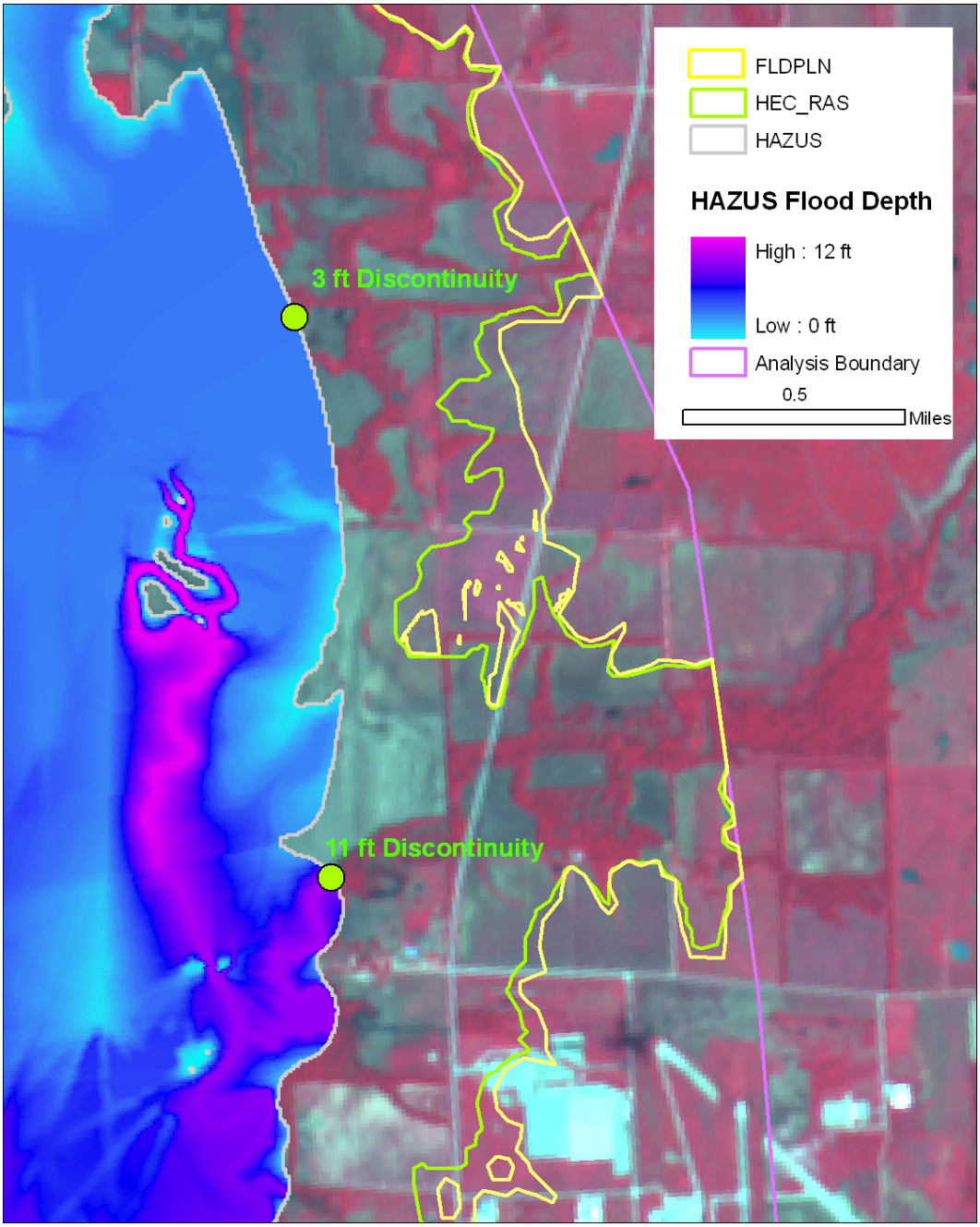

Figure 3-13. Two examples of flood boundary anomalies produced by HAZUS. Flood boundary flood depths should, under normal, gently sloping landscape conditions (as exist here) be zero-depth. These anomalies are likely produced by a stream buffer limit imposed by the software.

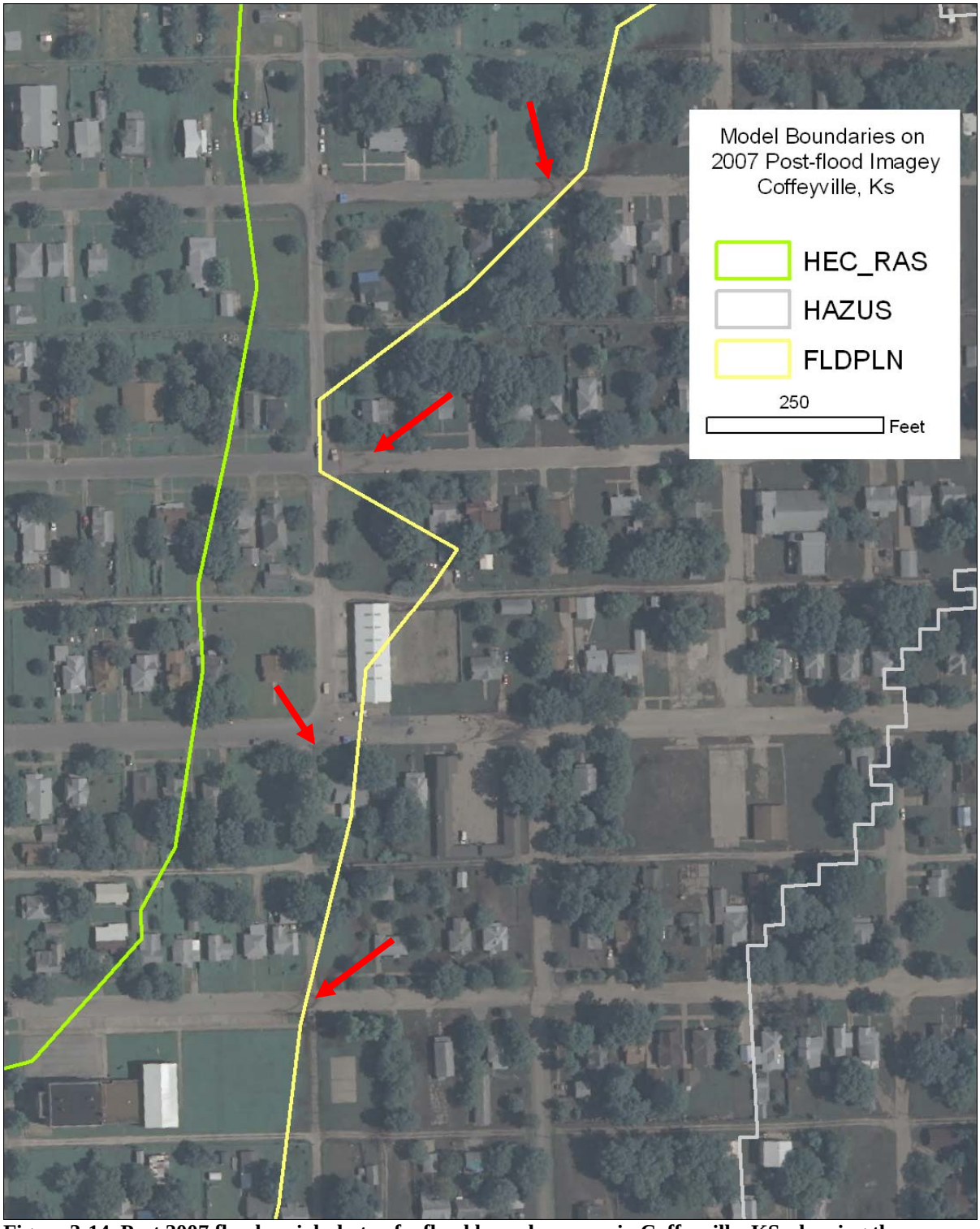

Figure 3-14. Post 2007 flood aerial photo of a flood boundary area in Coffeyville, KS, showing the modeled flood boundaries for the FLPLN, HEC-RAS, and HAZUS model. The red arrows point to shoreline debris on the streets. The peak discharge in this area was estimated to be 169,000 cfs.

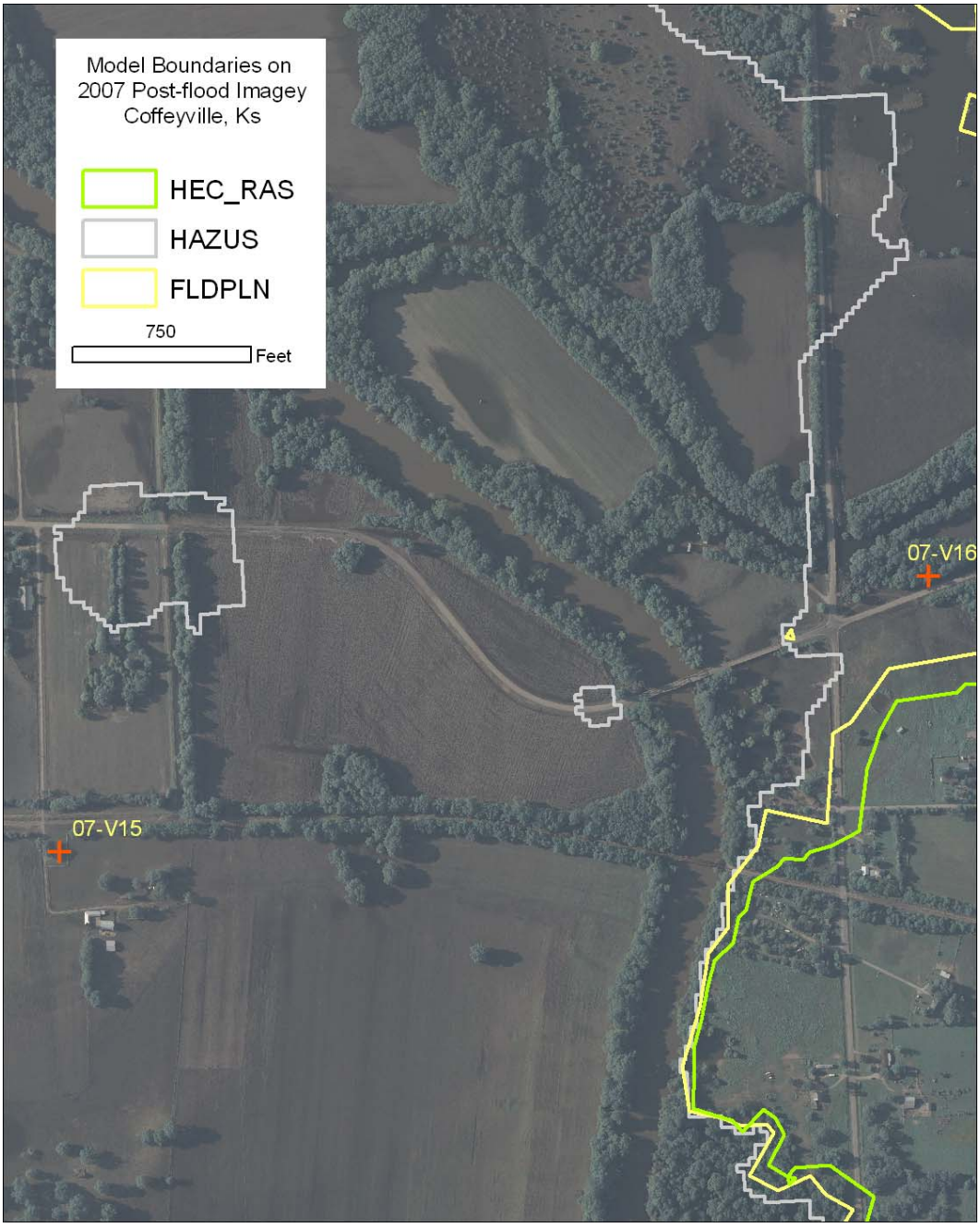

Figure 3-15. Two high water mark locations on either side of the Verdigris River on the east side of Coffeyville. Although the water surface elevations should be similar, based on proximity and orientation, the difference in surveyed elevations is 6.94 feet.

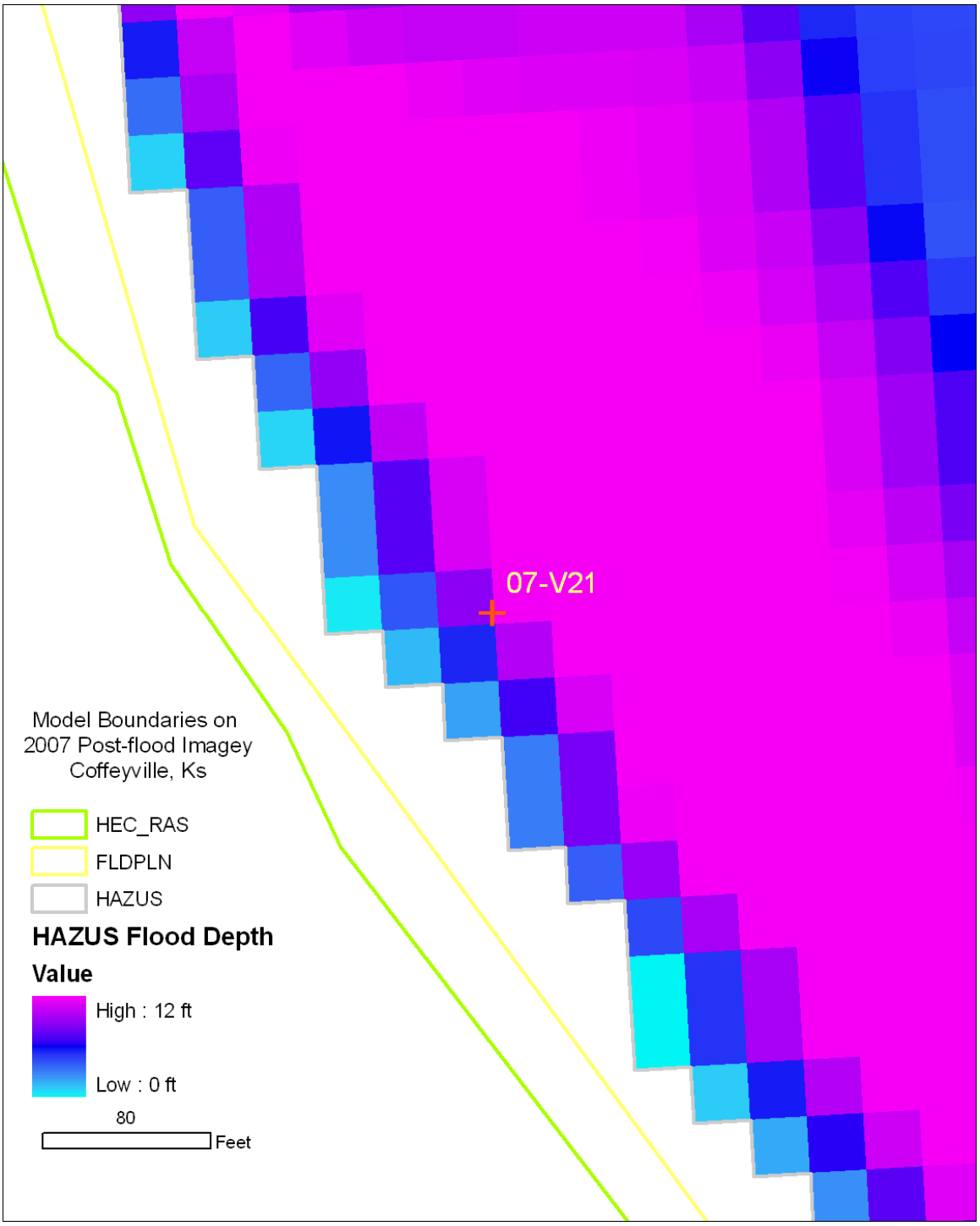

Figure 3-16. HWM location with a 16.9 ft underestimate in water surface elevation for the HAZUS model, while the HEC-RAS model overestimates by 1.71 ft and the FLDPLN model underestimates by 0.76 ft.

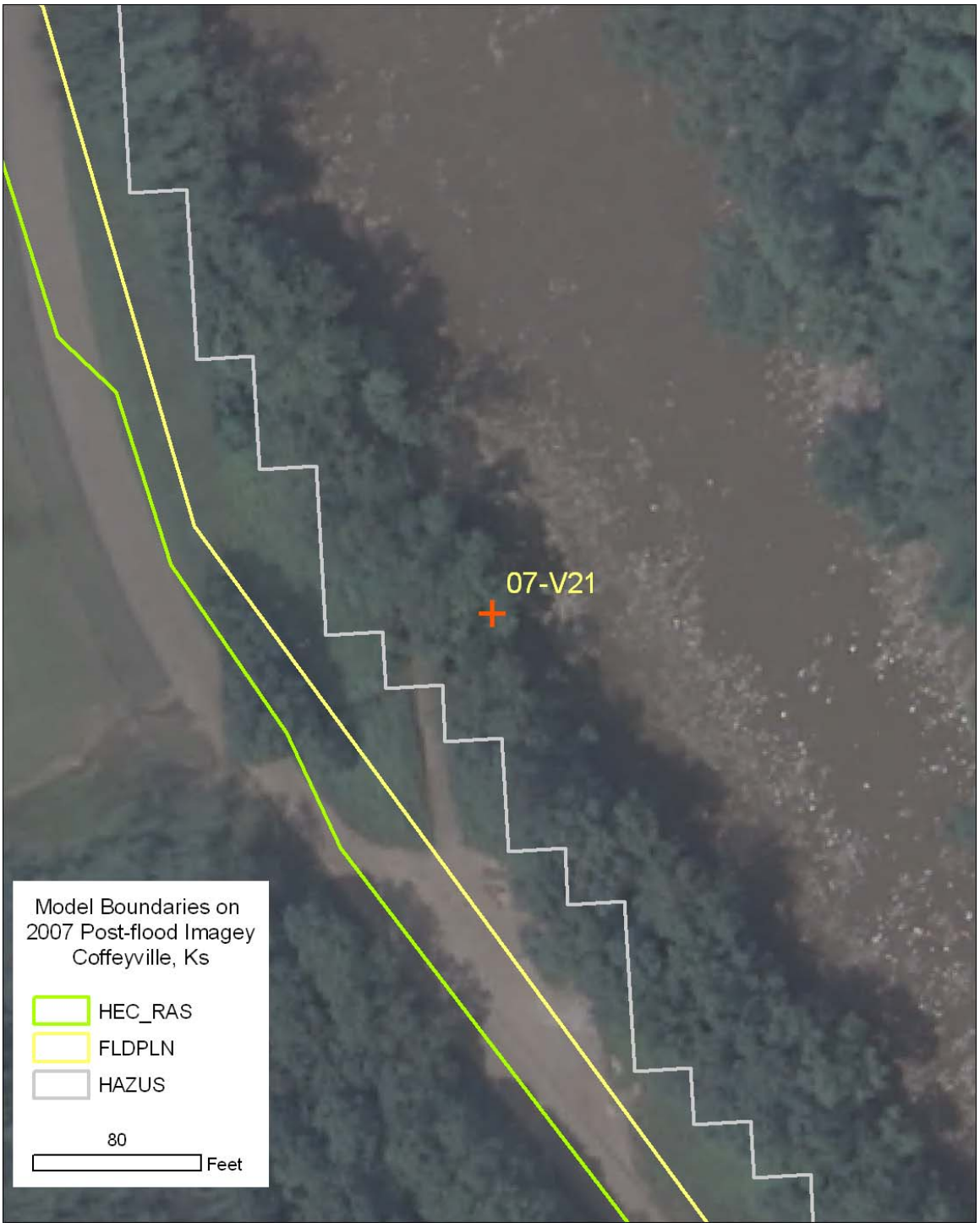

Figure 3-17. The same HWM location shown in Figure 3-16, but with aerial photography as the basemap. This location is at the western edge of the floodplain and is characterized by a very steep, tall embankment on the west side of the Verdigris River. Slight horizontal positional errors, either in the HWM or the underlying DEM can show as large errors with the analysis approach taken in this study.

References Cited

(IACWD), I. A. C. o. W. D. 1982. Guidelines for determining flood flow frequency. In *Bulletin 17B of the Hydrology Subcommittee*.

Bales, J. D. & C. R. Wagner (2009) Sources of uncertainty in flood inundation maps. *Journal of Flood Risk Management,* 2**,** 139-147.

Bates, P. D. & A. P. J. De Roo (2000) A simple raster-based model for flood inundation simulation. *Journal of Hydrology,* 236**,** 54-77.

Brasington, J. & K. Richards (1998) Interactions between model predictions, parameters and DTM scales for TOPMODEL. *Computers & Geosciences,* 24**,** 299-314.

Casas, A., G. Benito, V. R. Thorndycraft & M. Rico (2006) The topographic data source of digital terrain models as a key element in the accuracy of hydraulic flood modelling. *Earth Surface Processes and Landforms,* 31**,** 444-456.

Cook, A. & V. Merwade (2009) Effect of topographic data, geometric configuration and modeling approach on flood inundation mapping. *Journal of Hydrology,* 377**,** 131-142.

Crosetto, M., S. Tarantola & A. Saltelli (2000) Sensitivity and uncertainty analysis in spatial modelling based on GIS. *Agriculture, Ecosystems & Environment,* 81**,** 71-79.

England, J. F., R. D. Jarrett & J. D. Salas (2003) Data-based comparisons of moments estimators using historical and paleoflood data. *Journal of Hydrology,* 278**,** 172-196.

FEMA. 2008. Base Flood Elevation Determination, Mongomery County, Kansas. Wahshington, DC.

Gall, M., B. J. Boruff & S. L. Cutter (2007) Assessing Flood Hazard Zones in the Absence of Digital Floodplain Maps: Comparison of Alternative Approaches. *Natural Hazards Review,* 8**,** 1-12.

Griffis, V. W. & J. R. Stedinger (2007a) The use of GLS regression in regional hydrologic analyses. *Journal of Hydrology,* 344**,** 82-95.

--- (2007b) Evolution of Flood Frequency Analysis with Bulletin 17. *Journal of Hydrologic Engineering,* 12**,** 283-297.

Hancock, G. R. (2005) The use of digital elevation models in the identification and characterization of catchments over different grid scales. *Hydrological Processes,* 19**,** 1727-1749.

Harmel, R. D., D. R. Smith, K. W. King & R. M. Slade (2009) Estimating storm discharge and water quality data uncertainty: A software tool for monitoring and modeling applications. *Environmental Modeling & Software,* 24**,** 832-842.

Horritt, M. S. & P. D. Bates (2001) Effects of spatial resolution on a raster based model of flood flow. *Journal of Hydrology,* 253**,** 239-249.

Kastens, J. H. 2008. Some New Devolopments On Two Separate Topoics: Statistical Cross Validation and Floodplain Mapping. In *Mathematics*, 191. Lawrence: The University of Kansas.

Kenward, T., D. P. Lettenmaier, E. F. Wood & E. Fielding (2000) Effects of Digital Elevation Model Accuracy on Hydrologic Predictions. *Remote Sensing of Environment,* 74**,** 432-444.

Marks, K. & P. Bates (2000) Integration of high-resolution topographic data with floodplain flow models. *Hydrological Processes,* 14**,** 2109-2122.

Merwade, V., A. Cook & J. Coonrod (2008a) GIS techniques for creating river terrain models for hydrodynamic modeling and flood inundation mapping. *Environmental Modelling & Software,* 23**,** 1300-1311.

Merwade, V., F. Olivera, M. Arabi & S. Edleman (2008b) Uncertainty in Flood Inundation Mapping: Current Issues and Future Directions. *Journal of Hydrologic Engineering,* 13**,** 608-620.

National Research Council (U.S.). Committee on FEMA Flood Maps., United States. Federal Emergency Management Agency. & United States. National Oceanic and Atmospheric Administration. 2009. *Mapping the zone : improving flood map accuracy*. Washington, D.C.: National Academies Press.

NWS. 2010. Advanced Hydrologic Prediction Service; http://www.weather.gov/ahps/inundation.php.

Pielke, J., R.A., M.W. Downton, and J.Z. Barnard Miller. 2002. Flood Damage in the United States, 1926–2000: A Reanalysis of National Weather Service Estimates. Boulder, CO: UCAR.

Ries, K. G. & J. B. Atkins. 2007. *The National streamflow statistics program : a computer program for estimating streamflow statistics for ungaged sites*. Reston, Va.: U.S. Department of the Interior, U.S. Geological Survey.

Scawthorn, C., N. Blais, H. Seligson, E. Tate, E. Mifflin, W. Thomas, J. Murphy & C. Jones (2006) HAZUS-MH Flood Loss Estimation Methodology. I: Overview and Flood Hazard Characterization. *Natural Hazards Review,* 7**,** 60-71.

Singh, V. P. (1997) Effect of spatial and temporal variability in rainfall and watershed characteristics on stream flow hydrograph. *Hydrological Processes,* 11**,** 1649-1669.

Smemoe, C., J. Nelson & A. Zundel. 2004. Risk Analysis Using Spatial Data in Flood Damage Reduction Studies. 262-262. Salt Lake City, Utah, USA: ASCE.

Tate, E. C., D. R. Maidment, F. Olivera & D. J. Anderson (2002) Creating a Terrain Model for Floodplain Mapping. *Journal of Hydrologic Engineering,* 7**,** 100-108.

Tayefi, V., S. N. Lane, R. J. Hardy & D. Yu (2007) A comparison of one- and two-dimensional approaches to modelling flood inundation over complex upland floodplains. *Hydrological Processes,* 21**,** 3190-3202.

Valeo, C. & S. M. A. Moin (2000) Variable source area modelling in urbanizing watersheds. *Journal of Hydrology,* 228**,** 68-81.

Vardi, N. (2007) Slick. *Forbes,* 180**,** 50-50.

Voigt, S., T. Kemper, T. Riedlinger, R. Kiefi, K. Scholte & H. Mehi (2007) Satellite Image Analysis for Disaster and Crisis-Management Support. *IEEE Transactions on Geoscience & Remote Sensing,* 45**,** 1520-1528.

Wang, Y. & T. Zheng (2005) Comparison of Light Detection and Ranging and National Elevation Dataset Digital Elevation Model on Floodplains of North Carolina. *Natural Hazards Review,* 6**,** 34-40.

Weichel, T., F. Pappenberger & K. Schulz (2007) Sensitivity and uncertainty in flood inundation modelling; concept of an analysis framework. *Advances in Geosciences,* 11**,** 31-36.

CHAPTER 4

SUMMARY

As a natural phenomenon that is governed by multiple spatial and time dependent variables, flooding is not a problem that is given to simple and accurate prediction, both in terms of where and when it will occur. The development of modeling software, increases in computational capacity, more reliable ancillary data like antecedent moisture conditions, land cover, land use, impervious surfaces, and high accuracy elevation data, and increasingly accessible inputs such as recent and predicated rainfall and stream flow set the stage for development of systems capable of integrating these inputs in near real-time and producing a continuous stream of information accessible by decision makers and the general public. However, while from a production standpoint these advances may be somewhere around the corner, at present there is not an operational system in place, nor is there one in widespread development. Indeed, the current weather forecasting systems upon which so many people rely took decades to develop. Unlike weather, which affects nearly everyone every day, when flooding is a concern it often only directly affects a small portion of the population, and the duration of its direct impact is very short and widely spaced in time, sometime by years or even decades.

Until more advance flood warning systems come online, it is clear from recent flood events in the Midwest, particularly those of 2007 in Kansas and Missouri and 2008 in Arkansas, Iowa, and Wisconsin, that some type of food extent estimation is needed beyond the FEMA 100-year floodplain. Current research at the Kansas Biological

Survey is attempting to bridge this gap by producing a segmented library of inundation extents basted on the FLDPLN model.

The objectives of this study were to determine the accuracy of the pre-LiDAR and post-LiDAR National Elevation Dataset for Douglas County, to identify potential impacts of errors in the data on modeled flood estimates, and to compare modeled flood extents for the FLDPLN model against other models and evaluate model performance against empirical flood data to determine the utility of both the NED and the FLDPLN model for flood inundation extent library development.

Elevation data evaluations

For Douglas County, the GPSBM data analysis showed the NED10L data are of sufficiently high accuracy to serve as a reference standard for evaluating the NED10 elevation accuracy. Although only 12 GPSBM point were available and valid, the results for the LiDAR-derived elevation datasets, the LiDAR2, NED3L, NED10L, and NED30L showed RMS errors of 0.13, 0.45 , 0.20 , and 0.50 m, respectively. The LiDAR2 data was produced to meet FEMA specifications, and these results support that these standards were met. The degradation in accuracy from 0.13 m to 0.20 m (LIDAR2 vs. NED10L) is not unreasonable considering the downsampling that is necessary to produce the 10 m pixels of the NED10L from the 2 m LiDAR2 pixels.

The NED10 vertical accuracy analysis showed the overall error for 2660 randomly selected points across Douglas County, Kansas to be 1.51 m (RMSE). These results are better than the 2.44 m absolute accuracy reported by Gesch (2007). As expected, the accuracy of the woodland and urban classes was slightly lower than for the

cropland and grassland classes: 1.84, 1.56, 1.39, and 1.42 m, respectively. The greater errors are in urban and woodland areas caused by the vertical buildings and trees that obscure the ground surface, making ground surface elevation determination more prone to error. The overall error (1.51 m RMSE) is much lower than the often cited ±7 m accuracy of the NED. This is actually a production goal, not a measure of the NED accuracy (Gesch 2007). Steep, mountainous terrain is generally the only place where such error magnitudes are observed with any degree of significance.

The 100 and 50 yr flood event model analysis comparing the affects of using the NED10 and NED10L as inputs was performed on segments of the Kansas and Wakarusa Rivers. The results showed a range of flood extent correspondence, with a low F-statistic of 64.4 using the FLDPLN model on Wakarusa River segment for the 50 yr flood, to a high of 90.6 using HAZUS on the Kansas River segment for the 100 yr flood. In general, for both models, the 100 yr floods always had higher correspondence than 50 yr floods. These results show that lower floods may be more sensitive to data quality, but that the NED10 data can provide valuable information in the absence higher quality data. The results also showed that the FLDPLN model, in all cases, was more sensitive to discrepancies between the NED datasets. In all cases the F-statistic for the FLDPLN model was at least 12.9 points lower that HAZUS, up to a maximum of 14.9.

Flood model evaluations

The modeled comparison and empirical data evaluations for the Verdigris River in Montgomery County offered valuable insight into the difficulties in evaluating model performance with empirical data and the variability of model output between models for

the same simulated flood events. The modeled flood extent comparisons between HAZUS, HEC-RAS, and the FLDPLN models for simulated floods between 10 and 45 ft stage showed that model correspondence generally increases with increasing stage, from a low F-statistic between all three models of 9.8 at 15 ft to a high of 77.2 at 45 ft. Between model pairs, the FLDPLN model corresponded most closely with the HEC-RAS model, with a low of 12.4 at 15 ft to a high of 91.4 at 45 ft, and actually corresponding slightly better at 91.6 for the 2007 flood level. These results indicate that at low flow conditions model performance is least reliable, while at major flood stages the reliability of all three models increases significantly. Presumably this is because of the floodplain and valley morphology that causes flood extent to be less sensitive to vertical rise at high stages.

The high water mark analysis (HWM), which measured the models' accuracy in modeling floods water surface elevation, showed that the FLDPLN model performed best closer to the stage reference, which was expected, actually outperforming the other two models for the 10 of 13 HWM points that were closest to the reference gage, with an RMSE of 3.15 ft, compared to the 3.80 and 6.02 ft for HEC-RAS and HAZUS, respectively. For all 13 points the RMSE was 5.64, 4.10, and 6.10 ft for FLDPLN, HEC-RAS, and HAZUS respectively. HEC-RAS overestimated the water surface elevation for every point, ranging from 0.86 ft to 9.96 ft, with an average of -3.47 ft, while the average FLDPLN and HAZUS errors were -1.96 and 3.34 ft for all 13 points, respectively.

The ASTER and aerial image derived flood boundary point elevation analysis also assessed modeled water surface elevation and showed significantly greater error than the HWM analysis, with 10.46, 8.30, and 5.32 ft RMSE for the aerial image-derived

points and 10.34, 7.53, and 5.30 ft for the ASTER-derived points for FLDPLN, HEC-RAS, and HAZUS, respectively. HAZUS was shown to be the least biased and HEC-RAS and the FLDPLN model were both biased toward overestimating water surface elevation, ranging between 5.37 and 6.55 ft collectively. The elevation values used for reference were, however, not as reliable as the HWM elevations. Between the difficulties of the subjective image analyst's interpretation of flood boundaries, and the use of the 10-meter NED as the reference elevation, with its approximate 5 ft RMSE, this method of evaluation was determined to be least favorable. Improved reference elevation data, however, could yield significantly improved results.

The results certainly point to the value of improved elevation data, while at the same time showing that the current NED can provide valuable flood mapping information and has better accuracy than is commonly perceived. From a modeling standpoint, the FLDPLN model corresponded well with HEC-RAS for major floods, and favorably to HAZUS, while all models tested showed significant inconsistencies at low flood levels. Future floods in the areas will provide additional empirical data for model testing, and operational implementation opportunities for the FLDPLN library of inundation extents, which now covers major streams in forty counties in eastern Kansas.

Current and Future Research

There are several current and planned research activates for the FLDPLN model at KBS. Intermap Technologies has provided interferometric synthetic aperture radar (IFSAR) data for the Doulas County study area. Data accuracy and modeled flood extent comparisons, using the same protocols as in Chapter 2, are in progress for the area. This

research will enable comparison of the IFSAR data to the NED10 and NED10L. This may show the IFSAR data to be an economical alternative to LiDAR data, especially for counties in western Kansas where updated elevation data may not be developed in the near future.

Montgomery County has recently acquired LiDAR data and discussions are underway with the county emergency planner to access the data to reevaluate the Chapter 3 results using improved data. This would allow an improved evaluation of the model performances, and would more accurately reflex model performance by reducing the influence of elevation data uncertainty, especially in the case of the image-derived flood boundary elevation analysis. Because the protocols have already been establish though this research, reevaluation using the LiDAR data would be greatly expedited.

Currently a proposal has been submitted to the State of Kansas GIS policy board to develop the SLIE for an additional 36 counties in central Kansas. This would extend coverage to cover a total of two-thirds of the state. This area comprises a majority of the state's population that is not already covered. The results of this study are an important part of the proposal justification.

Contract negotiations are underway with the US Environmental Protection Agency to develop a FLDPLN module for ArcGIS, or as a stand-alone package, that can be used for an ecological application called river-typing. There are two geometry variables, valley bottom width and valley side slope, that the FLDPLN model had be used to determine for a Kansas River basin study area by researchers at KBS. The success of this approach has warranted the FLDPLN model's inclusion in the software development.

The Kansas Water Office (KWO) is interested in using the FLDPLN model to aid in site selection for potential new reservoirs. Although there are no large reservoirs planned at this time, because Kansas reservoirs are slowly filling with sediment there is concern that additional reservoir capacity, in terms of water supply for industrial, irrigation, and human consumption, will be needed. By decreasing the stream segment size and applying the FLDPLN model to targeted areas, as library of reservoir options can be created and evaluated. By varying the DTF values and calculating depth, volume, and surface area, and determining affected populations, land uses, and infrastructure, site locations can be scored based on selected criteria and eliminated from consideration or targeted for further consideration. Initial funding for this research has been secured.

Collaboration is also ongoing with counterparts at the University of Wisconsin on a project to evaluate the FLDPLN model as an image mask for radar image classification. Wisconsin experienced major flooding in 2008, as did Iowa, which prompted a wealth of data collection, both in terms of satellite imagery and post-flood assessments. As part of this effort, additional resources may be put toward comparisons similar to those made in this study. The motivation for the collaboration is to provide tools for use during disaster response in connection with activations of the International Charter "Space and Major Disasters" program, an agreement among ten member nations for "the coordinated use of space facilities in the event of natural or technological disasters" (http://www.disasterscharter.org).

Continued evaluation and documentation of these FLDPLN applications will add to the body of knowledge for this new approach to inundation mapping and allow other researchers to explore novel applications.

References Cited

(IACWD), I. A. C. o. W. D. 1982. Guidelines for determining flood flow frequency. In *Bulletin 17B of the Hydrology Subcommittee*.

Bales, J. D. & C. R. Wagner (2009) Sources of uncertainty in flood inundation maps. *Journal of Flood Risk Management,* 2**,** 139-147.

Bates, P. D. & A. P. J. De Roo (2000) A simple raster-based model for flood inundation simulation. *Journal of Hydrology,* 236**,** 54-77.

Brasington, J. & K. Richards (1998) Interactions between model predictions, parameters and DTM scales for TOPMODEL. *Computers & Geosciences,* 24**,** 299-314.

Casas, A., G. Benito, V. R. Thorndycraft & M. Rico (2006) The topographic data source of digital terrain models as a key element in the accuracy of hydraulic flood modelling. *Earth Surface Processes and Landforms,* 31**,** 444-456.

Cook, A. & V. Merwade (2009) Effect of topographic data, geometric configuration and modeling approach on flood inundation mapping. *Journal of Hydrology,* 377**,** 131-142.

Crosetto, M., S. Tarantola & A. Saltelli (2000) Sensitivity and uncertainty analysis in spatial modelling based on GIS. *Agriculture, Ecosystems & Environment,* 81**,** 71-79.

Ding, A., J. F. White, P. W. Ullman & A. O. Fashokun (2008) Evaluation of HAZUS-MH Flood Model with Local Data and Other Program. *Natural Hazards Review,* 9**,** 20-28.

England, J. F., R. D. Jarrett & J. D. Salas (2003) Data-based comparisons of moments estimators using historical and paleoflood data. *Journal of Hydrology,* 278**,** 172-196.

FEMA. 2003. Guidelines and Specifications for Flood Hazard Mapping Partners.

---. 2008. Base Flood Elevation Determination, Mongomery County, Kansas. Wahshington, DC.

Gall, M., B. J. Boruff & S. L. Cutter (2007) Assessing Flood Hazard Zones in the Absence of Digital Floodplain Maps: Comparison of Alternative Approaches. *Natural Hazards Review,* 8**,** 1-12.

Gesch, D. B. 2006. An inventory and assessment of significant topographic changes in the United States. xvii, 217 leaves. Geography Dept., South Dakota State University, 2006.

---. 2007. Chapter 4 – The National Elevation Dataset. In *Digital Elevation Model Technologies and Applications: The DEM Users Manual,* ed. D. Maune, 99-118. Bethesda, Maryland: American Society for Photogrammetry and Remote Sensing.

Griffis, V. W. & J. R. Stedinger (2007a) The use of GLS regression in regional hydrologic analyses. *Journal of Hydrology,* 344**,** 82-95.

--- (2007b) Evolution of Flood Frequency Analysis with Bulletin 17. *Journal of Hydrologic Engineering,* 12**,** 283-297.

Hancock, G. R. (2005) The use of digital elevation models in the identification and characterization of catchments over different grid scales. *Hydrological Processes,* 19**,** 1727-1749.

Harmel, R. D., D. R. Smith, K. W. King & R. M. Slade (2009) Estimating storm discharge and water quality data uncertainty: A software tool for monitoring and modeling applications. *Environmental Modeling & Software,* 24**,** 832-842.
Horritt, M. S. & P. D. Bates (2001) Effects of spatial resolution on a raster based model of flood flow. *Journal of Hydrology,* 253**,** 239-249.
Joyce, K. E., S. E. Belliss, S. V. Samsonov, S. J. McNeill & P. J. Glassey (2009) A review of the status of satellite remote sensing and image processing techniques for mapping natural hazards and disasters. *Progress in Physical Geography,* 33**,** 183-207.
Kastens, J. H. 2008. Some New Devolopments On Two Separate Topoics: Statistical Cross Validation and Floodplain Mapping. In *Mathematics*, 191. Lawrence: The University of Kansas.
Kenward, T., D. P. Lettenmaier, E. F. Wood & E. Fielding (2000) Effects of Digital Elevation Model Accuracy on Hydrologic Predictions. *Remote Sensing of Environment,* 74**,** 432-444.
Mansourian, A., A. Rajabifard, M. J. Valadan Zoej & I. Williamson (2006) Using SDI and web-based system to facilitate disaster management. *Computers & Geosciences,* 32**,** 303-315.
Marks, K. & P. Bates (2000) Integration of high-resolution topographic data with floodplain flow models. *Hydrological Processes,* 14**,** 2109-2122.
Merwade, V., A. Cook & J. Coonrod (2008a) GIS techniques for creating river terrain models for hydrodynamic modeling and flood inundation mapping. *Environmental Modelling & Software,* 23**,** 1300-1311.
Merwade, V., F. Olivera, M. Arabi & S. Edleman (2008b) Uncertainty in Flood Inundation Mapping: Current Issues and Future Directions. *Journal of Hydrologic Engineering,* 13**,** 608-620.
Moffatt, S. & D. Laefer An Open-Source Vision for HAZUS. *Journal of Computing in Civil Engineering,* 24**,** 1-2.
National Research Council (U.S.). Committee on FEMA Flood Maps., United States. Federal Emergency Management Agency. & United States. National Oceanic and Atmospheric Administration. 2009. *Mapping the zone : improving flood map accuracy*. Washington, D.C.: National Academies Press.
NDEP. 2004. Guidelines for Digital Elevation Data, Version 1.0. In *National Digital Elevation Program (NDEP)*.
NGS. 2010. GPS On Bench Marks (GPSBM) Used To Make GEOID09; http://www.ngs.noaa.gov/GEOID/GPSonBM09/.
NWS. 2010. Advanced Hydrologic Prediction Service; http://www.weather.gov/ahps/inundation.php.
Pielke, J., R.A., M.W. Downton, and J.Z. Barnard Miller. 2002. Flood Damage in the United
States, 1926–2000: A Reanalysis of National Weather Service Estimates. Boulder, CO: UCAR.
Ries, K. G. & J. B. Atkins. 2007. *The National streamflow statistics program : a computer program for estimating streamflow statistics for ungaged sites*. Reston, Va.: U.S. Department of the Interior, U.S. Geological Survey.

Roman, D. R., Y. M. Wang, J. Saleh & X. Li. 2009. National Geoid Height Models for the United States: USGG2009 and GEOID09. In *ACSM-MARLS-UCLS-WFPS Conference*.

Sagun, A., D. Bouchlaghem & C. J. Anumba (2009) A scenario-based study on information flow and collaboration patterns in disaster management. *Disasters,* 33**,** 214-238.

Scawthorn, C., N. Blais, H. Seligson, E. Tate, E. Mifflin, W. Thomas, J. Murphy & C. Jones (2006a) HAZUS-MH Flood Loss Estimation Methodology. I: Overview and Flood Hazard Characterization. *Natural Hazards Review,* 7**,** 60-71.

Scawthorn, C., P. Flores, N. Blais, H. Seligson, E. Tate, S. Chang, E. Mifflin, W. Thomas, J. Murphy, C. Jones & M. Lawrence (2006b) HAZUS-MH Flood Loss Estimation Methodology. II. Damage and Loss Assessment. *Natural Hazards Review,* 7**,** 72-81.

Schmitt, T., C. National Research, R. R. Ramesh & E. Jon. 2007. *Improving Disaster Management: The Role of IT in Mitigation, Preparedness, Response, and Recovery*. National Academy Press.

Singh, V. P. (1997) Effect of spatial and temporal variability in rainfall and watershed characteristics on stream flow hydrograph. *Hydrological Processes,* 11**,** 1649-1669.

Smemoe, C., J. Nelson & A. Zundel. 2004. Risk Analysis Using Spatial Data in Flood Damage Reduction Studies. 262-262. Salt Lake City, Utah, USA: ASCE.

Tate, E. C., D. R. Maidment, F. Olivera & D. J. Anderson (2002) Creating a Terrain Model for Floodplain Mapping. *Journal of Hydrologic Engineering,* 7**,** 100-108.

Tayefi, V., S. N. Lane, R. J. Hardy & D. Yu (2007) A comparison of one- and two-dimensional approaches to modelling flood inundation over complex upland floodplains. *Hydrological Processes,* 21**,** 3190-3202.

USACE. 2010. HEC-RAS; http://www.hec.usace.army.mil/software/hec-ras/.

USGS. 2010. National Elevation Dataset (NED) 1/3 Arc Second; http://seamless.usgs.gov/products/3arc.php.

Valeo, C. & S. M. A. Moin (2000) Variable source area modelling in urbanizing watersheds. *Journal of Hydrology,* 228**,** 68-81.

Vardi, N. (2007) Slick. *Forbes,* 180**,** 50-50.

Voigt, S., T. Kemper, T. Riedlinger, R. Kiefi, K. Scholte & H. Mehi (2007) Satellite Image Analysis for Disaster and Crisis-Management Support. *IEEE Transactions on Geoscience & Remote Sensing,* 45**,** 1520-1528.

Wang, Y. & T. Zheng (2005) Comparison of Light Detection and Ranging and National Elevation Dataset Digital Elevation Model on Floodplains of North Carolina. *Natural Hazards Review,* 6**,** 34-40.

Weichel, T., F. Pappenberger & K. Schulz (2007) Sensitivity and uncertainty in flood inundation modelling; concept of an analysis framework. *Advances in Geosciences,* 11**,** 31-36.

Zerger, A. & S. Wealands (2004) Beyond Modelling: Linking Models with GIS for Flood Risk Management. *Natural Hazards,* 33**,** 191-208.